

## Review

# Silver nanoparticles: Synthesis, medical applications and biosafety

Li Xu<sup>1,2,3,4#</sup>, Yi-Yi Wang<sup>1,2#</sup>, Jie Huang<sup>1,2,3</sup>, Chun-Yuan Chen<sup>1,2,3</sup>, Zhen-Xing Wang<sup>1,2,3</sup>, Hui Xie<sup>1,2,3,5,6,7,8</sup>✉

1. Department of Orthopedics, Xiangya Hospital, Central South University, Changsha, Hunan 410008, China.
2. Movement System Injury and Repair Research Center, Xiangya Hospital, Central South University, Changsha, Hunan 410008, China.
3. Xiangya Hospital of Central South University–Amcan Medical Biotechnology Co. Ltd. Joint Research Center, Changsha, Hunan 410008, China.
4. Institute of Reproductive and Stem Cell Engineering, School of Basic Medical Science, Central South University, Changsha 410013, China.
5. Department of Sports Medicine, Xiangya Hospital, Central South University, Changsha, Hunan 410008, China.
6. Hunan Key Laboratory of Organ Injury, Aging and Regenerative Medicine, Changsha, Hunan 410008, China.
7. Hunan Key Laboratory of Bone Joint Degeneration and Injury, Changsha, Hunan 410008, China.
8. National Clinical Research Center for Geriatric Disorders, Xiangya Hospital, Central South University, Changsha, Hunan 410008, China.

#These authors contributed equally to this work.

✉ Corresponding author: Hui Xie, Department of Orthopedics, Xiangya Hospital, Central South University, Changsha, Hunan 410008, China; E-mail: huixie@csu.edu.cn.

© The author(s). This is an open access article distributed under the terms of the Creative Commons Attribution License (<https://creativecommons.org/licenses/by/4.0/>). See <http://ivyspring.com/terms> for full terms and conditions.

Received: 2020.02.27; Accepted: 2020.06.26; Published: 2020.07.11

## Abstract

Silver nanoparticles (AgNPs) have been one of the most attractive nanomaterials in biomedicine due to their unique physicochemical properties. In this paper, we review the state-of-the-art advances of AgNPs in the synthesis methods, medical applications and biosafety of AgNPs. The synthesis methods of AgNPs include physical, chemical and biological routes. AgNPs are mainly used for antimicrobial and anticancer therapy, and also applied in the promotion of wound repair and bone healing, or as the vaccine adjuvant, anti-diabetic agent and biosensors. This review also summarizes the biological action mechanisms of AgNPs, which mainly involve the release of silver ions (Ag<sup>+</sup>), generation of reactive oxygen species (ROS), destruction of membrane structure. Despite these therapeutic benefits, their biological safety problems such as potential toxicity on cells, tissue, and organs should be paid enough attention. Besides, we briefly introduce a new type of Ag particles smaller than AgNPs, silver Ångstrom (Å, 1 Å = 0.1 nm) particles (AgÅPs), which exhibit better biological activity and lower toxicity compared with AgNPs. Finally, we conclude the current challenges and point out the future development direction of AgNPs.

Key words: Silver nanoparticles; Silver Ångstrom particles; Synthesis; Antimicrobial; Anticancer; Toxicity; Mechanisms

## Introduction

Silver and its compounds have been used for antibacterial and therapeutic applications for thousands of years [1, 2]. Ancient Greeks and Romans used silverwares to store water, food, and wine to avoid spoilage. Hippocrates used silver preparations to treat ulcers and promote wound healing. Silver nitrate was also used for wound care and instrument disinfection. In 1852, Sims sutured the vesicovaginal fistulas caused by delivery with fine silver wires which significantly decreased infection. At the beginning of the 19th century, silver preparations were developed for wound infection and burn care.

However, in the 1940s, the medical applications of silver gave way to the clinical introduction of antibiotics [1]. With the abuse of antibiotics, bacterial resistance has become a worldwide problem especially since the 1980s, and silver began to receive attention again especially with the development of nanotechnology in the early of this century.

Nanomaterials (1–100 nm materials) have been attracting much attention in the past few decades in many fields such as biomedicine, catalysis, energy storage, and sensors, due to their unique physicochemical properties as compared to their bulk

forms. Silver nanoparticles (AgNPs) have received special interest, especially in biomedicine. AgNPs are famous for their broad-spectrum and highly efficient antimicrobial and anticancer activities. Other biological activities of AgNPs have been also explored, including promoting bone healing and wound repair, enhancing the immunogenicity of vaccines [3], and anti-diabetic effects [4]. Deciphering the biological mechanisms and potential cytotoxicity of AgNPs will facilitate their better medical applications.

Herein, we review the achievements of AgNPs in the past decade, especially focused on the past five years. This review intends to provide a valuable reference for researchers who are interested in the biomedical applications of AgNPs. The main contents include:

- Synthesis of AgNPs, including physical, chemical and biological synthesis methods;
- Medical applications of AgNPs, focusing on antimicrobial and anticancer properties and potential mechanisms, as well as other medical applications, including wound repair, bone healing, dental applications, vaccine adjuvant, antidiabetic agent, and biosensing;
- The potential toxicity of AgNPs, including potential damages of AgNPs to many systems and organs *in vivo*, including skin, eyes, respiratory system, hepatobiliary system, central nervous system, urinary system, immune system and reproductive system.

Numerous studies focus on the synthesis of AgNPs with controlled size and shape, and a variety of specific synthetic methods have been developed, including physical, chemical, and biological methods [5]. The predominant processes of the physical methods are classified into two parts: mechanical and vapor-based processes [6]. Conventional physical methods may involve mill, pyrolysis, and spark discharging [7]. Physical synthesis can obtain AgNPs with uniform size distribution and high purity [8]. Chemical synthesis is the most commonly used method to obtain AgNPs [8]. This method involves reducing silver ions to silver atoms [9], and the process can be divided into two steps, nucleation and growth [10]. Size- and shape-controlled AgNPs can be obtained by regulating the growth rate of nucleation. Besides reducing agents, capping agents and stabilizers also play important roles in obtaining AgNPs with good dispersion stability and uniform size distribution [11]. In addition, external energy can synergistically synthesize AgNPs, such as microwave, light, heat, and sound [12-15]. Although chemical synthesis methods of AgNPs are widely used, the

toxicity and pollution caused by chemicals must be highlighted and more attention should be given. Compared with physical and chemical methods, the biological method proves an economical and environmental approach for AgNPs [8]. Microorganisms include bacteria, fungi, and algae, as well as plant parts, include bark, peel, callus, leaves, flower, fruit, stem, seed, and rhizome are widely used in biological synthesis [16]. The organics, like enzymes, alkaloids, phenolic compounds and terpenoids, are abundant in extracts of microorganisms and plants, which can be available to reduce silver salts [16, 17]. Furthermore, some organic substances among these can also be used as stabilizers and capping agents [17]. Among the different methods, the additives mentioned may influence the subsequent medical applications of AgNPs.

AgNPs are recognized for wide-spectrum and high antimicrobial activity, they can effectively kill a variety of pathogens even at very low concentrations [18], including (i) bacteria, such as *Escherichia coli*, *Klebsiella pneumoniae*, *Staphylococcus aureus*; (ii) fungi, such as *Candida albicans*, *Aspergillus niger*; (iii) virus, such as Hepatitis B virus (HBV) and human immunodeficiency virus (HIV). Besides, some studies have shown that AgNPs have nematocidal and anthelmintic activity. The mainstream recognition of the antimicrobial mechanisms of AgNPs includes destructing bacterial cell walls, producing reactive oxygen species (ROS) and damaging DNA structure [18, 19]. Unlike the risk of antibiotic resistance which may limit medical applications, rare AgNPs resistance of bacteria is observed [20]. This may be attributed to the simultaneous multiple antibacterial mechanisms of AgNPs.

In recent years, the anticancer effect of AgNPs has been widely studied. AgNPs play an efficient role against a variety of cancer both *in vitro* and *in vivo*, including cervical cancer, breast cancer, lung cancer, hepatocellular carcinoma, nasopharyngeal carcinoma, glioblastoma, colorectal adenocarcinoma, and prostate carcinoma [21-23]. The anticancer activity of AgNPs is affected by inherent properties, including size, shape and surface charge [24-26]. Generally speaking, the smaller the particle size, the higher the biological activity. To obtain an ideal anticancer agent with high biological activity, our team successfully synthesized a kind of very small silver particles which reached up to Ångstrom (Å; one-tenth of a nanometer) scale and determined the stronger anticancer activities of silver Ångstrom particles (AgÅPs) compared with AgNPs [21]. In addition, exposure time and dose are also considered as crucial factors. Longer exposure time and higher dosage will trigger stronger anticancer effects. Some

possible mechanisms involving the anticancer effects of AgNPs have been proposed. AgNPs can cause apoptosis or necrosis by destroying the ultrastructure of cancer cells, inducing ROS production and DNA damage, inactivating enzymes, as well as regulating signaling pathways [27-29]. In addition, AgNPs can also block the invasion and metastasis of tumor cells by inhibiting angiogenesis [30-32]. Due to the enhanced permeability and retention (EPR) effect, tumor cells preferentially absorb NPs-sized bodies than normal tissues [33, 34]. While the poor lymphatic drainage in the tumor enables nanoparticles to stay and penetrate [35]. This may enhance the targeted drug delivery of AgNPs. Further studies of anticancer mechanisms of AgNPs are essential to develop economical, reliable, and broad-spectrum anticancer agents.

Besides the most studied antimicrobial and anticancer activities, AgNPs have also received attention in other cutting-edge medical applications, including wound repair, bone healing, dental material filling, vaccine adjuvants, antidiabetic agents, and bioimaging. In this review, we will also briefly introduce these biomedical applications.

Considering various products containing AgNPs, such as dressings, creams, solvents, and scaffolds, it seems necessary to assess the potential toxicity of AgNPs in cells, tissues, and organs. Generally speaking, primary exposure routes include skin contact, inhalation, ingestion, and injection [36-38]. These routes will distribute AgNPs to different tissues and organs, such as skin, respiratory, circulatory, nervous, hepatobiliary, urinary and reproductive systems [36-41]. The deposited AgNPs may be potentially toxic to these tissues or organs by inducing cell necrosis, apoptosis or genetic mutations [42-45]. For example, AgNPs deposited in the lungs can cause pneumonia and asthma [46]. AgNPs may cross the blood testis barrier (BTB) and reduce the fertility of model animals and cause teratogenicity in offspring [42]. Some toxicological studies on model animals have shown that the potential toxicity of AgNPs is related to the inherent properties [25, 47]. Large surface area may lead to increased silver ions ( $Ag^+$ ) released from AgNPs, which may enhance the toxicity of nanoparticles. Besides the unique properties, the potential toxicity of AgNPs is closely related to dose, concentration and exposure time [24, 48-50]. Exploring the pharmacodynamics of AgNPs *in vivo* may contribute to the development of bio-friendly and safe agents.

In recent years, a considerable amount of researches involving AgNPs prove enough evidence of promising medical applications of silver nano-materials. However, the potential toxicities of AgNPs

to mammals *in vivo* and cell lines *in vitro* alert us to be cautious about its utilization. This reminds us to carry out more researches to obtain safe, bio-friendly agents containing AgNPs. This article provides a review of the applications of AgNPs and potential toxicology from an objective stance with insights toward understanding deep implications for medicine.

## Synthesis of AgNPs

The synthesis methods of nanoparticles (NPs) are mainly divided into two processes: top-down and bottom-up (Figure 1). The top-down approach refers to the formation of metal NPs from bulk materials using various physical forces to synthesis NPs, such as mechanical energy used in ball milling, crushing and grinding; electrical energy used in the electrical arc-discharge method and laser ablation method; and thermal energy used in vapor condensation method [51]. These approaches can obtain NPs between 10 and 100 nm in size. The top-down approach, mainly the physical method, may acquire pure nanoparticles without chemical additives. NPs synthesized by physical method may exhibit uniform particle size distribution and high purity. Though the physical approach does not contain chemical reagents which may harm human and environment, it brings a great challenge to prevent agglomeration due to absence of stabilizer or capping agents. Furthermore, these methods need complex equipment and external energy in the process. The bottom-up approach involves the construction of complex clusters to obtain NPs from molecular components by employing nucleation and growth processes [51, 52]. The commonly used bottom-up approaches include chemical synthesis and biological synthesis, both can obtain NPs by reducing the precursor salt [52]. The chemical synthesis can be coupled with alternative energies, such as photochemical [53], electrochemical [54], microwave-assisted [55] and sonochemical methods [12]. Though the chemical method is carried out to quickly obtain various shapes of NPs, the use of harmful chemical additives may limit the medical applications of NPs. To overcome the shortcomings of the chemical method, the biological method has been regarded as an alternative option. The biological method usually relies on macromolecular substances in bacteria, fungi, and algae [16], such as exopolysaccharide, cellulose, and enzymes, and organic components in plant extracts such as enzymes, alcohol, flavonoids, alkaloids, quinines, terpenoids, phenolic compounds [16, 56-59]. Biological synthesis is an economical, environmentally friendly, simple and reliable approach, but the components on the surface of

nanoparticles must be adequately considered in the application. Based on these two approaches, frequently used methods for synthesizing AgNPs, including physical, chemical and biological methods are discussed herein.

### Physical Method

The physical synthesis of AgNPs involves mechanical processes and vapor-based processes. Energies are used to reduce particle size, including mechanical energy (ball milling method) [60], electrical energy (electrical arc-discharge method) [61], light energy (laser ablation method) [62], and thermal energy (physical vapor deposition) [6] (Table 1). During the ball milling progress, high-speed collisions between rigid balls, such as ceramics, flint pebbles, and stainless steels, can produce localized high pressures, which grind the metal into very fine powders [60]. The electrical arc-discharge method can obtain NPs via arc discharge device under direct current (DC) power [63]. The device uses the powder reagent layer as the anode and the electrodes are immersed in dielectric liquids such as hydrocarbons, liquid inert gas, and deionized water. Laser ablation method refers to the ablation of a metal plate by a high-power laser, the metal target absorbs the laser beam energy and photoions, followed by nucleation and growth of metal particles during the plasma plume cooling process and eventually synthesize NPs [62, 64]. Sputtering and evaporation are two processes in physical vapor deposition. Sputtering refers to bombarding a target coating material with a high-energy electrical charge to sputter off atom or molecule that can be deposited on the substrate. While evaporation refers to heating the coating material to the boiling point in a vacuum environment and evaporating, and the evaporated material rises in the vacuum chamber and condenses on the substrate. Although physical synthesis can produce AgNPs on a large scale, AgNPs may aggregate and form large-sized particles which will affect subsequent applications. In order to avoid the re-aggregation of

AgNPs, some stabilizers are used to obtain stable colloids AgNPs. For example, polyvinyl pyrrolidone (PVP) may be used as both the electrolyte and stabilizer in the synthesis of AgNPs by laser ablation method [65]. Our team prepared Ångstrom silver particles, capped with fructose as stabilizer, can be stable for a long time [21]. In summary, the physical method can quickly produce NPs with uniform size distribution and high purity, but complex equipment and external energy are required.

### Ball Milling Method

Mechanical ball milling technique is to put milling balls and metal materials with a specific mass ratio as well as gas (air or inert gas) in a container rotated at a high speed. The milling time, rotating speed and the atmospheric medium in the process of ball milling are playing essential roles in the morphology of metal materials. A suitable milling time is closely related to the production of particles with a satisfactory size. The smaller size of particles, the higher surface energy, therefore particles prefer to aggregate. The temperature of the powder in the ball milling process influences the diffusivity and phase of nanoparticles [60]. Generally speaking, a higher temperature of powder tends to synthesize intermetallic compounds, while lower temperature tends to obtain amorphous and nanocrystalline phases [52].

### Electrical Arc-Discharge Method

The electrical arc-discharge apparatus consists of DC power between two silver rods, which are immersed in dielectric liquids [61, 66]. During the process of arc discharge, the silver electrode is etched in the dielectric medium, and the surface of the silver electrode is vaporized because of the high temperature near the electrode. Subsequently, the silver vapor is condensed into AgNPs and suspended in the dielectric liquid. This apparatus can obtain pure AgNPs with a simple and low-cost device.

**Table 1.** Synthesis of Silver Nanoparticles by Physical Methods

Method	Silver precursor	Stabilizer/Surfactant/Dispersant	Operating conditions	Size (nm)	Shape	Reference
Ball milling method	Silver powder	-	Dry, under protective Ar gas atmosphere, below -160 ± 10°C	4-8	Spherical	[85]
	Silver wire	-	Multi-walled carbon nanotubes-aqueous nanofluids, 15-40°C, DC power	About 100	Spherical	[86]
Electrical arc-discharge method	Silver wire	-	25°C, current, voltage, deionized water	-	-	[66]
	Silver wire	-	DC arc-discharge system, 70°C, stirring	72	Spherical	[63]
	Silver wire	-	DC arc-discharge system, room temp.	19	Cubic	[87]
	Silver wire	-	DC arc-discharge system, deionized water, stirring	20-30	Spherical	[61]
Laser ablation method	Silver plate	-	Laser pulses, organic solvent	4-10	Spherical	[88]
	Silver plate	PVP	Laser pulse, stirring	20-50	Spherical	[65]
	Silver plate	-	Laser pulse, solution of chlorobenzene, stirring	25-40	Spherical	[89]
Physical vapour condensation	Silver wire	Fructose	High voltage power, rapid cooling	19.2±3.8 Ång	Spherical	[21]

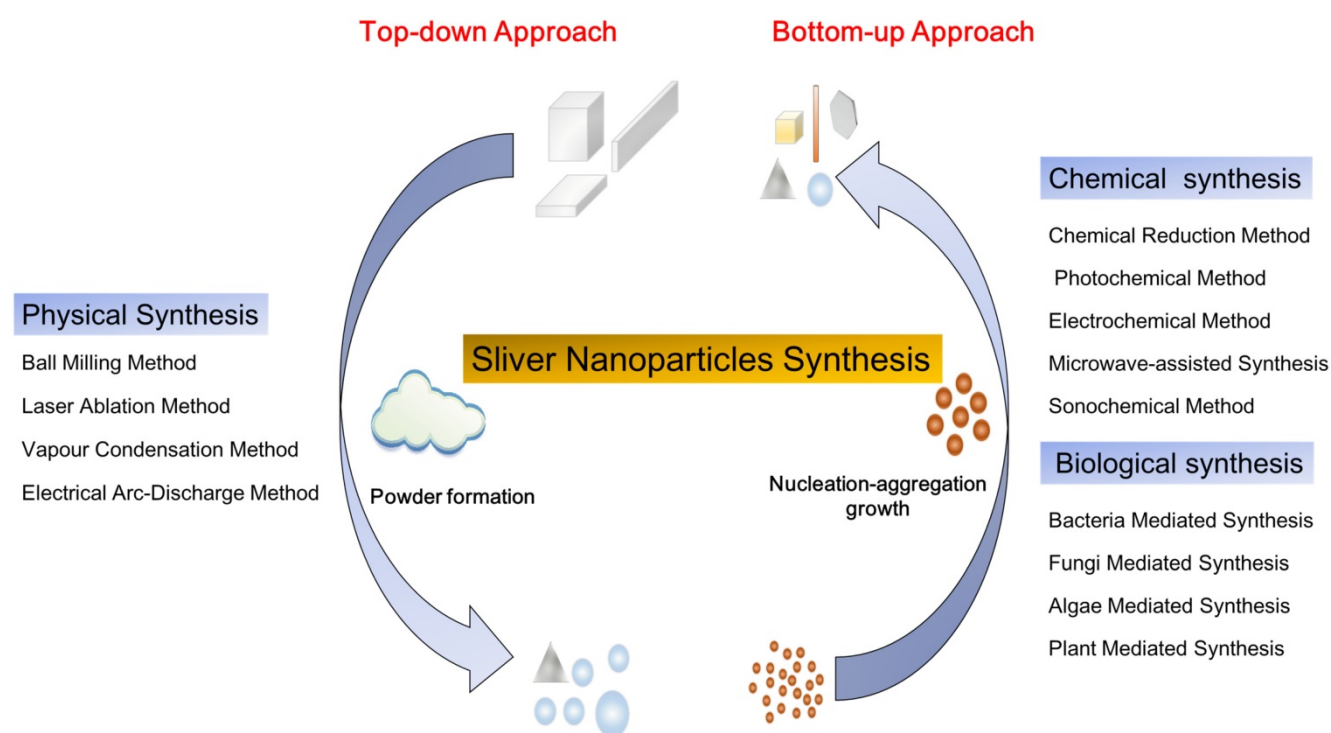


**Figure 1.** Silver nanoparticles synthesis: top-down approach and bottom-up approach, i.e. physical synthesis method, chemical and biological synthesis methods, separately. The top-down approach refers to the formation of metal nanoparticles from bulk materials, while the bottom-up approach refers to the growth of complex clusters and obtained nanoparticles from molecular components.

### Laser Ablation Method

Laser ablation method refers to a pulsed laser instantaneously heat the target bulk metal immersed in water or an organic solvent to form plasma plume, followed by nucleation and growth of metal particles during the plasma plume cooling process and eventually form nanoscale clusters [62, 64]. During the process of laser ablation, nanoparticles can absorb photons through multiple pathways, including plasmon excitations, interband transitions, and multiphoton absorption, which are closely related to pulse time, laser wavelength, and laser fluence. These factors, as well as the type of aqueous medium, may affect the characteristics of NPs [62]. Different synthesis conditions, such as laser fluences, pulse wavelength, as well as solvent type, may affect the size of the NPs. The addition of organic stabilizers such as cetyltrimethylammonium bromide (CTAB) and PVP can enhance the dispersibility of AgNPs [11]. However, it is difficult for laser ablation method to control the size distribution of NPs [62].

### Physical Vapor Deposition Method

The basic and most commonly used physical vapor deposition processes are divided into two general categories: arc evaporation and sputtering [67]. The former refers to the utilization of a cathodic arc source in a vacuum chamber or protective gases to obtain metal vapor and deposit it on a target coating

material to form a thin, adherent pure metal or alloy coating. During this process, highly ionized metal vapor generates plasma [68]. And the latter refers to using a high-energy electrical charge to bombard the target coating material and deposit metal on the substrate. In this process, ions and energetic atoms impact atoms and mechanically eject them from the target material. Recently, our team successfully synthesized a kind of very small silver particles which reached up to Ångstrom (Å) scale for the first time with a self-developed evaporation–condensation system [21]. A pure silver wire was fed into an explosion chamber filled with protective gas Argon, following by a high voltage of 25 kV when the wire contacted the positive electrode plate. The silver wire was exploded and evaporated to yield silver vapor plasma. Then the silver vapor was rapidly cooled and coagulated to form Ag particles in the rapid cooling chamber with a water chiller at 0–4 °C. High-intensity ultrasonic and demagnetization devices were used successively to prevent re-agglomeration of Ag particles. In conclusion, the physical vapor deposition method can obtain pure and dispersible AgNPs with small particle size, but complicated devices and external energy are required.

### Chemical Method

Chemical synthesis is currently the most common method to synthesize AgNPs (Table 2). The process involves the reduction of Ag<sup>+</sup> (supply by

silver salt precursor) to elemental silver (AgNPs) through electron transfer under certain conditions [8, 69]. In general, chemical synthesis can be promoted by reducing agents such as sodium borohydride (NaBH<sub>4</sub>) and sodium citrate (TSC). The chemical method can be combined with external energy sources to prepare AgNPs, such as photochemical, electrochemical, microwave-assisted and sonochemical methods. Among these methods, the generation process of AgNPs can be divided into two parts: nucleation and growth. The monomer concentration in the solution rapidly rises above the critical level of supersaturation, and triggers “burst-nucleation” and precipitation [70, 71]. The precipitation of the monomer forms the nucleus, and the repetitive nucleation process promotes the continuous birth of new seeds. As the seed formation, monomer concentration drops below the critical level of supersaturation. After nucleation, the increased addition of monomer induces the growth of nuclei and forms NPs with a larger size. During the synthesis process, stabilizers such as PVP and CTAB are usually used to stabilize and disperse AgNPs. Even though the chemical method of AgNPs is a reliable, high-yield, time-saving and controllable route, it must be noted that chemicals used in this method may cause environmental pollution.

### Chemical Reduction Method

Chemical reduction is a reliable method for

preparing colloidal AgNPs in organic solutions or water. AgNPs with desired shapes can be obtained by chemical reduction method, such as nanosphere, nanoprism, nanoplate, nanowire, nanocube, and nanorod. The chemical reduction method includes three components: salt precursor, reducing agent, and stabilizer. Silver precursors can be effectively reduced to AgNPs by different reducing agents with the presence of a stabilizer. There are several alternative silver precursors continuously providing monomers for nucleation, such as silver nitrate [69], silver ammonia (ie. Tollens reagent) [72], silver sulfate [73], and silver chlorate [74]. Frequently used reducing agents may affect the growth of nuclei, including NaBH<sub>4</sub>, hydrazine, N, N-dimethylformamide, TSC, ascorbic acid, ethylene glycol, polysaccharides, and formaldehyde. The types and ratio of precursors and reducers, as well as the temperature and pH of the solution, may influence the characteristics of AgNPs [75-78]. The nucleation and subsequent growth of the particles in the chemical reduction process can be controlled by alternating the components and adjusting the reaction parameters. For example, Jiang et al. [78] studied the role of temperature in the synthesis of AgNPs by chemical reduction method (**Figure 2**). At the reaction temperature range of 0 to 55 °C, the low temperature significantly slowed down the generation of nuclei and growth, therefore, it took a longer time to complete the reduction of precursors. From 17 to 55 °C, the reaction rate increased with

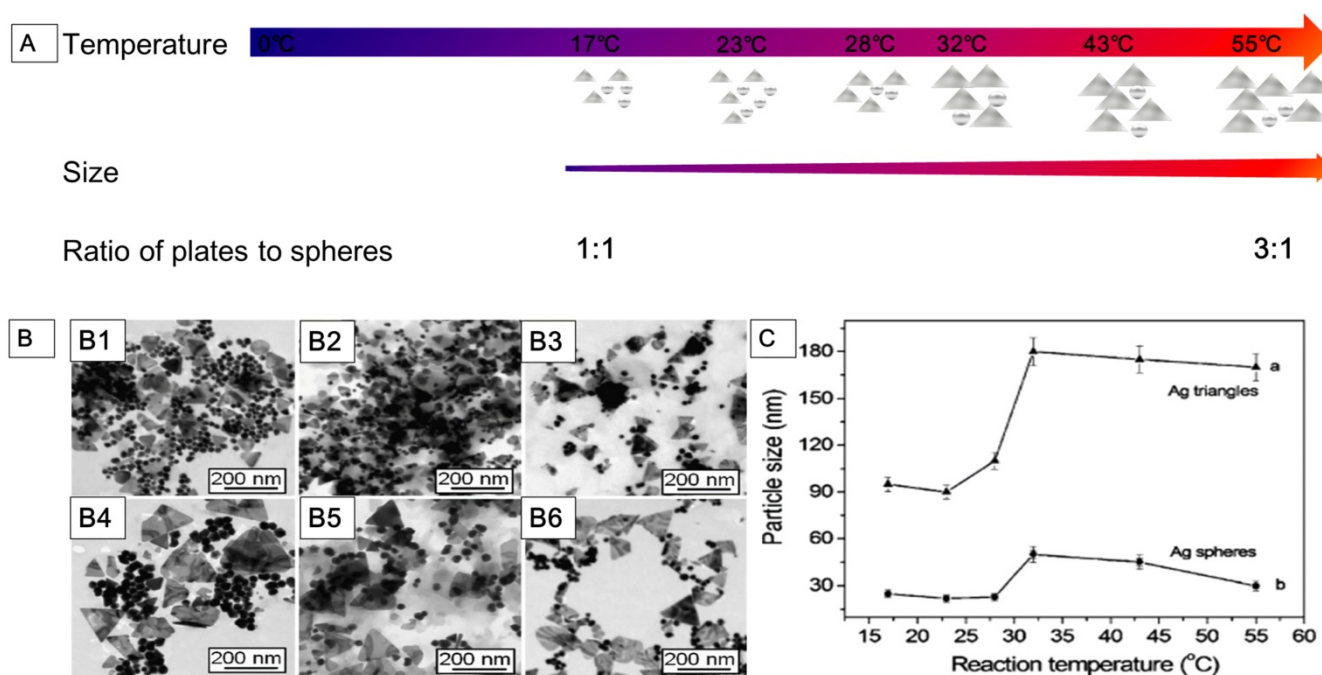


**Figure 2.** AgNPs synthesized at various temperatures. **(A)** The shape and size of AgNPs obtained in reaction systems at different temperatures ranged from 17 °C to 55 °C. **(B)** Transmission electron microscope (TEM) images of the AgNPs synthesized at different temperatures: (B1) 17 °C; (B2) 23 °C; (B3) 28 °C; (B4) 32 °C; (B5) 43 °C; (B6) 55 °C. **(C)** The average size of AgNPs (curve a: silver nanoplates; curve b: silver nanospheres) synthesized at different temperatures. Adapted with permission from [78], copyright 2011 Nanoscale Research Letters.

rising temperature, as well as the size of nanoparticle (Figure 2A, 2B). There was a size jump in the reaction synthesis at around 32 °C, i.e., the size of nanoparticles increased rapidly from around 90 nm to 180 nm for the edge length of plate AgNPs and from around 25 nm to 48 nm for the diameter of spherical AgNPs (Figure 2C). The ratio of the plate to spherical nanoparticles might be fundamentally dependent on the amount of single-crystal and twin structures formed at the nucleation process. In this experiment, the amount of spherical AgNPs decreased while the plate ones increased with the temperature rising. The ratio of the plate to spherical AgNPs was 1:1 at 17 °C, while 3:1 at 55 °C (Figure 2A).

### Photochemical Method

The photochemical method refers to reduce the precursors to AgNPs under the illumination. The silver precursors and solution in the luminescent region produce reduced free radicals and hydrated ions, which can reduce Ag<sup>+</sup> to Ag<sup>0</sup> *in situ* directly.

Light sources involving in the photochemical method include ultraviolet light, sunlight, and laser light, among which ultraviolet light is most commonly used. The source, intensity and wavelength of the light, and the irradiation time may affect the synthesis of AgNPs [79]. For example, prolonging the irradiation time and increasing the irradiation intensity during photochemical synthesis may promote the reduction of Ag<sup>+</sup> [79]. The photochemical method has the unique advantage of synthesizing highly dispersible nanoparticles *in situ* in the illumination region. Therefore, the photochemical method can obtain AgNPs on the surface of various media, such as polymeric films, glass, and cells which are illuminated. The photochemical method typically requires relatively simple equipment and can be carried out at room temperature without harmful or strong reducing agents. The reactions can be terminated or attenuated by stopping the illumination.

**Table 2.** Synthesis of Silver Nanoparticles by Chemical Methods

Method	Silver precursor	Reducing agent	Stabilizer/Surfactant/Dispersant	Operating conditions	Size (nm)	Shape	Reference
Chemical reduction	Tollens reagent	Triazole sugar	-	Room temp.	9.7 ± 1.9	Spherical	[72]
	AgNO <sub>3</sub>	Sodium citrate and tannic acid	-	Room temp., 100°C	About 30	Spherical	[90]
	AgNO <sub>3</sub>	Trisodium citrate/sodium borohydride/ascorbic acid	Sodium borohydride	Heat	-	-	[91]
	AgNO <sub>3</sub>	Hydrazine hydrate	Sodium dodecyl sulphate	Room temp.	40–60	Spherical	[92]
Photochemical method	AgNO <sub>3</sub>	Sodium borohydride	Trisodium citrate	Room temp., LED of specific wavelength	40–220	Decahedron, plate, prism	[93]
	AgNO <sub>3</sub>	NaCl	-	Room temp., UV light, stirring	About 8.6	Spherical	[13]
	AgNO <sub>3</sub>	Sodium borohydride	Trisodium citrate	Mixed light irradiation, DC power	31.4 ± 1.4	Triangular plate	[53]
	AgNO <sub>3</sub>	2-hydroxy-2-methylpropionone	-	Polychromatic Xe-Hg lamp, stirring	0.74–1.12	Spherical	[79]
	AgNO <sub>3</sub>	Sodium borohydride, tri-sodium citrate dihydrate	Polyvinylpyrrolidone	LED of different wavelength	4–20	Spherical, rod, polyhedrons	[94]
	AgNO <sub>3</sub>	Sodium citrate	-	25°C, Hg-halide floodlight	4.92±1.17	-	[95]
Electrochemical method	Silver plates	-	-	Room temp., galvanostatic	20	-	[96]
	Ag electrodes	-	-	20–95°C, 20 V, direct current, stirring	2–20	Spherical	[80]
	Ag electrodes	-	N-vinyl-2-pyrrolidone and sodium lauryl sulfate	Room temp., alternating polarity, 5–10 mA direct current, stirring	10–55	Spherical	[97]
	Silver plate	-	Chitosan	25°C, constant potential, UV irradiation, stirring	2–16	Spherical	[98]
	AgNO <sub>3</sub>	Sodium borohydride	Chitosan	Room temp., voltalab potentiostat/galvanostat	About 50	-	[69]
Microwave-assisted synthesis	AgNO <sub>3</sub>	Apple extract	-	Microwave, 100 °C	22.05 ± 1.05	Elongated and spherical-like	[99]
Sonochemical method	AgNO <sub>3</sub>	Glucose	Gelatin	High-intensity ultrasound irradiation, ambient conditions	About 5.3	Spherical	[84]
	AgNO <sub>3</sub>	-	J-carrageenan	Room temp., ultrasound irradiation	7.07 ± 2.54; 4.08 ± 2.09; 5.01 ± 6.48	Spherical	[12]
	AgNO <sub>3</sub>	-	Dihydrolipoic acid	Ultrasound irradiation, 50°C	5–10	Nanocluster	[100]
	AgNO <sub>3</sub>	-	Dihydrolipoic acid	Ultrasound irradiation, UV, room temp.	2–4	Nanocluster	[101]
	AgNO <sub>3</sub>	Polyacrylic acid	Acrylate	Ultrasound irradiation, 50°C	10–15	Spherical	[102]
	AgNO <sub>3</sub>	Sodium borohydride	Poly(vinyl alcohol)	Ultrasound irradiation, 60°C	13, 15, 18	Spherical	[103]
	AgNO <sub>3</sub>	-	Dihydrolipoic acid	Ultrasound irradiation, room temp.	2–3; 5–10	Nanocluster	[104]

### Electrochemical Method

Electrochemical method can form an electric potential in the electrolyte and reduce  $\text{Ag}^+$  to  $\text{Ag}^0$  [80]. The nucleation and growth of AgNPs occur almost simultaneously under the external electric field. Electrochemical method can synthesize AgNPs with different sizes by adjusting the current density. Besides, electrode types, electrolytes, and solvents are also important in the synthesis of size-controlled AgNPs. In the synthesis process, increased precursor concentration and enhanced current intensity, as well as prolonged implementation time, will obtain more AgNPs with smaller size [81]. To obtain dispersed and stable AgNPs, stabilizers and capping agents are optional additives. The steric hindrance formed by these additives will prevent the aggregation of AgNPs. The electrochemical method has the advantages of easy reaction control, mild reaction conditions, and less environmental pollution.

### Microwave-assisted Method

Microwave-assisted method refers to rapid heating the silver precursor by microwave irradiation, which may promote the generation of nuclei *in site* [82]. Several factors may influence the microwave-assisted synthesis of AgNPs, including the concentration of precursor and the type of stabilizer, power input and irradiation time of the microwave, dielectric constant, refractive index of the medium and chirality of reducing agents [55]. Water and alcohol are ideal media for microwave heating stabilizer because of their high dielectric losses [83]. For example, polar molecules such as  $\text{H}_2\text{O}$  attempt to orient the electric field in the microwave. When dipolar molecules attempt to reorient relative to an alternating electric field, they lose energy in the form of heat which may contribute to the reduction of  $\text{Ag}^+$ . Microwave-assisted method has the advantages of high energy conversion efficiency, time-saving, cleanliness, and convenience, most importantly, it can be used to obtain large-scale production of high dispersive AgNPs.

### Sonochemical Method

Sonochemical method refers to the cavitation effect generated by ultrasonic irradiation, which produces a local hot spot and promotes the synthesis of AgNPs [84]. The instantaneous high pressure and microjet generated by ultrasonic irradiation can uniformly mix the solution and generate bubbles, which may suddenly collapse when the bubbles grow. The adiabatic compression of the gas phase in the bubble creates a local hot spot, which accelerates the contact of  $\text{Ag}^+$  with the reducing agent and rapidly reduces it to AgNPs. Ultrasound prevents the

agglomeration of nanoparticles in the aqueous solution to decrease the size of AgNPs. Besides the high temperature, other factors such as pressure, pH, high-speed microjet, and high cooling rate may also contribute to the synthesis process. In summary, the sonochemical method is a simple, economical, and environment-friendly technique for preparing colloidal silver nanoparticles.

### Biological Method

In recent decades, a variety of microorganism- and plant-mediated biological syntheses of AgNPs are developed. The microorganisms can evolve metal tolerance genes and metal bioconcentration capability to survive in an extreme silver-rich environment [105, 106]. These adaptive evolutionary mechanisms include altering and decreasing the cytotoxicity of metal and resulting formation of AgNPs. AgNPs can be regarded as “by-product” of the resistance mechanism of microorganisms against free  $\text{Ag}^+$ . Plant mediated synthesis can reduce  $\text{Ag}^+$  to  $\text{Ag}^0$  using functional groups such as O-H and =C-H in organic components and their derivatives contained in the extract of plant parts [107]. Commonly used plant parts include bark, peel, callus, leaves, flower, fruit, stem, seed, and rhizome. In the process of biosynthesis, various biological components act as reducing agents, such as exopolysaccharide, peptides, nitrate reductase, reducing cofactors, c-type cytochromes, separated from microorganisms, and starch, cellulose, chitin, dextran, alginates, separated from plants. However, the organic components in the biosynthesis of AgNPs require to be further studied due to their complex interaction with AgNPs and the diversity of plants. Compared with physical or chemical methods, biological method can be carried out at normal temperature and pressure and avoid the use of toxic or hazardous additives. In this part, we will introduce several microbial and plant synthesis approaches of AgNPs, as well as the mechanisms involved in these processes.

### Bacteria-Mediated Synthesis

Since Tanja Klaus et al. firstly reported the phenomenon of aggregation of AgNPs in *Pseudomonas stutzeri* AG259 in 1999 [105], series of bacteria, both Gram-negative and Gram-positive, are been screened for the synthesis of AgNPs (Table 3). The property of bacteria to survive in an extreme silver-rich environment might contribute to the accumulation of AgNPs [105, 108]. Depending upon the location of the nanoparticles distribution, AgNPs may be synthesized intracellularly or extracellularly using biomass, supernatant, cell-free extracts, and derived components of the bacteria. Among these two modes, extracellular method is advantageous over

intracellular method due to the convenience of recovery of AgNPs. The abilities and mechanisms of strains used in the biosynthesis of AgNPs are different from each other due to the organic substances. Various organic substances in bacteria can be used as reducing agents, such as exopolysaccharide, peptides, reductase, cofactors, c-type cytochromes, and silver-resistant genes. Among these, several enzymes have been involved in synthesizing AgNPs, such as nitrate reductase and lactate dehydrogenase; and peptides with special amino acid, such as methionine, cysteine, lysine, and arginine, may attach on the surface of nuclei and act as reducing agents [109]. Nitrate reductase, a kind of NADH-dependent enzymes, has gained more attention in the bacteria-mediated synthesis of AgNPs. Nitrate reductase can participate in the electron transport chain, and subsequently creates a miniature reducing environment by transferring hydrogen atoms. The enzyme gains electron from NADH, oxidizes it to  $\text{NAD}^+$ , and undergoes oxidation to reduce silver ions to AgNPs [18, 109]. Some organic substances can also act as stabilizers and capping agents for AgNPs to prevent particle aggregation [18, 110]. The mechanisms of bacteria-mediated synthesis of AgNPs still need to be further explored. In conclusion, bacterial-mediated synthesis of AgNPs is a simple, effective, and environmentally friendly method.

### Fungi-Mediated Synthesis

Fungi-mediated synthesis of AgNPs is an effective and straightforward approach [111, 112]. According to the location of nanoparticles, fungi-mediated synthesis can obtain intracellular and extracellular AgNPs using mycelia and fungal cell-free filtrate, respectively [113, 114] (Table 3). Compared with intracellular synthesis, the extracellular synthesis of AgNPs using fungi is preferred due to the advantages of convenient collection and downstream processing. Plenty of fungi, due to their unique abilities of metal bioconcentration, high tolerance in the metal-rich environment, rapid mycelial growth, various extracellular enzymes secretion, and economic viability, are selected for biosynthesis of AgNPs [115], such as *Fusarium oxysporum* [116], *Trichoderma harzianum* [57], *Penicillium polonicum* [117], *Phomopsis liquidambaris* [118]. However, some fungi, such as *F. oxysporum* [111], are recognized to be potentially pathogenic, which may result in health risk in subsequent applications. While the AgNPs synthesized by extracellular method using the fungal extract can be purified by washing or precipitating unnecessary fungal components. Various organic components of fungi play an important role in the

synthesis of AgNPs, such as nitrate-dependent reductase, xylanases [119], naphthoquinones and anthraquinones, and quinine derivatives of the latter two, are involved in the reduction of silver precursor. In addition, some proteins secreted by fungi can be used as capping agents to form shape-controlled AgNPs [120]. Various incubation conditions might influence the characteristics of AgNPs, such as the types of carbon and nitrogen sources, temperature and light source [56]. In conclusion, fungi mediated synthesis of AgNPs is a convenient, effective, low-cost and energy-saving biological method. However, reducing potential pathogens on the surface of AgNPs should be considered to obtain safe products.

### Algae-Mediated Synthesis

Algae, as one of the most potential coastal renewable living resources, have received more attention in the biosynthesis of nanometer materials in recent years (Table 3). Algae contain a variety of biologically active organic matters, such as carbohydrates, polysaccharides, enzymes, proteins, vitamins, pigments and secondary metabolites [17, 121, 122]. These abundant organic compounds make algae an ideal candidate for biosynthesis of AgNPs. These active organic matters may be used as reducing agents to form size- and shape-controlled AgNPs, including spheres, triangles, cubes, rods, wires, hexagons, pentagons and wires. The roles of many algae in biosynthesis of AgNPs are verified, including *Cyanophyceae*, *Chlorophyceae*, *Phaeophyceae*, *Rhodophyceae* [123]. These studies support algae as a promising bioresource for the synthesis of AgNPs with various shapes and sizes. Biomolecules in algae extracts, such as amino acids, proteins and sulfated polysaccharides, can also act as stabilizers or capping agents in the biosynthesis of AgNPs with variable properties [124]. The specific factors involved in the algae-mediated synthesis of AgNPs are necessary to be identified and determined, including the ratio of silver precursor to algae extract, mixture pH, incubation time and temperature [125]. In conclusion, the biosynthesis of AgNPs using algae extract provides a facile, sustainable and eco-friendly method. Various algae can be considered as candidates in the biosynthesis of AgNPs due to their unique properties of rapid growth, high metal accumulation ability and abundant organic content.

### Plant-Mediated Synthesis

Plant-mediated synthesis of AgNPs, as a promising approach, has received great attention in recent years. Extracts from different parts of the plants, including bark, peel, callus, leaves, flower, fruit, stem, seed and rhizome, are involved in

biosynthesis of AgNPs with various sizes and shapes [59] (Table 4). These extracts from different plant parts contain organic components such as enzymes, alcohols, flavonoids, alkaloids, quinines, oils, terpenoids and phenolic compounds [126, 127]. There are different functional groups in these organic components [58], like hydroxyl, carbonyl, amidogen, which may contribute to the reduction of  $\text{Ag}^+$  to  $\text{Ag}^0$ . A variety of plant extracts, including the components mentioned above and plant derivatives such as starch, cellulose, chitin, dextran and alginates, act simultaneously as reducing agents and stabilizers [128]. The plant-mediated synthesis of AgNPs is influenced by different reaction parameters such as temperature, reaction time, pH and concentration of plant extracts and precursors [129, 130]. The AgNPs with different size and shape can be obtained by changing the synthesis parameters [129]. In summary, plant-mediated synthesis of AgNPs can be controlled by a variety of reaction conditions. In addition, different parts of plant exhibit various abilities in the synthesis of AgNPs [131]. The mechanisms of plant-mediated synthesis of AgNPs need more exploration. In conclusion, the plant-mediated synthesis of AgNPs using plant extract is a promising method due to its easy availability, nontoxicity, simplicity, cost-effectiveness and high reducing potential.

## Medical Applications of AgNPs

Antimicrobial and anticancer properties of AgNPs have been widely studied. Studies have shown that AgNPs have broad-spectrum antimicrobial properties against pathogens including bacteria, fungi and viruses [19, 49]. Besides, AgNPs can effectively damage or kill nematodes [152] and worms [153]. A variety of factors affect the antimicrobial activities of AgNPs, including size, shape, dose and stabilizer of AgNPs [49, 154, 155]. Interestingly, AgNPs may have different antibacterial effects against Gram-positive and Gram-negative bacteria [156]. AgNPs exhibit broad-spectrum anticancer properties. Anticancer activity of AgNPs is also affected by a variety of factors, including size, shape, dose, and exposure time [22, 157, 158]. It is also realized that the surface charge of AgNPs is a potential factor. Although current specific mechanisms of antimicrobial and anticancer properties of AgNPs are still unclear, many studies have carried out hypothesis. AgNPs can inhibit the growth of bacteria or kill them by inducing membrane destruction, ROS generation, DNA damage, enzyme inactivation and protein denaturation [4, 56, 159]. However, the anticancer mechanisms of AgNPs are much more complicated. Until now, it has been

approved that AgNPs can inhibit the growth of tumor cells by destroying the cellular ultrastructures, inducing ROS production and DNA damage [21-23, 160]. In addition, AgNPs can induce tumor cell apoptosis through inactivating proteins and regulating signaling pathways, or blocking tumor cell metastasis by inhibiting angiogenesis within lesion [31, 161]. Besides antimicrobial and anticancer properties, AgNPs can also be used in other medical applications, such as bone repair [162] and wounding repair [163]. And AgNPs can be regarded as an additive in dental materials or an adjuvant in vaccine. In this part, we will discuss the antimicrobial and anticancer properties and possible mechanisms of AgNPs, as well as other promising medical applications.

## Antimicrobial Application of AgNPs

### Antibacterial Properties of AgNPs

AgNPs have been proven to effectively inhibit various pathogenic bacteria, fungi and viruses, including *Staphylococcus aureus* [164], *Escherichia coli* [165], *Pseudomonas aeruginosa* [166], *dermatophyte* [167], HIV-1, etc. [168, 169]. The antibacterial effect of AgNPs against various strains of bacteria is different [156]. Rather than Gram-positive bacteria, AgNPs show a stronger effect on the Gram-negative ones. This may be due to the different thickness of cell wall between two kinds of bacteria [170]. Besides the bacteria strains, AgNPs may also exhibit size-, shape-, concentration-, time-, and charge-dependent antibacterial activity. In general, as particle size decreases, the antibacterial effect of AgNPs increases significantly [171]. Especially when the size is less than 10 nm, AgNPs show better antibacterial activity [172]. The antibacterial effect can be significantly enhanced by prolonging the treatment time of AgNPs [173]. The increased bacterial mortality may be ascribed to the accumulation of AgNPs and silver ions during the exposure period. Besides, the shape of AgNPs may also influence the antibacterial activity [171, 174]. By comparing the antibacterial activity of spherical, triangular, linear and cubic AgNPs, it is observed that spherical shaped AgNPs exhibit superior antibacterial effect. This phenomenon suggests that AgNPs with larger surface to volume ratio, which relates to both higher effective contact and larger reaction surface, may show stronger antibacterial activity [174]. In addition, the antimicrobial activity of AgNPs is also affected by the surface charge [156, 175]. Due to the presence of lipopolysaccharide, peptidoglycan and multiple groups, including carboxyl, amino and phosphate groups, bacterial membranes are primarily loaded with negative charges [170, 176]. Positive charge can

facilitate the adherence of AgNPs on bacterial membranes through electrostatic attraction [156]. Therefore, adjusting the surface charges of AgNPs may contribute to the enhanced antibacterial effect [175]. The stabilizers may influence the size, dispersion, and surface charge of AgNPs, which may involve in the antibacterial effect of AgNPs [154, 177]. Some stabilizers, such as citrates, PVP [154] and polyvinylalcohol [177], have been shown to influence the bacterial effect by adjusting the characteristics of AgNPs.

Although AgNPs exhibit good antibacterial activity, the specific mechanisms have not been completely clarified. Many hypotheses have been proposed to explain the antibacterial mechanisms of AgNPs, including i) Destructing the bacterial membrane and leaking cellular contents; ii) Generating ROS and disabling the respiratory chains; iii) Destructing the DNA structure and blocking the DNA replication; iv) Inactivating enzymes and denaturing proteins. Due to these mechanisms,

AgNPs exhibit broad-spectrum and effective antibacterial properties. These make AgNPs an alternative for the implementation of novel biomedical strategies, such as catheter modification, dental application, wound healing and bone healing.

### Antifungal and Antiviral Activities of AgNPs

Some studies confirm that AgNPs exhibit good antifungal properties against *Colletotrichum coccodes*, *Monilinia sp.* [178], *Candida spp.* [179] and various plant pathogenic fungi in size- and dose-dependent manners [180]. Some studies also point out that the type of culture media used in their experiments may also affect the inhibition activity [180]. Besides, AgNPs also show good antiviral activity against hepatitis B virus (HBV) [181], human parainfluenza virus (HPIV) [182], herpes simplex virus (HSV) [183] and influenza A (H1N1) virus [184]. AgNPs with less than 10 nm size exhibit good antiviral activity [185, 186], which may be due to their large reaction area and strong adhesion to the virus surface.

**Table 3.** Bacteria-, Fungi-, Algae-mediated Synthesis of Silver Nanoparticles

Bacteria/Fungi/Algae	Position	Precursor	Responsible organic components/functional groups	Operating condition	Size (nm)	Shape	Reference
<i>Streptomyces violaceus</i>	Extracellular	AgNO <sub>3</sub>	Exopolysaccharide	37°C; shaking; pH 7.0;	10–60	Cubic; crystalline; spherical	[132]
<i>Penicillium polonicum</i>	Extracellular	AgNO <sub>3</sub>	Proteins	Room temp.; shaking; light	10–15	Spherical; near spherical	[133]
<i>Falcaria vulgaris</i>	Extracellular	AgNO <sub>3</sub>	Hydroxyl group	50°C	10–30	Spherical	[134]
<i>Pseudomonas</i>	Extracellular	AgNO <sub>3</sub>	Aromatic and aliphatic amines	28°C; shaking	10–40	Irregular	[135]
<i>Pantoea ananatis</i>	Extracellular	AgNO <sub>3</sub>	Proteins or amino acids	37°C; shaking	8–90	Spherical	[136]
<i>Fusarium oxysporum</i>	Extracellular	AgNO <sub>3</sub>	Proteins	28°C; shaking	21.3–37.3	Spherical; oval	[111]
<i>Botryosphaeria rhodina</i>	Extracellular	AgNO <sub>3</sub>	NADH-dependent nitrate reductase	Room temp.; dark	below 20	Spherical	[137]
<i>Monascus</i>	Extracellular	AgNO <sub>3</sub>	Lactone ring	28–30°C; shaking	10–30; 15–40	Spherical	[138]
<i>Aspergillus tamarii</i>	Extracellular	AgNO <sub>3</sub>	NADH-dependent nitrate reductase	25±2°C; shaking	3.5 ± 3	Spherical	[120]
<i>Nostoc linckia</i>	Extracellular	AgNO <sub>3</sub>	Phycocyanin	Room temp.; pH 10.0	9.39–25.89	Spherical	[139]
<i>Caulerpa serrulata</i>	Extracellular	AgNO <sub>3</sub>	Caulerpenyne; caulerpin	27–95°C; pH 4.1–9.5	10 ± 2	Crystalline; spherical	[125]
<i>Laurencia aldingensis</i>	Extracellular	AgNO <sub>3</sub>	Proteins	Dark; shaking	5–10	Spherical	[140]

**Table 4.** Plant-mediated Synthesis of Silver Nanoparticles

Plant	Plant part	Precursor	Responsible phytoconstituent	Operating condition	Size (nm)	Shape	Reference
<i>Coptis chinensis</i>	Leaf	AgNO <sub>3</sub>	-	Room temp.; dark	6–45	Spherical	[23]
<i>Phyllanthus pinnatus</i>	Stem	AgNO <sub>3</sub>	Phytochemicals	Room temp.; sterility	below 100	Cubical	[141]
<i>Parkia speciosa</i>	Leaf	AgNO <sub>3</sub>	Polyphenols	60°C; pH 11.0	26–39	Spherical	[142]
<i>Plantago major</i>	All	AgNO <sub>3</sub>	-	85°C; dark	10–20	Spherical	[130]
<i>Avicennia marina</i>	Leaf, stem and root	AgNO <sub>3</sub>	-	Room temp.; shaking	About 75	Spherical	[131]
<i>Origanum vulgare L.</i>	Aerial part	AgNO <sub>3</sub>	-	-	2–25	Cubic	[143]
<i>Gossypium hirsutum</i>	Shoot	AgNO <sub>3</sub>	-	60°C; shaking	20–100	Spherical	[144]
<i>Flacourtia indica</i>	Leaf	AgNO <sub>3</sub>	Phenolic, lignin and sterols	50°C	14–24	Spheroid	[145]
<i>Walnut</i>	Fruit	AgNO <sub>3</sub>	-	37–40°C; shaking; dark	About 31.4	Spherical	[128]
<i>Cleome viscosa L.</i>	Fruit	AgNO <sub>3</sub>	-	Room temp.; dark	20–50	Spherical	[146]
<i>Alpinia katsumadai</i>	Seed	AgNO <sub>3</sub>	Phytochemicals	Room temp.; shaking; dark; pH 10	About 12.6	Quasispherical	[147]
<i>Ocimum Sanctum</i>	Leaf	AgNO <sub>3</sub>	Quercetin	-	250–600	Spherical	[129]
<i>Mimosa Pudica</i>	Root	AgNO <sub>3</sub>	-	Room temp.	35–42.5	Spherical	[148]
<i>Aloe vera</i>	Leaf	AgNO <sub>3</sub>	Lignin, hemicellulose, and pectins	100°C or 200°C; shaking	70.70 ± 22, 192.02 ± 53	Spherical	[149]
<i>Carambola</i>	Fruit	AgNO <sub>3</sub>	Polysaccharide and ascorbic acid	Stirring at 40°C	10–40	Face-centered-cubic	[150]
<i>Anogeissus latifolia, Boswellia serrata</i>	Gum ghatti, gum olibanum	AgNO <sub>3</sub>	-	121°C, 15 psi	5.7 ± 0.2; 7.5 ± 3.8	-	[151]

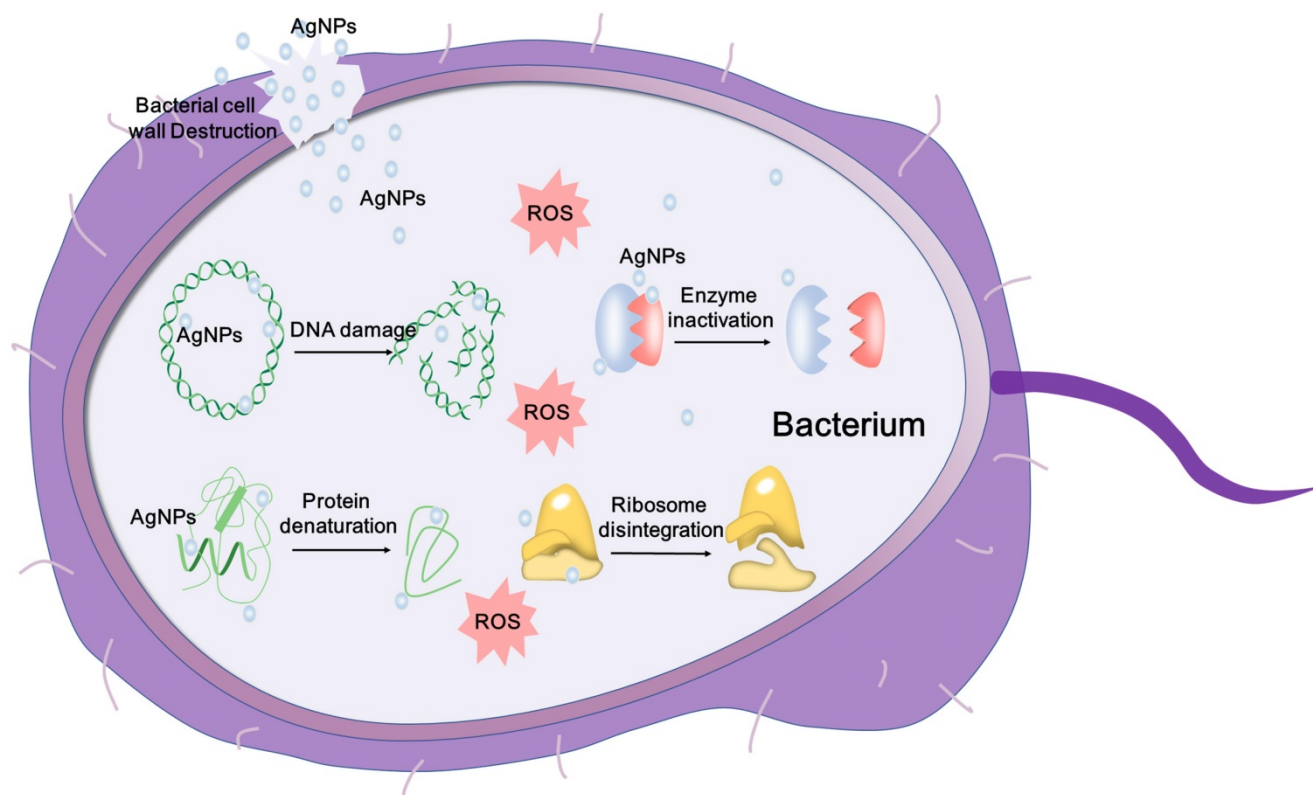


**Figure 3.** Schematic representation of the mechanisms of AgNPs against bacteria, depicting ROS-dependent pathway, DNA damage, protein denaturation and enzyme inactivation for antibacterial action of AgNPs.

For example, AgNPs can bind to the glycoprotein knobs and inhibit the reverse transcriptase (RT) of HIV-1 and interact with the virus in size- and dose-dependent manner [169, 185]. To develop AgNPs for antimicrobial applications, the detailed mechanism needs to be further studied.

### Antimicrobial Mechanisms of AgNPs

The antimicrobial effect of AgNPs has been widely studied, and the mechanisms are being explored. It is observed that AgNPs can anchor and then penetrate the bacterial membrane, and subsequently trigger the destruction of cell membrane and leakage of content [187]. Besides, AgNPs can influence crucial intracellular activities, such as attacking the respiratory chain, disturbing DNA replication and inhibiting cell division [188]. The antibacterial mechanisms of AgNPs are illustrated in **Figure 3**. AgNPs also have a good microbicidal effect in drug-resistant fungi via influencing the cellular targets, which are involved in the drug resistance and pathogenicity. For example, Venkatraman et al. [189] demonstrated that AgNPs could affect drug sensitivities by acting on multiple cellular targets of *Candida albicans*, including fatty acids like oleic acid, which were important in the hyphal morphogenesis involved in the pathogenicity. Some studies speculate

that AgNPs can saturate and adhere to the fungal hypha and eventually inactivate the fungus [180]. The antiviral mechanism of AgNPs has also been deeply explored. AgNPs can be used to prevent viral infection against several virus by blocking virus contact with cells and entry steps, or directly inactivating the virus, including herpes simplex virus (HSV), human parainfluenza virus 3, vaccinia virus, chikungunya virus and respiratory syncytial virus [182, 190-192]. These studies indicate that AgNPs can be used as a novel promising virucide agent. In order to develop safe and effective antimicrobial agents, the yet-to-be-determined mechanisms of antimicrobial properties of AgNPs are needed to be further studied.

### Nematicidal and Anthelmintic Activity

Worm infection via contact with contaminated soil is one of the most common diseases among children from middle and low-income countries [193]. Worm infections often lead to stunted growth, malnutrition and lagging academic performance [193, 194]. According to recent studies, AgNPs may become a candidate as a novel insecticide. Saha et al. [195] confirmed that AgNPs were effective in killing filaria and larvae. AgNPs induced the cell apoptosis and destroyed parasites mainly through the generation of ROS. It was worth noting that the carbohydrate

polymer not only participated in the synthesis of AgNPs, but also enhanced the filaricide activity of AgNPs. This suggested that AgNPs may be a potential preparation for filariasis control. In addition, they also tried to use AgNPs synthesized by *Acacia auriculiformis* to kill filaria, and also achieved impressive results [196]. Tomar et al. [197] realized the biologically synthesized AgNPs might inhibit both egg hatch and adult motility in dose-dependent manner. That was, a higher dose of AgNPs might exhibit better anthelmintic activity. Shabad et al. [198] confirmed the AgNPs synthesized by *Ziziphus jujuba* leaf extract showed ideal ovicidal and anthelmintic activity against *Haemonchus contortus* via nutrient depletion. The combination of AgNPs and organic components separated from plants can produce a synergistic effect which may enhance anthelmintic activity. Mamun et al. [199] speculated that organic substances in *M. charantia* fruit extracts, such as glycosides, alkaloids, reducing sugars and free acids, can help biosynthetic AgNPs to protect against parasitic infections. The phytochemicals might exert effect by adhering to the gastrointestinal tract or parasite cuticles. AgNPs exhibited larvicidal activities against larvae of *Anopheles stephensi* and *Culex quinquefasciatus*, thus contributed to the prevention of malaria and filariasis [200]. In conclusion, AgNPs may be used as an effective insecticidal agent to kill eggs, larvae and adult parasites. However, the mechanisms still need to be further explored.

## Anticancer Application of AgNPs

### Anticancer Properties of AgNPs

Cancer is currently considered an important factor in morbidity and mortality worldwide [201]. About 14 million new cancer cases are predicted by 2035, which will lead to a substantial impact on the economy and society around the world [202]. Therefore, there is an urgent need to develop effective and advanced treatment methods to reduce the adverse effects of cancer incidence. Common treatments of cancer or tumor include surgery, chemotherapy and radiotherapy. However, side effects and limitations of conventional treatments influence the outcomes. For example, standard chemotherapy may cause serious side effects, including local reactions, such as thrombophlebitis and tissue necrosis, and systemic reactions, including myelosuppression, dysfunction of liver and kidney and immunosuppression [203]. In addition, malignant tumors can develop multi-drug resistance (MDR), which may lead to chemotherapy failure [204]. Therefore, it is essential to develop novel drugs to improve the therapeutic effects. In recent years,

nanoparticles have attracted more attention in cancer therapeutics due to their special physical and chemical properties, which gives rise to a new field of anticancer – cancer nanomedicine [205, 206]. Compared to traditional anticancer agents, metallic nanoparticles (MNPs) can be used as novel therapeutic agents or drug carriers in combination with drug candidates, and undesirable side-effects can be prevented by providing a targeted approach [207]. Among these nanoparticles, AgNPs represent an ideal one in the search for anticancer or antitumor therapeutic agents [207].

AgNPs have been observed to exhibit good anticancer activities in breast cancer [158], cervical cancer [208], colon cancer [209], ovarian cancer [210], pancreatic ductal adenocarcinoma [211], lung cancer [212], hepatocellular carcinoma [213], melanoma [214], osteosarcoma [215], etc. (Table 5). Several studies confirm that the anticancer activities of AgNPs with various sizes, shapes and doses/concentrations are discrepant in different cancer cells [210-212, 215]. In addition, other factors, such as pH of lesions, exposure time, cell lines and tumor microenvironment, also influence the anticancer activity of AgNPs [210, 211, 214]. Generally speaking, AgNPs exhibit wide spectrum anticancer activity in size-, dose-/concentration- and time-dependent manners. AgNPs with smaller size can elicit enhanced endocytosis, and induce more significant cytotoxicity and genotoxicity. Compared with other shapes, spherical AgNPs exhibit better cytotoxicity due to the higher surface-to-volume ratio [216]. And higher dose of AgNPs usually leads to more apoptosis than lower one. In this section, we highlight these factors.

### Size- and Shape-dependent Manners

Nanoparticles motility in capillaries, as well as endocytosis and metabolism in tumor cells, are significantly affected by the size of AgNPs [217, 218]. It has been found that the kinetics of uptake, intracellular accumulation and excretion, and the resulting cytotoxicity and genotoxicity, varied with the different sized AgNPs. In general, smaller AgNPs have higher endocytosis and exocytosis efficiency, therefore are supposed to produce greater cytotoxicity than larger particles [49, 217]. To investigate the effect of nanoparticle size on distribution within tumor, Gavin Fullstone et al. [219] simulated the transport of nanoparticles in blood flow using an agent-based approach, testing the ability of 10 nm, 20 nm, 50 nm, 70 nm, 80 nm, 100 nm and 160 nm nanoparticles to traverse fenestrations with pore size of normal blood vessels and tumor-associated blood vessels.

**Table 5.** Anticancer Mechanisms of Silver Nanoparticles

Cancer cell lines	AgNPs		Concentration, IC <sub>50</sub> , exposure time	Manners	Mode of action	References
	Synthesis methods	Size; Shape				
HeLa cells	Plant	40 nm; spherical and pentagonal	25, 50, 100, 250 µg/mL; 24 h	Dose-dependent	ROS generation; ultrastructural changes; mitochondrial dysfunction	[229]
HeLa cells	Plant	33 nm; face-centered-cubic	0–100 µg/ml; 24 h	Concentration-dependent	Sub G1 cell cycle arrest; ROS generation; down-regulation of MMP	[261]
HeLa cells	Chemical	20–40 nm; spherical	1.35 µg/mL and 13.5 µg/mL; 24 h and 48 h	Dose-, concentration- and time-dependent	Decreased the number of cells at S and G2/M phase; increased the number of cells at sub-G1 phase	[244]
HeLa cells	Chemical	26.5 ± 8.4 nm; spherical	10, 20, 50 µg/mL; 10 h and 24 h	Dose- and time-dependent	Regulation of PtdIns3K signaling pathway	[22]
A549	Fungi	25 nm; round and triangular	1–10 µg/mL; 48 h	-	ROS generation; nucleus damage	[273]
A549	Plant	17–25.8 nm	25 µg/ml	-	Activation of apoptotic gene; inhibition of cell migration and invasion	[274]
MCF-7	Plant	22 nm; spherical	IC <sub>50</sub> : 20 µg/ml; 24 h and 48 h	Dose- and time-dependent	ROS generation; DNA damage; disruption of the cell membrane	[275]
MCF-7	Plant	12 nm; different shapes	IC <sub>50</sub> : 20 µg/mL; 24 h	Dose-dependent	Regulation of Bax and Bcl-2 gene expression	[276]
MCF-7	Peptides	31.61 nm; spherical	IC <sub>50</sub> : 104.1 µg/mL; 24 h	Dose-dependent	ROS generation; disruption of mitochondrial respiratory chain	[277]
MCF-7, EAC	Algae	7.1–26.68 nm; spherical	IC <sub>50</sub> : 13.07 ± 1.1 µg/mL; 48h	Dose-dependent	Inhibition of proliferation; mitochondria dysfunction	[278]
A549	Plant	6–45 nm; spherical	10 µg/mL and 25 µg/mL; 24h	Dose-dependent	Inhibition of proliferation, migration and invasion	[23]
MCF-7; MDA-MB-231	Plant	15–30 nm; spherical	IC <sub>50</sub> : 20 µg/mL (MCF-7), 30 µg/mL (MDA-MB-231)	Dose-dependent	Regulation of p53, Bax and Bcl-2 expressions	[279]
A549	Plant	45.12 nm; spherical	IC <sub>50</sub> : 62.82 µg/mL (24 h) and 42.44 µg/mL (48 h)	Dose- and time-dependent	S phase cycle arrest; decrease of cell population in sub G1 phase	[280]
A549; Hep G2	Purchased	21 ± 8 and 72 ± 11 nm; spherical	1–20 µg/mL; 48 h	Concentration- and dose-dependent	Inhibition of telomerase activity and telomere dysfunction	[240]
HT29	Plant	9.13 ± 4.86 nm; spherical	IC <sub>50</sub> : 38.55 µg/mL; 24 h	Dose-dependent	Induction of apoptosis pathway	[281]
HCT116	Bacteria	15 nm; spherical	IC <sub>50</sub> : 0.069 µg/mL; 24 h	Dose- and time-dependent	Induction of nuclear condensation and fragmentation	[159]
HCT-116	Plant	24–150 nm; spherical, triangular	IC <sub>50</sub> : 100 µg/ml; 24 h	Dose-dependent	Up-regulated modulators of apoptosis, Caspase-3, Caspase-8 and Caspase-9; mitotic arrest; DNA fragmentation	[282]
PANC-1	Purchased	2.6 and 18 nm; spherical	IC <sub>50</sub> : 1.67 µg/mL (2.6 nm), and 26.81 µg/mL (18 nm); 1 h, 24 h	Size- and concentration-dependent	Ultrastructural change; regulation of p53, Bax, Bcl-2, RIP-1, RIP-3, MLKL and LC3-II expression, Chromosome instability; mitotic arrest; regulation of gene expression	[211]
SCC-25	Purchased	10 ± 4 nm; spherical, cubic	IC <sub>50</sub> : 37.87 µg/mL; 24 h	Dose-dependent	Chromosome instability; mitotic arrest; regulation of gene expression	[24]
HOS; HCC	Fungi	8 ± 2.7 nm; spherical	IC <sub>50</sub> : < 5 µg/mL (Huh7 cells), 10 µg/mL (OS cells)	Dose-dependent	ROS generation; activation of JNK signaling	[283]
CNE; HEp-2	Chemical	20 nm; spherical	IC <sub>50</sub> : 9.909 µg/mL; 24 h	Dose-dependent	Mitotic arrest; regulation of Bax and P21 and Bcl-2 expression	[284]
PC-3	Plant	9 – 32 nm; spherical	IC <sub>50</sub> : < 10 µg/mL; 24 h	Dose-dependent	Decrease of stat-3 and bcl-2 expression; increase of caspase-3 expression	[285]
DU145; PC-3; SKOV3; A549	Plant	10 – 30 nm; spherical	IC <sub>50</sub> : 4.35 µg/mL (DU145); 7.72 µg/mL (PC-3); 4.2 µg/mL (SKOV3); 24.7 µg/mL (A549)	Dose-dependent	ROS generation; regulation of LPO and GSH level; regulation of caspase, p53 and Bax and Bcl-2	[29]
DLA	Bacteria	50 nm; spherical	IC <sub>50</sub> : 500 nmol/L; 6 h	Dose- and time-dependent	Activation of caspase 3; DNA fragmentation	[286]
SKBR3; 8701-BC; HT-29; HCT 116; Caco-2	Bacteria	11 ± 5 nm; spherical	IC <sub>50</sub> : 5 µg/ml (SKBR3); 8 µg/ml (8701-BC); 20 µg/ml (HT-29); 26 µg/ml (HCT116); 34 µg/ml (Caco-2)	Dose- and time-dependent	Decrease of MMP-2 and MMP-9 activities; ROS generation	[269]
Murine fibrosarcoma	Chemical	10 nm; spherical	IC <sub>50</sub> : 6.15 mg/kg	Dose-dependent	ROS generation; alteration of the IL-1b function	[287]
BxPC-3; A549; PC-3; Hep G2; CNE1; AsPC-1; U-87 MG; SW480; EC109; MDA-MB-231	Physical	19.2 ± 3.8 Ång; spherical	IC <sub>50</sub> : 10.36–25.85 µg/ml; 0 – 400 min, 24h	Dose- and time-dependent	Ultrastructure change; ROS generation; mitochondrial dysfunction; cell cycle arrest	[21]

\*NOTE: ROS, reactive oxygen species; MMP, matrix metalloproteinase; LPO, lipid peroxidation; GSH, glutathione; JNK, c-jun N-terminal kinase; MCF-7, human breast cancer cell line; EAC, ehrlich ascites carcinoma; A549, human lung carcinoma cells; BxPC-3, human pancreas adenocarcinoma cells; PC3, prostate adenocarcinoma cells; HepG2, hepatocellular carcinoma cells; CNE1, nasopharyngeal carcinoma cells; AsPC-1, pancreas adenocarcinoma cells; U-87 MG, glioblastoma cells; SW480, colorectal adenocarcinoma cells; EC109, esophageal cancer cells; MDA-MB-231, breast adenocarcinoma cells; HT29, human colorectal adenocarcinoma cell line; HCT-116, human colon cancer cell line; PANC-1, human pancreatic ductal cell line; SCC25, human tongue squamous carcinoma; DU145 and PC-3, human prostate carcinoma cell lines; SKOV3, human ovarian carcinoma; CNE, human nasopharyngeal carcinoma cell line; HEp-2, laryngeal carcinoma cell line; DLA, Dalton's lymphoma ascites cell lines; SKBR3, human breast cancer cell line; Caco-2, heterogeneous human epithelial colorectal adenocarcinoma cells; HCC, human hepatocellular carcinoma cells; HOS, human osteosarcoma cells; MDA-MB-231, triple-negative breast cancer cell line.

Although 50 nm, 70 nm and 80 nm nanoparticles can effectively penetrate both, 100 nm nanoparticles cannot penetrate normal fenestrations, suggesting that there might be an optimal size for effective leakage of nanoparticles from the microvasculature into the tissue. Rona et al. [41] demonstrated that size of AgNPs could influence cellular uptake and toxicity. Smaller particles (10 nm, 20 nm) easily penetrate LoVo cells and then significantly increase intracellular ROS levels, while larger particles (100 nm) appeared mainly on the cell surface. Alicia et al. [220] also found that smaller AgNPs were more cytotoxic than larger AgNPs when studying the therapeutic effects of AgNPs on human hepatoma and leukemia. Our team [21] used an evaporation–condensation system to obtain silver particles approaching the Ångstrom dimension. By comparing AgNPs with larger size, we found Ångstrom-scale silver particles had greater cytotoxicity to tumor cells, but did not induce notable toxicity on normal tissues.

The applications of AgNPs can be extended by tailoring the shape of nanoparticle, which may optimize the physicochemical and biological properties of AgNPs [26, 221]. The shape-controlled AgNPs can be obtained by changing the parameters in different synthesis methods. Though AgNPs with various shapes are prepared, such as sphere, triangle, cuboid, rod, tube, disk and wire, only a few among these are chosen for anticancer therapy. The cellular uptakes of AgNPs, as well as particle-to-cell or particle-to-protein interactions, are partly dependent on the shape of nanoparticles [216, 222]. In general, spherical AgNPs may display stronger endocytosis and more active anticancer effect than other shapes. Because it is more efficient for spherical AgNPs than non-spherical nanoparticles to pass through vascular endothelium, and their higher specific surface area is more beneficial for them to enter cancer cells [216, 222]. In addition, the active or weak endocytosis may be related to the different membrane bending energies of various shaped AgNPs. Ying Li et al. [223] compared the internalization rates of spherical-, cubic-, disk- and rod-shaped nanoparticles to find out the shape effect on endocytosis. They realized that the spherical nanoparticles exhibited the fastest internalization rate, followed by the cubic nanoparticles, while the disk- and rod-shaped nanoparticles exhibited the slowest internalization rate. After analyzing the free energies of four shaped nanoparticles, they speculated that the membrane bending energy of nanoparticles during endocytosis might be the main factor inducing the shape effect of the nanoparticles. Among these four shaped nanoparticles, compared with the non-spherical, the spherical nanoparticles only needed to overcome a

minimal membrane bending energy barrier, while the disk shaped nanoparticles faced a larger free energy barrier caused by stronger membrane deformation. In order to understand the effect of more complex shaped particles on cellular uptake, Yuanzu He et al. [224] treated LnCAP cells with particles of different keyboard character shapes and compared the cell endocytosis. Compared with shapes without sharp features, like number 0, letter O and pound key, the rod-like microparticles, such as number 1, letter I, and arrow key, were more likely to adhere, penetrate and enter the cancer cells. The results explained that the shapes of microparticles with sharper angular features and higher aspect ratio might have a higher chance to contact and be internalized by cancer cells.

#### Dose and Exposure Time

The AgNPs exhibit dose- and time-dependent cytotoxicity against cancer [21, 225–227]. In general, increased dose and prolonged exposure time can cause more tumor cell apoptosis [228, 229]. Increasing dosage and prolonged exposure time can provide more opportunities for AgNPs to enter cells and trigger multiple anticancer mechanisms. Muthu et al. [226] studied the anticancer effect of AgNPs on Dalton's lymphoma ascites (DLA) cell lines and found that AgNPs showed dose-dependent cytotoxicity to DLA cells through activation of caspase 3 enzyme, ultimately inducing apoptosis. Bitu Mousavi et al. [230] found that AgNPs synthesized by *Artemisia turcomanica* leaf extract showed both dose- and time-dependent anticancer effect on gastric cancer cell line. Although increased dose of AgNPs and prolonged exposure time can result in better anticancer effects, the potential toxicity to normal tissues needs to be carefully considered.

#### Surface Charge and Protein Corona

Surface charges participate in the formation of AgNPs surface chemistry, which play an important role in cytotoxicity [231–233]. The surface charges of AgNPs determine the binding with serum albumin, as well as the adhesion and uptake of cells [25]. Negatively charged and neutrally charged AgNPs can adhere to cell membranes but internalize in small amounts, while positively charged AgNPs exhibit more efficient cell membrane penetration and internalization [25]. Besides, the positively charged AgNPs tend to stagnate on the surface of the tissue and the lumen of the blood vessels for a long time, which may be beneficial for the targeted delivery of anticancer agents [234]. AgNPs with opposite surface charges exhibit different cytotoxicity in tumor cells. The greater cytotoxicity and more ROS production are observed in tumor cells exposed to high positive charged AgNPs [234]. Nanoparticles exposed to a

protein-containing medium are covered with a layer of mixed protein called protein corona [235]. The electrostatic interactions between proteins and nanoparticles contribute to the formation of protein corona [236]. Some proteins may undergo conformational changes during the formation of protein corona [235]. Protein corona has an important effect on the absorption, accumulation and subsequent behaviors of nanoparticles in cells [237]. It is proved that AgNPs with protein coronas enter cells via receptor-mediated endocytosis and subsequently induce mitochondrial dysfunction and cell apoptosis [238]. By comparing nanoparticles without protein coronas, it is realized that the formation of protein coronas around AgNPs can be a prerequisite for their cytotoxicity.

### Anticancer Mechanisms

AgNPs have broad-spectrum anticancer activity via multiple mechanisms [21, 239, 240]. Numerous experiments *in vitro* and *in vivo* have proved that AgNPs can decrease the proliferation and viability of cancer cells. AgNPs can cause apoptosis and necrosis by destroying the ultrastructure of cancer cells, inducing the production of ROS and DNA damage [21, 241]. AgNPs can promote apoptosis by up- or down-regulating expression of key genes, such as p53 [242], and regulating essential signaling pathways, such as hypoxia-inducible factor (HIF) pathway [243]. Cancer cells treated with AgNPs may also show cell cycle arrest [160, 244]. Several cancer cells exposed to AgNPs undergo sub-G1 arrest and apoptosis. Besides, AgNPs can also reduce distant metastasis by inhibiting tumor cell migration and angiogenesis [28, 245]. Multiple anticancer mechanisms of AgNPs are described in **Figure 4**. In order to develop safe and effective anticancer agent, more mechanisms for anticancer effects of AgNPs remain to be explored. Here, we summarize the possible anticancer mechanisms of AgNPs both *in vitro* and *in vivo*.

### Ultrastructural Destructures of Cancer Cells

Destruction of ultrastructures such as cell membranes and intracellular organelles leads to cell apoptosis and necrosis [21]. Tumor cells exhibit intact cell structure under light microscope, such as round nuclei, intact nuclear membrane, homogeneous chromatin, normal mitochondria and rough endoplasmic reticulum [40]. The ultrastructural changes of AgNPs-exposed tumor cells are in a dose- and time-dependent manner [246]. Generally, the higher the concentration of AgNPs and the longer the exposure time, the more serious the damage of cell ultrastructure. TEM observation showed that AgNPs-exposed cells are suffering morphological change or

cytoplasmic organelle damage, and undergoing different death patterns: apoptosis, necrosis and autophagy [40]. Autophagosomes associated with apoptosis and necrosis are formed in the cytoplasm of AgNPs-treated tumor cells [247]. AgNPs promote autophagosome formation through the PtdIns3K pathway, and induce autophagy in tumor cells without inhibiting lysosomal function [22]. Structural and functional disruption of the actin cytoskeleton may be the cause of morphological deterioration of tumor cells exposed to AgNPs, and may be involved in inhibiting migration and invasion of tumor cells [248]. Free Ag<sup>+</sup> released from AgNPs is involved in the destruction of cellular membranes. Ag<sup>+</sup> released by AgNPs induces oxidation of glutathione, and increases lipid peroxidation in cellular membranes, resulting in cytoplasmic constituents leaking from damaged cells [249]. Our team found time-dependent morphological changes in cancer cells treated with F-AgNPs, such as organelle compaction, nuclear fragmentation and cell blebbing [21]. Tumor cells exposed to AgNPs lose their typical shape due to pseudopod contraction, decreased cell adhesion and reduced cell density. Scanning electron microscopy analysis of AgNPs-treated tumor cells reveal spherical appearance, foamed membrane and shorten filopodia [248]. Tumor cells exposed to AgNPs show apoptotic cell characteristics such as loss of intact membrane, decreased contact with adjacent cells, condensed and detached from the culture plate [250].

### ROS Production

ROS are by-products of biological aerobic metabolism, including oxygen ions, peroxides and oxygenated free radicals [251]. ROS are highly active due to the presence of unpaired free electrons. ROS are controlled at a low level by normal cellular antioxidant defense mechanisms and do not affect the normal physiological activities of the cells. However, excessive ROS can produce oxidative stress that reduces the activity of biological macromolecules and damages subcellular organelles and DNA structures [252, 253]. Oxidative stress trigger lipid peroxidation, impaired mitochondrial function, amino acid oxidation in proteins, enzyme inactivation and DNA/RNA damage [233], which may lead to autophagy, apoptosis and necrosis of cancer cells. AgNPs distributed in tumor cells via endocytosis can result in autophagy and apoptosis through a variety of ROS-mediated stress responses. In addition, AgNPs-induced formation of ROS may affect cellular signal transduction pathways, which may participate in the activation of apoptosis [254]. For example, the mitochondrial function can be inhibited by AgNPs via disrupting mitochondrial respiratory chain,

suppressing ATP production. Besides, ROS induced by AgNPs may ultimately lead to DNA damage [255]. Superoxide radicals directed to mitochondria may enhance mitochondrial outer membrane permeabilization (MOMP) and the release of Cyt *c*, destroy the electron transport chain, and impair mitochondrial function [256]. Some factors influence the generation of ROS induced by AgNPs. Smaller size and higher concentration of AgNPs exhibit higher induction of ROS and stronger cytotoxicity, and sharp increased ROS appear in different cancer cells treated with AgNPs [220].

#### DNA Damage

AgNPs can induce ROS production to disrupt DNA structure, or directly contact with DNA to cause DNA mutations [209, 241, 248]. High levels of ROS can generate damage to DNA double helix in a concentration-dependent manner, including breaking

the single or double-stranded DNA, affecting base modifications and DNA cross-links [241, 253, 257]. AgNPs-treated cancer cells may exhibit DNA methylation, DNA base pairing errors, DNA repair defects and increased chromosomal aberrations [209, 248, 258]. AgNPs may play an important role in the regulation of gene expression of cells. AgNPs inhibit the proliferation of cells and trigger DNA repair defects by down-regulating the functions of proteins involved in cell cycle progression and DNA repair [259]. For example, proliferating cell nuclear antigen (PCNA) gene plays an important role in DNA synthesis and repair as a cofactor for DNA polymerase. PCNA is down-regulated in AgNPs-exposed cells. While the up-regulation of the apoptotic precursor protein Bax suggests that AgNPs initiate apoptosis via the mitochondrial pathway [260]. AgNPs-treated cells may undergo S phase, G2/M phase and sub-G1 cell cycle arrests in a

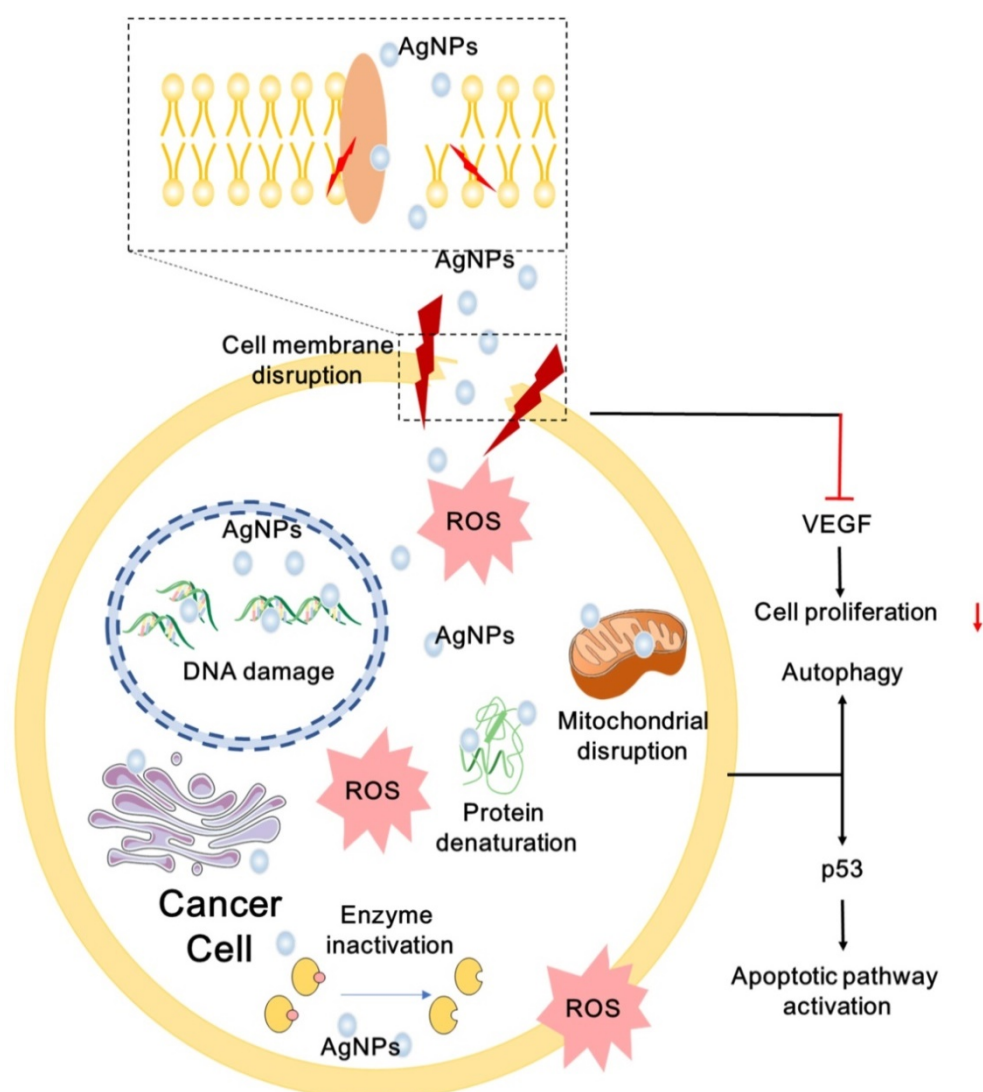


**Figure 4.** A schematic diagram of anticancer mechanisms of AgNPs. AgNPs can destroy the ultrastructure of cancer cell, induce ROS generation and DNA damage, promote apoptosis and autophagy by regulating multiple signaling pathways.

concentration-dependent manner, as well as the increased number of G0/G1 phase cells, which may be prone to apoptosis [244, 258, 261]. AgNPs can not only induce apoptosis through ROS-mediated DNA damage, but also destroy DNA structure directly via Ag<sup>0</sup> and Ag<sup>+</sup> released by AgNPs [157]. The DNA double helix structure is composed of four bases of adenine, guanine, cytosine and thymine by strictly complementary base pairing. Base pairs are bounded by hydrogen bonds to form a unit of DNA double helix. The destruction of hydrogen bonds decreases the stability of DNA structure. Tsuneo Ishida [157] analyzed the activities of AgNPs in the nucleus. Silver could form a complex containing silver within DNA. Ag<sup>+</sup> caused DNA damage by replacing the hydrogen bonds in the G≡C and A=T base pairs. The Ag atom was twofold coordinated by two N atoms to form N-Ag<sup>+</sup>-N complex in G≡C base pair, and other complex structures appearing in the base pair were O-Ag<sup>+</sup>-N (G≡C base pair), N-Ag<sup>+</sup>-O (both G≡C and A=T base pairs). DNA damage caused by these complexes might be a factor in triggering cancer cell apoptosis.

Generally speaking, AgNPs can exert anti-cancer effects through multiple pathways. Bandyopadhyay et al. [262] confirmed that AgNPs could exhibit antitumor properties through multiple channels, including triggering cell morphological changes, ROS generation, and nuclear fragmentation, while exhibited minimum toxicity in normal peripheral blood lymphocytes. The considerable anticancer activity and histocompatibility might relate to the types of reducing agent and stabilizer.

#### Inactivate Proteins and Regulate Signaling Pathways

In the development and progression of tumors, many signaling pathways are involved in controlling cell growth and proliferation, apoptosis and viability, and can participate in more complex signaling networks that contribute to tumor progression, such as tumor microenvironment (TME), angiogenesis and inflammation [263]. Some proteases and cytokines are also involved in these regulations, such as vascular endothelial growth factor (VEGF), matrix metalloproteinase (MMPs) and fibroblast growth factor 2 (FGF-2), etc. AgNPs have been confirmed to inhibit tumor proliferation, invasion and angiogenesis by regulating the associated signaling pathways or inactivating proteins. For example, AgNPs can regulate the HIF signaling pathway [161]. In general, rapid proliferation of tumor cells and irregular vasculature cause hypoxic TME [264-266]. HIF-1 level is up-regulated in hypoxic TME, followed by activation of target genes that in response to hypoxia. These genes contribute to cellular activities, such as

cell proliferation, angiogenesis, and eventually lead to failure of cancer treatment [161]. Therefore, HIF-1 is a potential target for cancer treatment. It has been demonstrated that hypoxia can weaken HIF-1 $\alpha$ -mediated autophagy [247]. Tieshan Yang et al. found that AgNPs could disrupt the HIF signaling pathway by attenuating HIF-1 protein accumulation and downstream target genes expression [161]. AgNPs can also inhibit the progression of tumors by inhibiting MMPs activity. MMPs are known as protein family and classified into different evolutionary groups according to their primary sequences [267]. MMPs play a dominant role in tumor progressions, such as tumor cell proliferation, invasiveness and distant metastasis, evasion of immune surveillance, and angiogenesis [267, 268]. Therefore, MMPs are considered as potential targets for cancer therapy [31]. In order to obtain antitumor drugs with targeting capabilities, some teams have attempted to develop inhibitors against members of MMPs.

Other signaling pathways and proteases involved in tumor progression have also been highlighted. Melissa M Kemp et al. [245] found that AgNPs could effectively inhibit FGF-2-induced angiogenesis. Their results suggested that AgNPs may have great potential for inhibiting pathological angiogenesis in cancer. Eom et al. [27] indicated that AgNPs induced cytotoxicity, including DNA damage, cell cycle arrest and apoptosis, by activating the p38 MAPK signaling cascades. These studies may inspire the development of anticancer agents containing AgNPs. In view of the complex signaling pathways and various proteins involved in the regulation of tumor development and progression, anticancer mechanisms of AgNPs by regulating intracellular signaling pathways and inactivating proteins still need to be further explored.

#### Inhibit Migration and Angiogenesis

Numerous studies have confirmed that AgNPs can inhibit migration and invasion of tumor cells in concentration- and dose-dependent manners [23, 30, 32, 269]. Migration and invasion are important hallmarks of cancer progression and deterioration [270]. Although it has been observed that AgNPs can inhibit tumor invasion [269], the specific mechanism is still unclear. It is hypothesized that AgNPs may decrease the protein expression of cytokines and growth factors within cancer cells, or reduce the enzymatic activity of MMPs. VEGF is an important signaling protein involved in vasculogenesis and angiogenesis, which plays a crucial role in tumor growth and metastasis [32]. Various studies support that AgNPs can deprive cancer cells of both nutrients

and oxygen via inhibiting angiogenesis. It has been demonstrated that AgNPs can inhibit VEGF-induced angiogenesis by inactivating PI3K/AKT pathway [271]. Besides, AgNPs can block VEGF-induced Akt phosphorylation, this may influence the proliferation and migration of cells [272]. Another study has proved that AgNPs can disrupt the HIF-1 signaling pathway, thus lead to inhibition of angiogenesis [161].

### Other Medical Applications

The special physicochemical properties of AgNPs make the nanoparticles and composites having considerable application prospects in the biomedical field. Besides the antimicrobial and anticancer applications mentioned above, AgNPs exhibit good properties in promoting wound repair and bone healing, as well as inhibition of inflammation. AgNPs can also be used as an additive in dental materials and adjuvant in vaccines.

### Wound Repair

The wound healing is closely related to the prognosis of surgical treatment. The rapid development of nanotechnology in recent years has provided a new therapeutic strategy for healing wounds, but the specific mechanisms of AgNPs on wound healing still need more exploration. Jun Tian et al. [288] found that AgNPs could increase wound healing rate with less hypertrophic scarring in the thermal injury model. Compared with the healing time of deep partial-thickness wounds treated with silver sulfadiazine, the AgNPs treated group could heal in a shorter period and a superior cosmetic appearance was observed, including nearly normal hair growth and less hypertrophic scarring. In the healing process, lower level of TGF- $\beta$  and increased level of interferon- $\gamma$  were detected at the same time in AgNPs treated group, while the former was related to keloids and hypertrophic scars, and the later was involved in the inhibition of fibroblast proliferation. In addition, higher level of VEGF mRNA detected in keratinocytes at the edge of the wound suggested that AgNPs might promote wound healing by inducing angiogenesis. These results indicated that AgNPs could participate in wound healing by regulating various cytokines and achieve cosmetic effects. Other mechanisms of AgNPs in wound repair are being explored. AgNPs can remain in the cytoplasm of fibroblasts in skin biopsies, and promote the reconstruction of dermis and epidermis [289]. Some studies prove that AgNPs can induce the proliferation and migration of keratinocytes, decrease the amounts of collagen and hydroxyproline, and promote the differentiation of fibroblasts into myofibroblasts, which may help wound early adhesion, contraction

and closure [290]. Besides, AgNPs can promote wound healing by regulating the production of cytokines or proteins, such as inflammatory cytokines, VEGF and MMPs [163, 291]. The above studies of AgNPs on wound repair broaden our understanding of the activity of AgNPs in cellular events. The role of AgNPs in wound repair is positive for clinical wound care and postoperative results.

### Bone Healing

Bone is an active tissue with regenerative and restorative capabilities. The self-repairing capability of bone is usually compromised when bacterial infection occurs in bone defects. Bone grafts are commonly implanted to replace or restore large defects that usually resulted from severe trauma, tumor resection or genetic malformation. Orthopedic infections are usually related to bone destruction and implant loose [292]. AgNPs can be used as doping materials for synthetic bone scaffolds. AgNPs-implanted crystallized hydroxyapatite (HA) or titanium scaffolds display strong antibacterial ability against both Gram-positive and Gram-negative bacterial strains [162]. AgNPs can promote fracture healing as an osteoconductive biomaterial. For example, AgNPs can naturally stimulate the osteogenic differentiation and matrix mineralization of MC3T3-1 cells [293]. In a mouse model, AgNPs has been proved to stimulate proliferation and osteogenic differentiation of mesenchymal stem cells (MSCs) *in vitro*, and promote the healing process of bone fracture [294].

### Dental Applications

Plaque biofilm formation is one of the causes of dental diseases. AgNPs have been incorporated into some dental biomaterials for reducing biofilm formation due to its antibacterial activity. Polymethyl methacrylate (PMMA), also known as acrylic resins, and composite resins are applied for the fabrication of dentures, but potential harmful organisms are likely to adhere to the rough surface of dentures [155]. AgNPs incorporated in PMMA can improve the antibacterial effect of dental material. It is proved that PMMA-AgNPs showed great anti-bacterial effect by continuous releasing of Ag<sup>+</sup> even in 28 days. It is highlighted that increased loading of AgNPs in PMMA also improved the mechanical properties [155]. While Acosta-Torres et al. demonstrated PMMA-AgNPs could efficiently decrease the adherence of *Candida albicans* and exhibit no obvious genotoxicity or cytotoxicity. Comparison study of the anti-bacterial and anti-biofilm efficacies of AgNPs capped with carboxymethyl cellulose and sodium alginate, respectively, showed that carboxymethyl cellulose-

capped AgNPs exhibited stronger inhibition to Gram-negative organisms, which were primarily responsible for periodontal infection [295].

### Vaccine Adjuvant

Vaccination is one of the most effective methods to prevent infectious diseases and manage healthcare costs [296]. Traditional vaccines have good immunogenicity due to the complex nature of the formulation and the presence of adjuvants. However, purified preparations lack immunogenicity, which makes the addition of adjuvants essential. Adjuvants can simultaneously reduce the amount of antigen required, shorten the time needed for a protective threshold of antibody production and improve the intensity of the elicited responses, stimulate long-term memory responses to reduce the requirement of repeated vaccinations. Yingying Xu et al. [297] firstly reported the remarkable immunological adjuvant effect of AgNPs both *in vitro* and *in vivo* using model antigens ovalbumin and bovine serum albumin in 2013. After intraperitoneal or subcutaneous immunization of mice, AgNPs increased the production of serum antigen-specific IgG, as well as antigen-specific IgE, indicating that AgNPs stimulated Th2-biased immune responses. Further study of the mechanism of adjuvant revealed that AgNPs could recruit and activate local leukocytes and macrophages. Vahid Asgary et al. [298] evaluated AgNPs as an adjuvant for the rabies vaccine in 2014 and 2016, respectively. They found that although the load of AgNPs could significantly increase the immune responses by arising neutralizing antibody against rabies virus in mice, the lowest concentration of virus-loaded AgNPs decreased cell viability. This limited the use of AgNPs as an adjuvant in rabies virus. They then challenged the green synthesis of AgNPs using leaf extract of *Eucalyptus procera* and added AgNPs as an adjuvant in rabies veterinary vaccine, following by estimating vaccine efficacy in mice and dogs. They confirmed that the vaccine loaded with a suitable concentration of AgNPs was nontoxic [299].

### Antidiabetic Agent

Diabetes mellitus (DM) is a group of metabolic diseases characterized by hyperglycemia. DM is due to either insufficient insulin secretion or insulin resistance of the cell. Commonly used hypoglycemic agents can lower blood sugar by promoting secretion of insulin or increasing cell sensitivity [300]. In recent studies, it is noticed that AgNPs synthesized by plant extracts exhibit antidiabetic potential. Arumugam et al. [301] synthesized AgNPs using leaf extract of *Solanum nigrum* and evaluated the anti-hyperglycemic

effect in alloxan-induced diabetic rats. They found that the blood glucose level of diabetic rats decreased when treated with AgNPs for 14 days and 21 days without significant acute toxicity. And they assessed glucose tolerance of AgNPs in diabetic rats. The results showed that AgNPs exhibited a good hypoglycemic effect compared to glibenclamide, a standard antidiabetic drug. Saratale et al. [4] demonstrated that AgNPs synthesized by leaf extract of *Argyrea nervosa* exhibited antidiabetic activity *via* inhibiting  $\alpha$ -amylase and  $\alpha$ -glucosidase. These two carbohydrate digestive enzymes contribute to decompose carbohydrates into monosaccharides. The antidiabetic mechanism of AgNPs is still unclear. Jihan Hussein et al. [302] hypothesized that AgNPs might influence insulin signaling pathway or insulin sensitivity in diabetic rats. The results supposed that AgNPs could activate protein kinase C and PI<sub>3</sub>K pathway at the insulin receptor substrate level, as well as inhibit protein kinase C isozymes, thus effectively enhance insulin secretion and sensitivity. It was highlighted that AgNPs were effective in reducing insulin resistance and DNA damage.

### Biosensing and Imaging

Surface-enhanced Raman scattering (SERS) has attracted the attention of noble metals with Raman signals in many application strategies, including biochemical sensing, analytical chemistry, and materials science [303]. Among these nanomaterials, AgNPs can be used as a cost-effective surface-enhanced Raman scattering substrate. Nanoparticles containing AgNPs can be used as biosensors to detect blood glucose, enzymes, molecular markers of tumor cells, pathogens, etc. For example, Jiang et al. [304] prepared silver-containing nanocomposites as acetylcholinesterase biosensors for electrochemical detection of organophosphorus pesticides. AgNPs improved the electrical conductivity and biocompatibility of nanocomposites and made them more suitable for enzyme activity and stability. Anderson et al. [305] prepared a high-sensitivity nonenzymatic biosensor for the detection of glucose using AgNPs as a conductive additive. Both the porous nanostructures of AgNPs and large surface areas of carriers enhanced the interaction sites between AgNPs and electrode/glucose, which could accelerate the electron transfer of AgNPs and therefore improve the sensitivity of the biosensor. Although the electrochemical characteristics and Raman scattering make AgNPs exhibit good application prospects in the field of biosensing, the matrix composition may affect their SERS and reduce the detection sensitivity. Therefore, it is necessary to modify AgNPs in order to improve the sensitivity of

re-creating platforms. For example, Zeng et al. [306] synthesized hybrid Ag@NGO nanoparticles by a one-step reduction method. Among these platforms, the nanosized graphene oxide (NGO) worked as inert protective layers and provided an ultrathin protective layer for AgNPs. Ag@NGO exhibited the advantages of both SERS biosensing and drug delivery, ie, monitoring biomolecule signals in tumor cells through SERS biosensing and interacting with the anticancer drug doxorubicin through formation of  $\pi$ - $\pi$  bonds. These results prove that AgNPs hold great application potential with capabilities of SERS biosensing.

Silver nanoclusters have unique optical and electrical properties and can be used as materials for synthetic probes. While proteins have multiple chelating and functional groups, therefore, they have unique advantages as ligands in biological imaging. Cunlan Guo and Joseph Irudayaraj [307] used denatured bovine serum albumin as a stabilizer to synthesize silver clusters, which could sensitively and selectively detect the content of mercury. The probe had important application value for detecting mercury content in water, soil and food. Sun et al. [308] used glutathione as a ligand to passivate silver nanoclusters and obtained highly sensitive fluorescent probes. During the passivation of glutathione, the specific recognition of silver nanoclusters modulated from  $Hg^{2+}$  to  $Cu^{2+}$ . This fluorescent probe was highly sensitive and selective in detecting  $Cu^{2+}$  in blood samples. The synthesis of silver nanoclusters with DNA as the backbone has excellent spectral and photophysical properties. The generation of this fluorophore is highly dependent on the DNA sequence. Oligonucleotide sequence changes may trigger the adjustment of the photoluminescence emission band, thus identifying the mutant nucleotide sequence. Guo et al. [309] designed a double-stranded DNA scaffold that hybridizes probe DNA strands and sickle cell anemia mutation target DNA to generate fluorescent silver nanoclusters. The fluorescent silver nanoclusters specifically recognized sickle cell anemia mutations. The research extended from DNA scaffold single-stranded oligonucleotide to hybrid DNA double-stranded mutation site recognition, which may have more applications in the field of biological analysis. These studies suggest that silver nanoclusters have great clinical application potential.

## Potential Toxicity of AgNPs

The potential harm of nanomaterials to organs and systems in the body has been gradually observed [310-312], which may influence the biomedical application of nanomaterial. Therefore, it is necessary

to review the dynamics of AgNPs *in vivo*. AgNPs can be taken and distributed to different organs through a variety of routes of administration, mainly include inhalation, ingestion, skin contact, and subcutaneous or intravenous injection (**Figure 5**). The absorbed AgNPs are distributed in many systems [310, 311], such as the dermis, respiratory, spleen, digestive, urinary, nervous, immune and reproductive system, and mainly distributed in the spleen, liver, kidney and lung, while little deposition of AgNPs is observed in teeth and bones. The small-sized AgNPs are easy to penetrate the body and cross biological barriers like the blood-brain barrier and the blood-testis barrier, and subsequently induce potential cytotoxicity. Besides the directly exposed tissues, AgNPs can also be transported to different organs via blood circulation. Therefore, the non-specific distribution of AgNPs may produce cytotoxicities such as dermal toxicity, ocular toxicity, respiratory toxicity, hepatobiliary toxicity, neurotoxicity and reproductive toxicity, which limit the applications of AgNPs. The potential cytotoxicity of AgNPs depends on the routes of administration and the properties or characteristics of the AgNPs, such as the size, shape, and concentration. At the cellular level, Wang et al. [313] used TEM and integrating synchrotron radiation-beam transmission X-ray microscopy (SR-TXM) with 3D tomographic imaging to capture the information of the cellular uptake, accumulation, degradation, chemical transformation, and removal of AgNPs. The experiment revealed that the cytotoxicity was caused by the chemical transformation of AgNPs, ie.  $Ag^0$  transformed into  $Ag^+$ ,  $Ag-O-$ , and  $Ag-S-$  species, which might induce the cellular biochemical changes. However, there is still inadequate acknowledge of the potential cytotoxicity, long-term adverse health effects, and the specific mechanisms of AgNPs accumulated in the different tissues and organs. In order to develop AgNPs with better biocompatibility for medical applications, it is urgent to systematically study their potential cytotoxicity. This chapter provides a brief overview of the potential toxicity and possible mechanisms of AgNPs in different organs, including skin, eye, kidney, respiratory system, hepatobiliary system, central nervous system, immune system and reproductive system (**Table 6**).

## Skin Toxicity

Even as early as in 1614, Angelo Sala reported the first case of a definitive diagnosis of argyria, a kind of disease induced by the deposition of silver in tissues [314]. Since the mid-19th century, it has been recognized that silver or silver compounds may induce some tissues to turn gray or blue-grey, especially involving the skin. The skin, as the largest

organ and the first-line barrier of the human body, can isolate the external pathogens from the internal environment. Topically applied AgNPs may induce cytotoxicity in the site and penetrate the skin and subsequently access the systemic circulation followed by adverse effects on other organs. For example, applying AgNPs gel and covering dressings will allow particles to penetrate and accumulate in the skin and produce potential cytotoxicity [315]. Before AgNPs, there are several reports on the skin toxicity of elemental silver, known as Argyria [316]. Argyria is a disease characterized by permanent gray-blue pigmentation of mucous membranes, eyes and skin, occurring in individuals exposed to high concentrations of silver for a long period. G D DiVincenzo et al. [317] previously reported that the skin of workers exposed to silver aerosols showed a distinctive gray bluish hue change, and deposited silver was also detected in worker's hair, urine and feces. Jennifer et al. [318] reported a Argyria case. The patient showed uniform accumulation of silver on the skin after long-term consumption of silver solution. Current studies show that AgNPs can enter the hair follicles to induce local deposition and deposit into the subcutaneous structure by penetration pathways. The follicular penetration pathway is most commonly used to explain the penetration of particles into the

skin [319-322]. Yu Kyung Tak et al. observed that AgNPs of different shapes would remain at different layers of skin. Rod-shaped, spherical, and triangular AgNPs penetrated the dermis, epidermis and stratum corneum layers, respectively. They observed the behavior of AgNPs in subcutaneous capillaries. And prolonged exposure time would increase the amount of nanoparticles. Notably, they found that the penetration of AgNPs was achieved by the follicular penetration pathway and intercellular penetration pathway [323]. Francesca et al. [324] attempted to use AgNPs to act on intact or damaged skin. They demonstrated a significantly higher penetration of AgNPs used on damaged skin as compared with intact skin, and they speculated that a small part of the particles would diffuse into the skin as silver ions. Radoslaw et al. [325] explored the cytotoxicity of AgNPs on epidermal keratinocytes (NHEK). The results showed that AgNPs inhibited cell proliferation and migration, induced activation of caspase 3 and caspase 7, and damaged DNA. In addition, by measuring the ATP content of cells treated with different concentrations (6.25, 12.5, 25 and 50  $\mu\text{g}/\text{ml}$ ), it was found that a high concentration of AgNPs significantly decreased the ATP production, and this phenomenon worsened with prolonging exposure time.

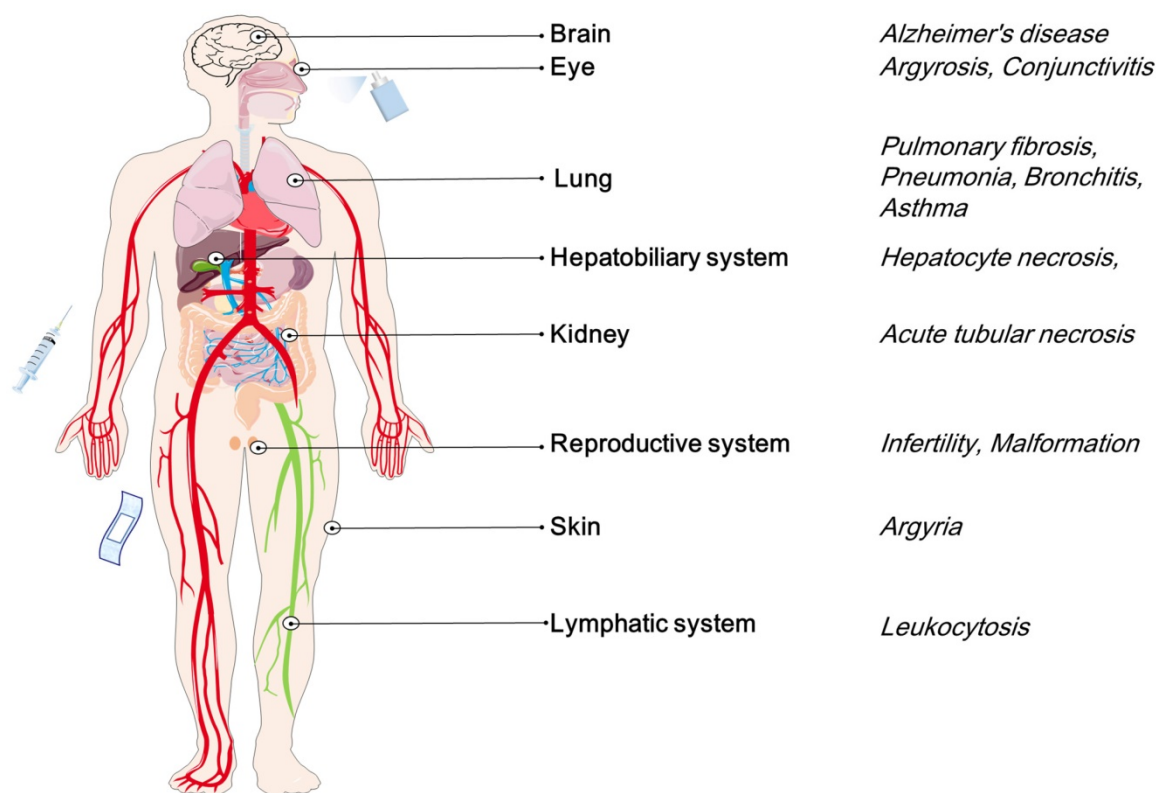


**Figure 5.** A schematic of potential toxicities of AgNPs in the human body. The exposure patterns of AgNPs include respiratory inhalation, intravenous injection and skin contact. Affected organs include the eye, kidney, skin, and nerves, respiratory, immune, hepatobiliary and reproductive systems. Diseases or pathologic changes induced by AgNPs are listed.

**Table 6.** Potential toxicity of AgNPs *in vivo* and *in vitro*

Objects		Exposure		Toxicity			References		
Animal model	<i>In vitro/ in vivo</i>	Cell lines/Tissues	Size; Shape	Dosages	Route	Time	Effect	Toxicity manners	
Pig	<i>In vitro and in vivo</i>	HEKs and porcine skin	20, 50 and 80 nm	0.34, 1.7 µg/mL	Incubation; skin contact	Acute: 18 and 24 h; chronic: 14 d	Focal inflammation	Dose-dependent	[350]
Mice	<i>In vivo</i>	Liver	Less than 30 nm	10 ppm	Skin contact	2, 7 and 14 d	Central venous dilation; hyperemia, cell swelling, Kupffer and inflammatory cells increase	Time-dependent	[332]
Mice	<i>In vivo</i>	Spleen, liver, lung and kidney	12–20 nm	7.5, 30 and 120 mg/kg	Intravenous administration	7 and 14 d	Induction of inflammatory reactions in lung and liver cells	Gender-, concentration- and time-dependent	[346]
Mice	<i>In vivo</i>	Lung	10–20 nm; spherical	10, 100, 1000 and 10,000 ppm	Intratracheally administration	1, 3, 7 and 15 d	Acute lung inflammation and bronchitis; hyperplasia of alveolar epithelial cells	Dose-dependent	[330]
Mice	<i>In vivo</i>	Liver, spleen, kidneys, heart, lungs, testes, stomach, intestine and seminal vesicles	3±1.57 nm; spherical	11.4–13.3 mg/kg	Intravenous injection	1, 28 d	Inflammatory response; alteration of hematological factors; change of gene expression; ROS generation	Dose-dependent	[351]
Mice	<i>In vivo</i>	Liver, kidneys and lung	10, 75 and 110 nm; spherical	25 µg/mice	Intravenous administration	1, 3 and 7 d	Peripheral inflammation in liver, kidneys and lungs	Time-, concentration- and size-dependent	[343]
Mice	<i>In vivo</i>	Lung	20 and 110 nm	0.05, 0.15, 0.45 and 1.35 mg/kg	Intratracheal instillation	1, 7 and 21 d	Alter SP-D level; deficit immune defense function	Size- and stabilization-dependent	[44]
Mice	<i>In vivo</i>	Brain, lung, liver, kidney and testis	22, 42 and 71 nm	0.25 mg/kg, 0.50 mg/kg, 1.00 mg/kg	Oral administration	14 and 28 d	Induce organ toxicity and inflammatory responses	Dose-dependent	[352]
Mice	<i>In vivo</i>	heart, lung, kidney, liver and blood	1.4–250nm	11.4–13.3mg/kg body weight	Intravenous administration	28 d	Induce gene expression; ROS generation; apoptosis	Dose-dependent	[351]
Mice	<i>In vitro and in vivo</i>	A549, BxPC-3; PC-3; Hep G2, CNE; AsPC-1; U-87 MG; SW480; EC109; MDA-MB-231; VSMC; HMEC; LO2; 293FT; tumor, brain, heart, kidney, lung, spleen, and liver	19.2±3.8 Ång, spherical or ellipsoidal	0–32ng/µl, 1.875 mg/kg	Intravenous administration	Acute: 24 h; chronic: 28 d	None	Dose- and time-dependent	[21]
Mice	<i>in vivo</i>	Lung	20 and 110 nm, spherical	0.1, 0.5 and 1.0 mg/kg	Inhalation	Acute: 40 h; chronic: 21 d	Pulmonary fibrosis	Size- and coating-dependent	[353]
Mice	<i>in vivo</i>	Kidney, liver and spleen	2.45–19.53 nm	0.37, 0.65, 13 and 21 mg/kg	Oral administration	27 d	Tissue destruction; cell necrosis and apoptosis	dose-dependent	[354]
Rat	<i>In vivo</i>	Brain	>100 nm	5 and 50 mg/kg	Oral administration	79 d	Cell death, disturbed neurotransmitter and cytokine production, ROS generation	--	[355]
Rat	<i>In vivo</i>	Sperm and testicular tissue	60–80 nm	30, 125 and 300 mg/kg	Intraperitoneal injection	28 d	Decrease normal sperm morphology, sperm vitality and sperm count	Dose-dependent	[348]
Rat	<i>In vivo</i>	Kidneys, liver and blood	20–65 nm	2,000 mg/kg	Intraperitoneal administration	3 d	Liver and kidney damage	Time- and dose-dependent	[356]
Rat	<i>In vivo</i>	Lung, spleen, liver, kidney, thymus and heart	6.3–629 nm	0.5 mg/kg	Intravenous administration	24 h	Liver and kidney damage; chromosome breakage; genotoxicity	Dose-dependent	[357]
Rat	<i>In vivo</i>	Epididymal sperm	20–30 nm	50, 100 and 200 mg/kg	Oral administration	90 d	Sperm anomalies; decrease sperm viability	Dose-dependent	[37]
Rat	<i>In vivo</i>	Brain	3–10 nm, spherical	1 and 10 mg/kg	Intragastric administration	14 d	Neuron shrinkage; cytoplasmic or foot swelling of astrocytes	Dose-dependent	[38]
Rats	<i>In vivo</i>	Kidney, liver and blood	20–60 nm, spherical	2,000 mg/kg bw, twice injections	Intraperitoneal injection	5 d	Liver and kidney damage; blood parameters disrupt	Dose- and time-dependent	[356]
Rat	<i>In vivo</i>	Spleen, liver, and lymph nodes and blood	20 nm and 100 nm	6 mg/kg	Intravenous administration	28 d	Suppression of the natural killer cell activity; stimulate LPS mitogen; increase cytokine production	Dose-dependent	[358]
Rat	<i>In vivo</i>	Liver and kidney	56 nm	30, 125 and 500 mg/kg	Oral administration	90 d	Liver damage; bile-duct hyperplasia	Dose- and gender-dependent	[341]

Objects			Exposure		Toxicity			References	
Animal model	<i>In vitro</i> / <i>in vivo</i>	Cell lines/Tissues	Size; Shape	Dosages	Route	Time	Effect	Toxicity manners	
Rat	<i>In vivo</i>	Kidney	52.7–70.9 nm	10 ml/kg	Oral administration	90 d	Deposite in kidneys	Dose-dependent	[340]
Female ICR mice; male guinea pigs	<i>In vivo</i>	Oral, skin and eye	10–20 nm, spherical	5,000 mg/kg (oral); 50 and 5,000 ppm (eye); 50 and 100,000 ppm (skin)	Oral administration; eye drops; skin contact	1, 2 and 3 day	Conjunctivae irritation	–	[326]
Male ICR mice	<i>In vivo</i>	Blood, liver, spleen, kidney, lungs and brain	10, 40 and 100 nm, spherical	10 mg/kg	Intravenous injection	24 h	Bleeding or necrosis of multiple internal organs	Size- and tissue-dependent	[331]
BN and SD rats	<i>In vivo</i>	Lung	20, 110 nm, spherical	0.1 mg/kg or 90 breaths/minute	Intratracheal administration	1, 7 and 21 d	Lung eosinophilia and bronchial hyperresponsiveness; destruction of blood/alveolar epithelial permeability barrier	Dose- and size-dependent; rat strains related	[46]
Mice and guinea pigs	<i>in vivo</i>	Lung, lymph node, heart, liver and kidney	10–20 nm, spherical	5,000 mg/kg, 5000 ppm	Oral administration, eye and skin contact	14 d	No mortality and toxic signs	–	[326]
Freshwater fish	<i>In vivo</i>	Embryo	25.9–36.7 nm, spherical	Acute: 0.3, 0.6, 1.2, 2.4 and 4.8 mg/L; subchronic: 0.05, 0.1, 0.25 and 0.5 mg/L	Incubation	14 d	Liver damage; deplete glutathione; deactivate lactate dehydrogenase and antioxidant enzymes	Time- and dose-dependent	[39]
Japanese medaka	<i>in vivo</i>	Embryo	20–37 nm, spherical	0, 0.5, 1.0, 2.0, 4.0 and 8.0 mg/L	Oral administration	48 h	death	dose-dependent	[327]
Zebrafish	<i>In vivo</i>	Embryo	20 and 110 nm, spherical	0.08, 0.4, 2, 1,0 and 50 mg/L	Hatch	5 d	Multiple developmental abnormalities	Size- and surface coating-dependent	[359]
Zebrafish	<i>In vitro</i> and <i>in vivo</i>	Brain, heart, yolk and blood of embryo	5–20 nm	5, 10, 25, 50 and 100 µg/mL	Hatch	24, 48 and 72 h	Multiple developmental abnormalities	Concentration-dependent	[43]
<i>Drosophila melanogaster</i>	<i>in vivo</i>	Parents, egg and offspring	2–20 nm	10, 20, 30, 40, 50 and 100 mg/L	Oral administration	5,10, 15, 30, 45, 60 and 95 min	Abdominal pigmentation	Dose-dependent	[360]
<i>Drosophila melanogaster</i>	<i>In vivo</i>	Germline stem cell; testis	20 nm	2, 3.5 and 5 mg/L	Oral administration	24h, 5 d	Delay the development of the F1 offsprings; ROS generation; premature GSC differentiation	Dose-dependent	[42]
<i>Caenorhabditis elegans</i>	<i>In vivo</i>	The worms' body	96.4±35.6 nm, spherical	0–1mg/L	Culture	6 and 24 h	DNA damage, ROS generation, inhibition of growth	Dose- and time-dependent	[361]
<i>Caenorhabditis elegans</i>	<i>In vitro</i>	The worms' body	< 100 nm, spherical	0.025, 0.05 and 0.075 µg/mL	Culture	24 h	ROS generation; DNA damage	Size-dependent	[152]
–	<i>In vitro</i>	rat brain microvascular endothelial cells, pericytes, and astrocytes	7±2 nm	1 and 10 µg/mL	Incubation	24 h	Trx system, Nr4a1 and Dusp1 regulaion , inflammation and apoptosis	Dose-dependent	[338]
–	<i>In vitro</i>	Mouse ESCs	20.2 ±4.1 nm, spherical	5.0 µg/ml	–	24 h	Heat shock protein and the metallothionein families regulation, induce oxidative stress and apoptosis	Dose-dependent	[362]
–	<i>In vitro</i>	Mouse microglia N9 cell line, N27 neuronal cells	49.7±10.5 nm, spherical	50 µg/mL	Incubation	24 h	Nitric oxide and TNFα production	Dose-dependent	[363]
–	<i>In vitro</i>	Mouse lymphoma cell line, human lymphoblastoid cells	20, 50 and 100 nm, spherical	0–400 µg/mL	Incubation	4, 8, and 24 h	DNA mutants	Size-, concentration- and coating-dependent	[47]
–	<i>In vitro</i>	Rat primary cerebral astrocytes	24.18±4.14 nm, spherical	0.01, 0.1, 1 and 10 mg/mL	Incubation	24 h	Neuroinflammation and apoptosis; increase caspase activities	Dose-dependent	[337]
–	<i>In vitro</i>	Primary astrocyte cell, rat glioma C6 cell line	6.9–8.7 nm, spherical	0.1, 1, 10, 50, 75 and 100 µg/mL	Incubation	24 h	Necrosis and apoptosis	Dose-dependent	[364]
–	<i>In vitro</i>	Murine brain ALT astrocytes, murine microglial BV-2 cells and mouse neuroblastoma Neuro-2a (N2a) cells	3–5 nm	0.5, 1, 5, 10 and 12.5µg/mL	Incubation	24 h	Cytokine secretion, Aβ amyloid deposition, inflammatory response	Dose-dependent	[339]
–	<i>In vitro</i>	UMR-106	6 nm, cubic	10, 25, 50, 100, 150 and 225 µM	Incubation	24h	Decrease lysosomal and mitochondrial activity	Dose-dependent	[365]
–	<i>In vitro</i>	U937 cell	4,20 and 70 nm, round	1.56, 3.12, 6.25, 12.5, 25 and 50 µg/mL	Incubation	24 h	Oxidative stress; cytokines release	Size-dependent	[50]
–	<i>In vitro</i>	HepG2 cell line	20 nm	2.5 to 50 µg/cm <sup>3</sup>	Incubation	24 h	Endogenous antioxidant defence regulation	Dose-dependent	[366]

Objects		Exposure		Toxicity			References		
Animal model	<i>In vitro</i> / <i>vivo</i>	Cell lines/Tissues	Size; Shape	Dosages	Route	Time	Effect	Toxicity manners	
–	<i>In vitro</i>	Jurkat T, NCI-H460, HeLa cells, HepG2, MCF-7, Beas-2B	5–10 nm	0.2, 0.5 and 1 mg/L	Incubation	4, 12 and 24 h	DNA damage; p38 MAPK activation; cell arrest; apoptosis	Time- and concentration-dependent	[27]
–	<i>In vivo</i>	Human lymphocytes and sperms	8–10 nm	Density gradient: 1:9, 1:3, 1:1	–	30 and 60 mins	Cell viability decrease	Concentration- and time-dependent	[367]
–	<i>In vitro</i>	Pk15	61.2±33.9 nm, nonuniform	50 mg/L	Incubation	24 and 48 h	Genotoxicity in Pk15 cells	Dose-dependent	[342]
–	<i>In vitro</i>	Zebrafish ovarian follicle cells	30–55 nm	30 µg/mL	Incubation	2 h	Apoptosis of ovarian follicle cells; germinal vesicle breakdown	Concentration-dependent	[349]

\*NOTE: UMR 106, rat osteosarcoma cells; MDA-MB-231, triple negative breast cancer cell line; PMBC, peripheral blood mononuclear cell; HepG2, human liver cancer cell line; Jurkat T, human T lymphocyte cell line; NCI-H460, human lung cancer cell line; MCF-7, human breast cancer cell line; Beas-2B, human bronchial epithelial cells; SPD, surfactant protein-D; U937, human histiocytic lymphoma cell line; Pk15, pig kidney cell line; BV-2, murine microglial cell line; N2a cells, mouse neuroblastoma; HEKs, human embryonic kidney cells; A549, human lung carcinoma; BxPC-3, human pancreas adenocarcinoma cells; PC3, prostate adenocarcinoma cells; HepG2, hepatocellular carcinoma cells; ESCs, embryonic stem cell; CNE, nasopharyngeal carcinoma cells; AsPC-1, pancreas adenocarcinoma cells; U-87 MG, glioblastoma cells; SW480, colorectal adenocarcinoma cells; EC109, esophageal cancer cells; VSMC, vascular smooth muscle cells; HMEC, human microvascular endothelial cells; LO2, hepatocytes; 293FT, embryonic kidney cells.

## Eye Toxicity

AgNPs agent may cause concentration-dependent acute conjunctival irritation, but there is still no reliable evidence for toxicological effects. Pattwat et al. [326] dripped 50 ppm and 2,5000 ppm colloidal AgNPs into the eyes of guinea pig and explored whether there were acute eye irritation or corrosion throughout the 78 hours observation period. Although transient mild conjunctival irritation, i.e. blood vessel hyperemia in conjunctivae, was observed within 24 hours after 5000 ppm AgNPs treatment, neither low-dose nor high-dose colloidal AgNPs caused any acute toxicological effects in guinea pigs. AgNPs may have developmental toxicity in the eyes of early-stage individuals, which can eventually result in multiple types of eye defects. Yuan Wu et al. [327] studied the developmental toxicity of AgNPs by using Japanese medaka at early-life stages as experimental models, including embryonic, larval and juvenile stages. The Japanese medaka was exposed to 100–1000 mg/mL AgNPs for 70 days and various morphological malformations were described and analyzed, such as edema, visceral deformities, heart malformations, spinal abnormality, especially eye defects. AgNPs-treated group showed different eye defects, such as microphthalmia, exophthalmia, cyclopia and anophthalmia. Histopathological examinations of 2-day-old larvae showed increased thickness of retinal pigment epithelium and missing of the retina in inner segments. Interestingly, comparing with the high-dose groups, the types and numbers of eye malformations in the low-dose groups were significantly higher. These morphological abnormalities and non-linear dose-response pattern suggest that the developmental toxicity of AgNPs may exhibit complex toxicological mechanisms.

## Respiratory toxicity

AgNPs can induce acute lung toxicity and therefore impair lung function, and the damage severity is related to particle accumulation and clearance. Akinori [328] et al. studied the pulmonary toxicity of nanometer particles in mouse models. Ultrafine particles may pass the air-blood barrier through the gap between alveolar epithelial cells, induce vacuolation and necrosis of bronchiolar epithelial cells, resulting in transient acute lung inflammation and tissue damage. The oxidative stress and apoptosis induced by ultrafine particles may contribute to lung damage. In addition, nanoparticles showed size-dependent pulmonary toxicity, i.e. the particles in smaller size exhibit higher capacity for inducing lung inflammation and tissue damage than larger size [36, 329]. On the other hand, AgNPs may induce dose-dependent lung toxicity. Kaewamatawong et al. [330] demonstrated dose-dependent acute lung toxicity in mice induced by AgNPs using a single intratracheal instillation of 0, 10, 100, 1000 or 10000 ppm of colloidal AgNPs. And they observed moderate to severe bronchitis and multifocal alveolitis in 100, 1000 and 10,000 ppm AgNPs treated groups. Proinflammatory cytokines such as IL-1 $\beta$  and TNF- $\alpha$  released by alveolar macrophages and airway epithelial cells might involve in the inflammatory lesions in mice. The aggregation of AgNPs had a direct effect on the basement membrane, and disrupted equilibrium between the synthesis and degradation of the extracellular matrix, thus may cause pulmonary fibrosis. Similarly, they also speculated that AgNPs induced oxidative stress in the lung. Furthermore, they recognized that metallothionein (MT) expression induced by AgNPs might be regarded as one of the possible protective mechanisms of lung. Different concentrations of AgNPs, which induce lung damage,

may also accumulate in peripheral organs and cause potential health risks. Joanna et al. [46] found that AgNPs disrupted the blood/alveolar epithelial permeability barrier, elicited oxidative stress, activated eosinophils and promoted the release of multiple cytokines. Most importantly, their results showed that AgNPs induced eosinophilic and neutrophilic inflammation, which was an important pathological change in asthma. This might suggest that exposure to AgNPs could trigger asthma.

### Hepatobiliary System Toxicity

Part of the ingested nanoparticles tend to be sequestered, degraded and accumulated in the liver, which means the liver may be responsible for the metabolism of nanoparticles as well as one of the most frequently attacked organs. On the other hand, the gallbladder collects, stores and excretes bile or biological waste to the intestine. Various metal nanoparticles, including AgNPs, are recognized to be exported from the liver through this pathway. Therefore, hepatocytes are widely studied in the liver toxicity of AgNPs. Maglie et al. [48] found that AgNPs induced severe hepatobiliary damage in mice, including significant hepatocyte necrosis and gallbladder hemorrhage. In this study, AgNPs exhibited size- and dose-dependent hepatobiliary toxicity, i.e. AgNPs in smaller size produced more serious toxic effects, and higher dose of AgNPs induced severer hepatobiliary damages. Camilla et al. [331] observed multi-system acute toxicities in mice with a single intravenous injection of AgNPs. First of all, significant hepatobiliary damages were recognized, including hepatocyte necrosis, micro-hemorrhage around the biliary tract, and portal vein injury. Secondly, they also observed that AgNPs could induce acute tubular necrosis and apoptosis, and moderate splenomegaly. The results of Mohammad et al. [332] showed that AgNPs penetrating via the skin induced time-dependent liver damage such as hyperemia, dilatation in central venous, swelling hepatocytes and increased inflammatory cells. Besides hepatocytes, Kupffer cells (KCs) are also responsible for the removal of AgNPs [333]. KCs are macrophages that reside in the hepatic sinusoids and have the active ability of phagocytosis, maintaining the normal immune response and removing nanoparticles from organisms [333, 334]. Therefore, KCs become the focus of research on liver toxicity and metabolism of AgNPs.

### Central Nervous System Toxicity

The central nervous system consists of two parts: the brain and the spinal cord. Lots of supporting non-nervous cells, i.e. neuroglial cells fill the

interneuronal space within the central nervous system. In recent years, some articles point out that AgNPs may penetrate the brain and subsequently induce neuronal death. Due to the limited self-repairing ability of nerve cells, the potential neurotoxicity of AgNPs is receiving more attention. Different exposure patterns can lead to the accumulation of AgNPs in the brain. Injected AgNPs cross blood-brain barrier (BBB) and then penetrate the brain, while inhaled AgNPs reach the central nervous system through the olfactory and/or BBB [335, 336]. Due to the unique physicochemical properties of AgNPs, deposited AgNPs in nerve cells, astrocytes and extravascular lymphocytes may cause and aggravate neurotoxicity and inflammation, and increase the permeability of BBB. In the study of the cytotoxicity of AgNPs on rat cerebral astrocytes, Cheng et al. [337] investigated the neurotoxicological effects of AgNPs and Ag<sup>+</sup> and compared the mechanisms. Both AgNPs and Ag<sup>+</sup> exposure could internalize silver in astrocytes in dose- and time-dependent manners. The AgNPs had higher bioaccumulation ability than Ag<sup>+</sup> after 24 h treatment. After the same treatment time, they found that AgNPs might induce intracellular ROS generation in rat cerebral astrocytes and caused cell apoptosis, however, there were undetectable alterations in Ag<sup>+</sup> group. More importantly, they confirmed that AgNPs could increase the level of phosphorylated JNK, a kind of kinase involved in mediating apoptosis. The non-cytotoxic dose of AgNPs, rather than Ag<sup>+</sup>, might induce neuroinflammation by promoting the secretion of multiple cytokines of astrocytes, including CINC-2a/b, CINC-3, IL-10, IP-10, L-selectin and thymus chemokine. Liming et al. [38] investigated the neurotoxicity of AgNPs in the rat after intragastric administration of low-dose (1 mg/kg, body weight) or high-dose (10 mg/kg, body weight) for two weeks. They observed a variety of cell morphological changes in the nervous system, including neuron shrinkage, astrocytes swelling and extravascular lymphocytes. They also observed significantly increased inflammatory factors such as IL-4 in the serum. These data supported the proinflammatory effects of AgNPs in the nervous system. Then they focused on the possible mechanisms for AgNPs or Ag<sup>+</sup> transporting across the blood-brain barrier. AgNPs or released Ag<sup>+</sup> might cross through the blood-brain barrier via ionic pores or channels and subsequently damage the nerve cells. Besides, AgNPs could enter the central nervous system via vesicular transport of endothelial cells and subsequently induced neuroinflammation. At the same time, they demonstrated the increased permeability of the blood-brain barrier in a rat model after AgNPs treatment. They also observed that

AgNPs might inhibit the antioxidant defense of astrocytes by increasing thioredoxin interacting protein, thus lead to the central neurotoxicity. AgNPs might induce ROS, inflammation and apoptosis through regulating the MAPK pathway, mTOR activity and Bcl-2 expression in astrocytes. AgNPs could cause severe ultrastructural changes in astrocytes, including mitochondrial contraction, endoplasmic reticulum expansion and nuclear atypia. Furthermore, AgNPs regulated the expression of multiple genes, inhibited metabolic and biosynthetic processes, thus affect astrocytes function and increase the neurotoxicity. More importantly, the impairing of learning, memory and cognition processes by AgNPs reduced the learning ability and cognition function of rats [338]. AgNPs may induce neurological diseases such as Alzheimer's disease by altering gene expression. Chin et al. [339] reported that AgNPs could induce the expression of amyloid precursor protein (APP) gene in nerve cells. APP gene promoted the deposition of amyloid- $\beta$  (A $\beta$ ) protein, a key pathological feature of Alzheimer's disease.

### Kidney Toxicity

The kidney participates in balancing body fluid volume and pH, regulating osmotic pressure and electrolyte concentration, drug metabolism, and toxic emissions. Abnormal renal function may occur in AgNPs-treated mammalian kidneys. AgNPs exhibits a dose-dependent accumulation in most examined tissues, such as the brain, lung, liver, dermis, blood and testes. However, there is a gender-related difference in silver accumulation in the kidney. Wan et al. [340] observed that female rats treated with AgNPs had a twofold higher concentration of silver in kidneys than male rats. Ag enhancement staining of the kidneys showed that AgNPs preferentially accumulated in the basement membrane of the glomerulus as well as renal tubules, while mildly accumulated in the adrenal capsule and cortex. There were two possible mechanisms of gender difference in the accumulation of AgNPs: the gender difference in the expression of organic cation transporters, and hormonal regulation. Renal metallothionein and zinc-binding protein, a kind of transporter or binding protein molecules in the kidney, might contribute to the silver accumulation. While organic anions secreted by kidneys might influence the clearance and accumulation of silver [341]. Mirta et al. [342] studied the uptake mechanism and potential cytotoxicity of AgNPs in porcine kidney (Pk15) cells *in vitro*. TEM results showed that there were aggregates in the lysosome and early endosomes. In addition to micropinocytosis, as an uptake pattern, clathrin- and caveolin-mediated endocytosis could also be the

possible endocytotic mechanisms. AgNPs could decrease the number of viable Pk15 cells *in vitro* in a dose-dependent manner. Hua et al. [343] studied the distribution, accumulation and potential toxicity of AgNPs in different sizes in liver, lung and kidney of mice. They found that AgNPs could be taken up by vascular endothelial cells, then induced the generation of intracellular ROS and down-regulated the expression of vein endothelial cadherin. Therefore, AgNPs destroyed the conjunction between endothelial cells, allowing AgNPs to cross the endothelial layer and accumulate in organs. Besides, the leaking AgNPs could also result in peripheral inflammation in a size-dependent manner. Mice receiving single or multiple intravenous injections of AgNPs showed basement membrane injury in glomeruli.

### Immune System Toxicity

Our immune system, a natural host defense barrier, is composed of immune cells, tissues and organs, can constantly interact with the internal environment and protect us from pathogens in the external environment, and provide the inherent knowledge to separate the friend and foe within our body [344]. Seung et al. [345] found that AgNPs inhibited the proliferation and the production of cytokines, including IL-5, INF- $\gamma$  and TNF- $\alpha$ , and induced cytotoxicity in peripheral blood mononuclear cells in a concentration-dependent manner. AgNPs may deposit in the immune organs and influence the number of immune cells and the production of cytokines. Wim et al. [45] investigated the effects of AgNPs on the immune system of rats by repeated intravenous administration of AgNPs with different sizes (20 nm and 100 nm) for 28 days. They found that AgNPs administered at the maximum dose (6 mg/kg) were still well tolerated by the rats. The size and weight of the spleen increased significantly, possibly due to the increased cell number of T cells and B cells. However, the cytotoxic activity of NK cells in the spleen was almost completely inhibited. For multiple immune-related cytokines in serum, levels of interferon- $\gamma$ , IL-10, IL-6 and TNF- $\alpha$  declined, while levels of IL-1 $\beta$ , IgM and IgE increased. The number of neutrophilic granulocytes in peripheral blood also increased. Besides, brown and black pigments were observed in histopathological sections of spleen and lymph nodes, indicating the accumulation of AgNPs in these immune organs. This study suggested that the immune system was sensitive to the potential adverse effects of AgNPs. The spleen may be one of the main organs for the accumulation and elimination of AgNPs, and both processes are in a sex-dependent manner. Yuying et al. [346] observed the potential

acute toxicity and biokinetics after repeated intravenous administration of AgNPs in mice. During the 14-day observation period, both the survival and behavior of the mice were normal. They found that AgNPs were widely distributed in tissues, especially in the spleen, followed by the liver. The biokinetics of AgNPs in the kidney and lung seem to show gender-related differences, i.e. the accumulation of silver in kidney and lung of female mice was higher than that of male mice, the longer elimination half-life and slower clearance of AgNPs in female mice than male mice. Besides, the KCs in the liver were mainly responsible for the retention and elimination of AgNPs. The silver content in the liver significantly decreased after one day. While in the spleen, the marginal zone and the red pulp macrophages contributed to the clearance of silver.

### Reproductive System Toxicity

Biological barriers, such as the blood-testis barrier, placental barrier and epithelial barrier, can protect the reproductive system from infection and toxicity. AgNPs can cross the biological barriers to deposit in reproductive organs including testis, epididymis, ovary and uterus. Thus, AgNPs may damage germ cells and related cells, such as primary and secondary follicles, germline stem cells, Sertoli cells and Leydig cells [42, 347]. Besides, AgNPs can also cause changes in sexual behavior by affecting the secretion of hormones within the reproductive organs and glands. Further studies confirmed that the reproductive toxicities of AgNPs are achieved by increasing inflammation, disrupting DNA structure, down-regulating gene expression, decreasing mitochondrial function, inducing ROS production and apoptosis. These toxicities of AgNPs to the reproductive system are size-, time- and dose-dependent [347, 348]. Zhang et al. [347] investigated the effects of AgNPs with different sizes (10 nm and 20 nm) on male somatic Leydig cells and Sertoli cells, and found that cell viability was inhibited by AgNPs in size- and concentration-dependent manners. The 10 nm AgNPs showed more cytotoxicity than the 20 nm AgNPs, and cell proliferation was significantly decreased as the concentration of AgNPs increased from 0 to 100  $\mu\text{g}/\text{ml}$ . AgNPs-treated Sertoli cells showed decreased mRNA levels of ZO-1 and Cx43, both are involved in encoding tight junction proteins which playing a crucial role in the formation of BTB. As well as AgNPs-treated somatic Leydig cells showed decreased mRNA levels of StAR,  $3\beta\text{-HSD}$  and  $17\beta\text{-HSD}$ , which are involved in the production of testosterone. It is widely acknowledged that spermatogonial stem cells (SSCs) can continuously proliferate, renew and produce sperms throughout

male's postnatal life. Cytokines secreted by Sertoli cells play an important role in the proliferation and renewal of SSCs. In this study, AgNPs-treated Leydig cells secreted decreased level of testosterone, which was responsible for inducing spermatogenesis and maintaining normal functions of Sertoli cells. These results suggest that AgNPs can impair the function of Leydig cells and Sertoli cells, then worsen the function of SSCs, ultimately suppress male fertility. Cynthia et al. [42] evaluated the fecundity and development of *Drosophila* fed with AgNPs at various concentrations from 0 to 5  $\mu\text{g}/\text{mL}$ . AgNPs decreased the viability and delayed the development of *Drosophila* in a dose-dependent manner. Germline stem cells (GSCs) and early germ cells were concentrated at the apical tip of the testis. Among different treated groups, a significantly increased ROS level was observed at this tip area of *Drosophila* treated with 5  $\mu\text{g}/\text{mL}$  AgNPs. They also proved that AgNPs might disrupt GSCs maintenance by triggering precocious differentiation of GSCs, thereby decreased the number of sperms. Besides, the first generation of *Drosophila* fed with a higher concentration of AgNPs showed delayed eclosion and decreased male offsprings as compared to control or lower concentration group. The mating success of *Drosophila* and the number of their second or third generations decreased in AgNPs-treated groups than the control group. This might suggest that AgNPs accumulated in GSCs could be passed onto offspring and affect the development and fecundity of the offspring. Lafuente et al. [37] studied parameters of epididymal sperm of rat fed with different doses of PVP-AgNPs (50, 100 and 200  $\text{mg}/\text{kg}/\text{day}$ ), including sperm morphology, motility and viability. PVP-AgNPs induced sperm morphology abnormalities in a dose-dependent manner. In their study, 100  $\text{mg}/\text{kg}/\text{day}$  of PVP-AgNPs significantly increased abnormal morphologies in epididymal sperms, such as banana head, tail bending, head loss and neck abnormalities. Abnormal sperm morphology reduced sperm motility and vitality. Some studies focus on the effects of AgNPs on female reproduction. Chen et al. [349] evaluated the potential toxicity of AgNPs and  $\text{Ag}^+$  on zebrafish oocytes. Vacuolation or swollen mitochondria, and condensed nucleus were observed in AgNPs- and  $\text{Ag}^+$ -treated follicular cells. Zebrafish oocytes treated with AgNPs or  $\text{Ag}^+$  showed a decreased concentration of cAMP, which plays a key role in the maintenance of meiosis arrest, and results in meiosis resumption and subsequent oocyte maturation. Besides, AgNPs and  $\text{Ag}^+$  up-regulated caspase 3 and caspase 9, respectively, both of which play important roles in the initiation and execution of apoptosis, ultimately leading to apoptosis in ovarian

follicle cells.

## Conclusion and prospect

Over decades, AgNPs have been studied rapidly and extensively due to the unique physical, chemical, optical, electronic and catalytic properties. These properties are closely related to characteristics of AgNPs, especially the size and shape. AgNPs with different characteristics can be produced by physical, chemical and biological routes. External energy sources such as light, heat, electricity, sound and microwave can be used in the synthesis process. Various factors should be considered in the synthesis of AgNPs with expected size and shape. Besides the types of precursor salts, additives such as reducing agents, capping agents and stabilizers, as well as the importance of reaction parameters, including reaction temperature, time, pH and extra energy sources should be recognized in the production process. Among these methods, biological synthesis using bacteria, fungi and plant extract proves a simple, environmentally friendly, cost-effective and reliable approach. Compared with physical and chemical methods, biological method does not require high temperature or toxic/hazardous additives, but the potential pathogens need to be carefully considered. We review the synthesis methods of AgNPs and compare the advantages and disadvantages to help understand how to obtain nanoparticles with controlled size and shape.

AgNPs have broad prospects in medical applications. Among them, antimicrobial and anticancer properties have received more attention. A variety of factors influence the antimicrobial and anticancer effects of AgNPs, including size, concentration/dose, exposure time, stabilizer and surface charges. The proposed mechanisms for antimicrobial activity of AgNPs involve destroying the structure of cell wall, inducing ROS production and DNA damage. Anticancer mechanisms of AgNPs are more complicated. AgNPs can induce apoptosis and necrosis of cancer cells by destroying cell ultrastructure, inducing ROS production and DNA damage, inactivating proteins and regulating multiple signaling pathways. Besides, AgNPs may block invasion and migration of cancer cells by inhibiting angiogenesis within the lesion. However, the potential cytotoxicity of AgNPs may limit their medical applications. In order to improve the compatibility of AgNPs, proper surface functionalization is widely concerned. The AgNPs surface allows coordination of multiple ligands and thus can be functionalized. The surface functionalization of AgNPs can simultaneously improve their biological safety and challenge their

drug delivery, which is conducive to the development of more antibacterial and antitumor agents involving AgNPs. AgNPs can also be used as an additive or adjuvant in bone scaffolds, dental materials and vaccines. The antidiabetic effect of AgNPs is also explored. Besides the impressive antimicrobial and anticancer activities, the unique optical properties of AgNPs make them great clinical potential in the field of biosensing and imaging. The AgNPs surface allows coordination of multiple ligands and thus can be functionalized.

Although most studies focus on the therapeutic purposes of AgNPs, the potential toxicities of AgNPs in multiple systems including skin, eyes, kidney, respiratory system, hepatobiliary system, immune and reproductive systems have been discussed. Further in-depth studies are required to evaluate the biocompatibility and potential cytotoxicity of AgNPs, which may help to develop safer and biocompatible AgNPs-based agents.

In this review, we separately introduce the synthesis method and anticancer properties of Ång-scale silver particles in the relevant sections. Compared with AgNPs mentioned in this review, we prepared pure and fine silver particles with Ångstrom size. This ultra-fine size may be a threshold for silver particles in the medical applications, that is, Ång-scale silver particles exhibit broad-spectrum anticancer activities without obvious cytotoxicity. This exciting discovery inspires us to explore more promising applications of Ång-scale silver particles in nanomedicine.

## Acknowledgments

This work was supported by the Special Funding for the Construction of Innovative Provinces in Hunan (Grant Nos. 2019SK2301, 2020SK3002), the National Natural Science Foundation of China (Grant Nos. 81670807, 81871822), the Non-profit Central Research Institute Fund of Chinese Academy of Medical Sciences (Grant No. 2019-RC-HL-024), the Science and Technology Plan Project of Hunan Province (Grant Nos. 2017XK2039, 2018RS3029) and the Innovation Driven Project of Central South University (Grant Nos. 2019CX014, 2018CX029).

## Author Contributions

H.X. guided the planning and writing of the review manuscript. L.X., H.X. and Y.-Y.W. wrote the manuscript. L.X. and J.H. prepared the figures. H.X., C.-Y. C., Z.-X.W., L.X. and Y.-Y.W. amended the manuscript.

## Competing Interests

The authors have declared that no competing

interest exists.

## References

- Alexander JW. History of the Medical Use of Silver. *Surg Infect*. 2009; 10: 289-292.
- Barillo DJ, Marx DE. Silver in medicine: a brief history BC 335 to present. *Burns*. 2014; 40: S3-S8.
- Asgary V, Shoari A, Baghbani-Arani F, Sadat Shandiz SA, Khosravy MS, Janani A, et al. Green synthesis and evaluation of silver nanoparticles as adjuvant in rabies veterinary vaccine. *Int J Nanomedicine*. 2016; 11: 3597-3605.
- Saratale GD, Saratale RG, Benelli G, Kumar G, Pugazhendhi A, Kim D-S, et al. Anti-diabetic potential of silver nanoparticles synthesized with *Argyrea nervosa* leaf extract high synergistic antibacterial activity with standard antibiotics against foodborne bacteria. *J Clust Sci*. 2017; 28: 1709-1727.
- Shanmuganathan R, Karuppusamy I, Saravanan M, Muthukumar H, Ponnuchamy K, Ramkumar VS, et al. Synthesis of Silver Nanoparticles and their Biomedical Applications - A Comprehensive Review. *Curr Pharm Des*. 2019; 25: 2650-2660.
- Stagon SP, Huang H. Syntheses and applications of small metallic nanorods from solution and physical vapor deposition. *Nanotechnol Rev*. 2013; 2: 259-267.
- Pourzahedi L, Eckelman MJ. Comparative life cycle assessment of silver nanoparticle synthesis routes. *Environ Sci Nano*. 2015; 2: 361-369.
- Iravani S, Korbekandi H, Mirmohammadi SV, Zolfaghari B. Synthesis of silver nanoparticles: chemical, physical and biological methods. *Res Pharm Sci*. 2014; 9: 385-406.
- Dong PV. Chemical synthesis and antibacterial activity of novel-shaped silver nanoparticles. *Int Nano Lett*. 2012; p:2-9.
- Zhang Z, Zhang X, Xin Z, Deng M, Wen Y, Song Y. Synthesis of monodisperse silver nanoparticles for ink-jet printed flexible electronics. *Nanotechnology*. 2011; 22: 425601.
- Díaz-Núñez P, González-Izquierdo J, González-Rubio G, Guerrero-Martínez A, Rivera A, Perlado J, et al. Effect of Organic Stabilizers on Silver Nanoparticles Fabricated by Femtosecond Pulsed Laser Ablation. *Appl. Sci*. 2017; 7: 793.
- Elsupikhe RF, Shameli K, Ahmad MB. Sonochemical method for the synthesis of silver nanoparticles in κ-carrageenan from silver salt at different concentrations. *Res Chem Intermediat*. 2015; 41: 8515-8525.
- Pu F, Ran X, Guan M, Huang Y, Ren J, Qu X. Biomolecule-templated photochemical synthesis of silver nanoparticles: Multiple readouts of localized surface plasmon resonance for pattern recognition. *Nano Res*. 2018; 11: 3213-3221.
- Joseph S, Mathew B. Microwave-assisted green synthesis of silver nanoparticles and the study on catalytic activity in the degradation of dyes. *J Mol Liq*. 2015; 204: 184-191.
- Pompilio A, Geminiani C, Bosco D, Rana R, Aceto A, Bucciarelli T, et al. Electrochemically Synthesized Silver Nanoparticles Are Active Against Planktonic and Biofilm Cells of *Pseudomonas aeruginosa* and Other Cystic Fibrosis-Associated Bacterial Pathogens. *Front Microbiol*. 2018; 9: 1349.
- Pantidos N. Biological Synthesis of Metallic Nanoparticles by Bacteria, Fungi and Plants. *J Nanomed Nanotechnol*. 2014; 5:233.
- de Morais MG, Vaz BdS, de Morais EG, Costa JAV. Biologically active metabolites synthesized by microalgae. *Biomed Res Int*. 2015; 435265.
- Otari S, Patil R, Ghosh S, Thorat N, Pawar S. Intracellular synthesis of silver nanoparticle by actinobacteria and its antimicrobial activity. *Spectrochim Acta A*. 2015; 136: 1175-1180.
- Prabhu S, Poulouse EK. Silver nanoparticles: mechanism of antimicrobial action, synthesis, medical applications, and toxicity effects. *Int Nano Lett*. 2012; 2: 32.
- Panacek A, Kvitek L, Smekalova M, Vecerova R, Kolar M, Roderova M, et al. Bacterial resistance to silver nanoparticles and how to overcome it. *Nat Nanotechnol*. 2018; 13: 65-71.
- Wang ZX, Chen CY, Wang Y, Li FXZ, Huang J, Luo ZW, et al. Ångstrom scale silver particles as a promising agent for low toxicity broad spectrum potent anticancer therapy. *Adv Funct Mater*. 2019; 29: 1808556.
- Lin J, Huang Z, Wu H, Zhou W, Jin P, Wei P, et al. Inhibition of autophagy enhances the anticancer activity of silver nanoparticles. *Autophagy*. 2014; 10: 2006-2020.
- Pei J, Fu B, Jiang L, Sun T. Biosynthesis, characterization, and anticancer effect of plant-mediated silver nanoparticles using *Coptis chinensis*. *Int J Nanomedicine*. 2019; 14: 1969-1978.
- Dziedzic A, Kubina R, Buldak R, Skonieczna M, Cholewa K. Silver nanoparticles exhibit the dose-dependent anti-proliferative effect against human squamous carcinoma cells attenuated in the presence of berberine. *Molecules*. 2016; 21: 365.
- El Badawy AM, Silva RG, Morris B, Scheckel KG, Suidan MT, Tolaymat TM. Surface charge-dependent toxicity of silver nanoparticles. *Environ sci technol*. 2010; 45: 283-287.
- Jo DH, Kim JH, Lee TG, Kim JH. Size, surface charge, and shape determine therapeutic effects of nanoparticles on brain and retinal diseases. *Nanomedicine*. 2015; 11: 1603-1611.
- Eom H-J, Choi J. p38 MAPK activation, DNA damage, cell cycle arrest and apoptosis as mechanisms of toxicity of silver nanoparticles in Jurkat T cells. *Environ sci technol*. 2010; 44: 8337-8342.
- Homayouni-Tabrizi M, Soltani M, Karimi E, Namvar F, Pouresmaeil V, Es-haghi A. Putative mechanism for anticancer properties of Ag-PP (NPs) extract. *IET nanobiotechnol*. 2019; 13: 617-620.
- Bethu MS, Netala VR, Domdi L, Tartte V, Janapala VR. Potential anticancer activity of biogenic silver nanoparticles using leaf extract of *Rhynchosia suaveolens*: an insight into the mechanism. *Artif cell nanomed B*. 2018; 46: 104-114.
- Hashemi Goradel N, Ghiyami-Hour F, Jahangiri S, Negahdari B, Sahebkar A, Masoudifar A, et al. Nanoparticles as new tools for inhibition of cancer angiogenesis. *J cell physiol*. 2018; 233: 2902-2910.
- Fields GB. Mechanisms of action of novel drugs targeting angiogenesis-promoting matrix metalloproteinases. *Front Immunol*. 2019; 10: 278.
- Zhao Y, Adjei AA. Targeting angiogenesis in cancer therapy: moving beyond vascular endothelial growth factor. *Oncologist*. 2015; 20: 660-673.
- Cho K, Wang X, Nie S, Chen Z, Shin DM. Therapeutic nanoparticles for drug delivery in cancer. *Clin Cancer Res*. 2008; 14: 1310-1316.
- Maeda H, Sawa T, Konno T. Mechanism of tumor-targeted delivery of macromolecular drugs, including the EPR effect in solid tumor and clinical overview of the prototype polymeric drug SMANCS. *J Control Release*. 2001; 74: 47-61.
- Xie Y, Bagby TR, Cohen MS, Forrest ML. Drug delivery to the lymphatic system: importance in future cancer diagnosis and therapies. *Expert Opin Drug Deliv*. 2009; 6: 785-792.
- Kaewamatawong T, Kawamura N, Okajima M, Sawada M, Morita T, Shimada A. Acute pulmonary toxicity caused by exposure to colloidal silica: particle size dependent pathological changes in mice. *Toxicol pathol*. 2005; 33: 745-751.
- Lafuente D, Garcia T, Blanco J, Sánchez D, Servent J, Domingo J, et al. Effects of oral exposure to silver nanoparticles on the sperm of rats. *Reprod Toxicol*. 2016; 60: 133-139.
- Xu L, Shao A, Zhao Y, Wang Z, Zhang C, Sun Y, et al. Neurotoxicity of silver nanoparticles in rat brain after intragastric exposure. *J Nanosci Nanotechnol*. 2015; 15: 4215-4223.
- Wu Y, Zhou Q. Silver nanoparticles cause oxidative damage and histological changes in medaka (*Oryzias latipes*) after 14 days of exposure. *Environ Toxicol Chem*. 2013; 32: 165-173.
- Sooklert K, Wongjarupong A, Cherdchom S, Wongjarupong N, Jindatip D, Phungnoi Y, et al. Molecular and morphological evidence of hepatotoxicity after silver nanoparticle exposure: a systematic review, in silico, and ultrastructure investigation. *Toxicol Res*. 2019; 35: 257-270.
- Miethling-Graff R, Rumpker R, Richter M, Verano-Braga T, Kjeldsen F, Brewer J, et al. Exposure to silver nanoparticles induces size- and dose-dependent oxidative stress and cytotoxicity in human colon carcinoma cells. *Toxicol In vitro*. 2014; 28: 1280-1289.
- Ong C, Lee QY, Cai Y, Liu X, Ding J, Yung L-YL, et al. Silver nanoparticles disrupt germline stem cell maintenance in the *Drosophila* testis. *Sci rep*. 2016; 6: 20632.
- Asharani P, Wu YL, Gong Z, Valiyaveetil S. Toxicity of silver nanoparticles in zebrafish models. *Nanotechnology*. 2008; 19: 255102.
- Botelho DJ, Leo BF, Massa CB, Sarkar S, Tetley TD, Chung KF, et al. Low-dose AgNPs reduce lung mechanical function and innate immune defense in the absence of cellular toxicity. *Nanotoxicology*. 2016; 10: 118-127.
- De Jong WH, Van Der Ven LT, Sleijffers A, Park MV, Jansen EH, Van Loveren H, et al. Systemic and immunotoxicity of silver nanoparticles in an intravenous 28 days repeated dose toxicity study in rats. *Biomaterials*. 2013; 34: 8333-8343.
- Seiffert J, Hussain F, Wiegman C, Li F, Bey L, Baker W, et al. Pulmonary toxicity of instilled silver nanoparticles: influence of size, coating and rat strain. *PLoS one*. 2015; 10: e0119726.
- Guo X, Li Y, Yan J, Ingle T, Jones MY, Mei N, et al. Size- and coating-dependent cytotoxicity and genotoxicity of silver nanoparticles evaluated using *in vitro* standard assays. *Nanotoxicology*. 2016; 10: 1373-1384.
- De Maglie M, Cella C, Bianchessi S, Argenti S, Scanziani E, Recordati C. Dose and batch-dependent hepatobiliary toxicity of 10 nm silver nanoparticles after single intravenous administration in mice. *Int J Health Anim Sci Food Safety*. 2015; 10: 13130.
- Jeong Y, Lim DW, Choi J. Assessment of size-dependent antimicrobial and cytotoxic properties of silver nanoparticles. *Adv Mater Sci Eng*. 2014; 763807.
- Park J, Lim D-H, Lim H-J, Kwon T, Choi J-S, Jeong S, et al. Size dependent macrophage responses and toxicological effects of Ag nanoparticles. *Chem Commun*. 2011; 47: 4382-4384.
- Ju-Nam Y, Lead JR. Manufactured nanoparticles: An overview of their chemistry, interactions and potential environmental implications. *Sci Total Environ*. 2008; 400: 396-414.
- Yadav TP, Yadav RM, Singh DP. Mechanical milling: a top down approach for the synthesis of nanomaterials and nanocomposites. *Nanosci Nanotechnol*. 2012; 2: 22-48.
- Zheng X, Peng Y, Lombardi JR, Cui X, Zheng W. Photochemical growth of silver nanoparticles with mixed-light irradiation. *Colloid Polym Sci*. 2016; 294: 911-916.

54. Kuntiy O, Kytsya A, Mertsalo I, Mazur A, Zozula G, Bazylyak L, et al. Electrochemical synthesis of silver nanoparticles by reversible current in solutions of sodium polyacrylate. *Colloid Polym Sci.* 2019; 297: 689-695.
55. Chung DS, Kim H, Ko J, Lee J, Hwang B, Chang S, et al. Microwave Synthesis of Silver Nanoparticles Using Different Pentose Carbohydrates as Reducing Agents. *J Chem.* 2018; 12: 1-10.
56. Hamed S, Ghaseminezhad M, Shokrollahzadeh S, Shojaosadati SA. Controlled biosynthesis of silver nanoparticles using nitrate reductase enzyme induction of filamentous fungus and their antibacterial evaluation. *Artif Cells Nanomed Biotechnol.* 2017; 45: 1588-1596.
57. Al Abboud MA. Fungal biosynthesis of silver nanoparticles and their role in control of fusarium wilt of sweet pepper and soil-borne fungi *in vitro*. *Int J Pharmacol.* 2018; 14: 773-780.
58. Khan MA, Khan T, Nadhman A. Applications of plant terpenoids in the synthesis of colloidal silver nanoparticles. *Adv Colloid Interface Sci.* 2016; 234: 132-141.
59. Kuppusamy P, Yusoff MM, Maniam GP, Govindan N. Biosynthesis of metallic nanoparticles using plant derivatives and their new avenues in pharmacological applications—An updated report. *Saudi Pharm J.* 2016; 24: 473-484.
60. Khayati G, Janghorban K. The nanostructure evolution of Ag powder synthesized by high energy ball milling. *Adv Powder Technol.* 2012; 23: 393-397.
61. Tien D, Liao C, Huang J, Tseng K, Lung J, Tsung T, et al. Novel technique for preparing a nano-silver water suspension by the arc-discharge method. *Rev Adv Mater Sci.* 2008; 18: 750-756.
62. Amendola V, Meneghetti M. Laser ablation synthesis in solution and size manipulation of noble metal nanoparticles. *Phys Chem Chem Phys.* 2009; 11: 3805-3821.
63. Wongrat E, Wongkrajang S, Chuejetton A, Bhoomanee C, Choopun S. Rapid synthesis of Au, Ag and Cu nanoparticles by DC arc-discharge for efficiency enhancement in polymer solar cells. *Mater Res Innov.* 2019; 23: 66-72.
64. Sadrolhosseini AR, Mahdi MA, Alizadeh F, Rashid SA. Laser Ablation Technique for Synthesis of Metal Nanoparticle in Liquid. In: Yufei Ma Ed. *Laser Technology and its Applications: IntechOpen*, 2nd ed. London: Croatia; 2018;p: 63-81.
65. Rhim JW, Wang LF, Lee Y, Hong SI. Preparation and characterization of bio-nanocomposite films of agar and silver nanoparticles: laser ablation method. *Carbohydr Polym.* 2014; 103: 456-465.
66. Tien D-C, Tseng K-H, Liao C-Y, Huang J-C, Tsung T-T. Discovery of ionic silver in silver nanoparticle suspension fabricated by arc discharge method. *J Alloys Compd.* 2008; 463: 408-411.
67. Shang S, Zeng W. *Conductive nanofibres and nanocoatings.* Hong Kong: Woodhead Publishing Series in Textiles. 2013.
68. Mubarak AMA, Hamzah EHE, Tofr MTM. Review of physical vapour deposition (PVD) techniques for hard coating. *Jurnal Mekanikal.* 2005; 20: 42-51.
69. Laghrib F, Farahi A, Bakasse M, Lahrach S, El Mhammedi M. Chemical synthesis of nanosilver on chitosan and electroanalysis activity against the p-nitroaniline reduction. *J Electroanal Chem.* 2019; 845: 111-118.
70. Vreeland EC, Watt J, Schober GB, Hance BG, Austin MJ, Price AD, et al. Enhanced nanoparticle size control by extending LaMer's mechanism. *Chem Mater.* 2015; 27: 6059-6066.
71. Naik AN, Patra S, Sen D, Goswami A. Evaluating the mechanism of nucleation and growth of silver nanoparticles in a polymer membrane under continuous precursor supply: tuning of multiple to single nucleation pathway. *Phys Chem Chem Phys.* 2019; 21: 4193-4199.
72. Dondi R, Su W, Griffith GA, Clark G, Burley GA. Highly Size-and Shape-Controlled Synthesis of Silver Nanoparticles via a Templated Tollens Reaction. *Small.* 2012; 8: 770-776.
73. Li X, Odoom-Wubah T, Chen H, Jing X, Zheng B, Huang J. Biosynthesis of silver nanoparticles through tandem hydrolysis of silver sulfate and cellulose under hydrothermal conditions. *J Chem Technol Biotechnol.* 2014; 89: 1817-1824.
74. Zielinska A, Skwarek E, Zaleska A, Gazda M, Hupka J. Preparation of silver nanoparticles with controlled particle size. *Procedia Chem.* vol. 1. 2009; p:1560-1566.
75. Ahmad N, Ang BC, Amalina MA, Bong CW. Influence of precursor concentration and temperature on the formation of nanosilver in chemical reduction method. *Sains Malays.* 2018; 47: 157-168.
76. Ajitha B, Divya A, Harish G, Sreedhara Reddy P. The influence of silver precursor concentration on size of silver nanoparticles grown by soft chemical route. *Res J Phys Sci.* 2013; 2320: 4796.
77. Alqadi M, Noqta OA, Alzoubi F, Alzoubi J, Aljarrah K. pH effect on the aggregation of silver nanoparticles synthesized by chemical reduction. *Mater Sci-Poland.* 2014; 32: 107-111.
78. Jiang X, Chen W, Chen C, Xiong S, Yu A. Role of temperature in the growth of silver nanoparticles through a synergetic reduction approach. *Nanoscale Res Lett.* 2011; 6: 32.
79. Zaarour M, El Roz M, Dong B, Retoux R, Aad R, Cardin J, et al. Photochemical preparation of silver nanoparticles supported on zeolite crystals. *Langmuir.* 2014; 30: 6250-6256.
80. Khaydarov RA, Khaydarov RR, Gapurova O, Estrin Y, Scheper T. Electrochemical method for the synthesis of silver nanoparticles. *J Nanopart Res.* 2009; 11: 1193-1200.
81. Jovanović Ž, Stojkovića J, Obradović B, Mišković-Stanković V. Alginate hydrogel microbeads incorporated with Ag nanoparticles obtained by electrochemical method. *Mater Chem Phys.* 2012; 133: 182-189.
82. S Horikoshi, N Serpone. *Microwaves in Nanoparticle Synthesis: Fundamentals and Applications.* Weinheim, Germany. Wiley Online Library. 2013.
83. Pal A, Shah S, Devi S. Microwave-assisted synthesis of silver nanoparticles using ethanol as a reducing agent. *Mater Chem Phys.* 2009; 114: 530-532.
84. Darroudi M, Zak AK, Muhamad M, Huang N, Hakimi M. Green synthesis of colloidal silver nanoparticles by sonochemical method. *Mater Lett.* 2012; 66: 117-120.
85. Kumar N, Biswas K, Gupta RK. Green synthesis of Ag nanoparticles in large quantity by cryomilling. *RSC Adv.* 2016; 6: 111380-111388.
86. Munkhbayar B, Tanshen MR, Jeoun J, Chung H, Jeong H. Surfactant-free dispersion of silver nanoparticles into MWCNT-aqueous nanofluids prepared by one-step technique and their thermal characteristics. *Ceram Int.* 2013; 39: 6415-6425.
87. El-Khatib AM, Doma AS, Abo-Zaid GA, Badawi MS, Mohamed MM, Mohamed AS. Antibacterial activity of some nanoparticles prepared by double arc discharge method. *Nano-Structures & Nano-Objects.* 2020; 23: 100473.
88. Amendola V, Polizzi S, Meneghetti M. Free silver nanoparticles synthesized by laser ablation in organic solvents and their easy functionalization. *Langmuir.* 2007; 23: 6766-6770.
89. El-Kader FA, Hakeem N, Elashmawi I, Menazea A. Synthesis and characterization of PVK/AgNPs nanocomposites prepared by laser ablation. *Spectrochim Acta Part A.* 2015; 138: 331-339.
90. Ranošek-Soliwoda K, Tomaszewska E, Socha E, Krzyczmonik P, Ignaczak A, Orłowski P, et al. The role of tannic acid and sodium citrate in the synthesis of silver nanoparticles. *J Nanopart Res.* 2017; 19: 273.
91. Rashid MU, Bhuiyan MKH, Quayum ME. Synthesis of silver nano particles (Ag-NPs) and their uses for quantitative analysis of vitamin C tablets. *Dhaka Univ J Pharm Sci.* 2013; 12: 29-33.
92. Guzmán MG, Dille J, Godet S. Synthesis of silver nanoparticles by chemical reduction method and their antibacterial activity. *Int J Chem Biomol Eng.* 2009; 2: 104-111.
93. Saade J, de Araújo CB. Synthesis of silver nanoprisms: a photochemical approach using light emission diodes. *Mater Chem Phys.* 2014; 148: 1184-1193.
94. Krajczewski J, Kołataj K, Parzyszek S, Kudelski A. Photochemical synthesis of different silver nanostructures. Rome, Italy: IEEE. 2015.
95. Petrucci OD, Hilton RJ, Farrer JK, Watt RK. A ferritin photochemical synthesis of monodispersed silver nanoparticles that possess antimicrobial properties. *J Nanomater.* 2019; 9535708.
96. Starowicz M, Stypuła B, Banaś J. Electrochemical synthesis of silver nanoparticles. *Electrochem commun.* 2006; 8: 227-230.
97. Dobre N, Petică A, Buda M, Anicăi L, Vișan T. Electrochemical synthesis of silver nanoparticles in aqueous electrolytes. *UPB Sci Bull.* 2014; 76: 127-136.
98. Reicha FM, Sarhan A, Abdel-Hamid MI, El-Sherbiny IM. Preparation of silver nanoparticles in the presence of chitosan by electrochemical method. *Carbohydr Polym.* 2012; 89: 236-244.
99. Nthunya LN, Derese S, Gutierrez L, Verliefe AR, Mamba BB, Barnard TG, et al. Green synthesis of silver nanoparticles using one-pot and microwave-assisted methods and their subsequent embedment on PVDF nanofibre membranes for growth inhibition of mesophilic and thermophilic bacteria. *New J Chem.* 2019; 43: 4168-4180.
100. Naaz S, Chowdhury P. Sunlight and ultrasound-assisted synthesis of photoluminescent silver nanoclusters: A unique 'Knock out' sensor for thiophilic metal ions. *Sens Actuators B Chem.* 2017; 241: 840-848.
101. Naaz S, Poddar S, Bayen SP, Mondal MK, Roy D, Mondal SK, et al. Tenfold enhancement of fluorescence quantum yield of water soluble silver nanoclusters for nano-molar level glucose sensing and precise determination of blood glucose level. *Sens Actuators B Chem.* 2018; 255: 332-340.
102. Chowdhury P, Hazra A, Kr. Mondal M, Roy B, Roy D, Prasad Bayen S, et al. Facile synthesis of polyacrylate directed silver nanoparticles for pH sensing through naked eye. *J Macromol Sci A.* 2019; 56: 773-780.
103. Saha SK, Chowdhury P, Saini P, Babu SPS. Ultrasound assisted green synthesis of poly(vinyl alcohol) capped silver nanoparticles for the study of its antifilarial efficacy. *Appl Surf Sci.* 2014; 288: 625-632.
104. Bayen SP, Mondal MK, Naaz S, Mondal SK, Chowdhury P. Design and sonochemical synthesis of water-soluble fluorescent silver nanoclusters for Hg<sup>2+</sup> sensing. *J Environ Chem Eng.* 2016; 4: 1110-1116.
105. Klaus T, Joergner R, Olsson E, Granqvist C-G. Silver-based crystalline nanoparticles, microbially fabricated. *Proc Natl Acad Sci India Sect B Biol Sci.* 1999; 96: 13611-13614.
106. Eckhardt S, Brunetto PS, Gagnon J, Priebe M, Giese B, Fromm KM. Nanobio silver: its interactions with peptides and bacteria, and its uses in medicine. *Chem Rev.* 2013; 113: 4708-4754.
107. Rengasamy M, Anbalagan K, Kodhaiyoli S, Pugalenth V. Castor leaf mediated synthesis of iron nanoparticles for evaluating catalytic effects in transesterification of castor oil. *RSC Adv.* 2016; 6: 9261-9269.
108. Deshpande LM, Chopade BA. Plasmid mediated silver resistance in *Acinetobacter baumannii*. *Biometals.* 1994; 7: 49-56.
109. Ali J, Ali N, Wang L, Waseem H, Pan G. Revisiting the mechanistic pathways for bacterial mediated synthesis of noble metal nanoparticles. *J Microbiol Methods.* 2019.

110. Galvez AM, Ramos KM, Teja AJ, Baculi R. Bacterial exopolysaccharide-mediated synthesis of silver nanoparticles and their application on bacterial biofilms. *J Microbiol Biotechnol Food Sci.* 2019; 9: 970-978.
111. Ahmed A-A, Hamzah H, Maarof M. Analyzing formation of silver nanoparticles from the filamentous fungus *Fusarium oxysporum* and their antimicrobial activity. *Turk J Biol.* 2018; 42: 54-62.
112. Singhal A, Singhal N, Bhattacharya A, Gupta A. Synthesis of silver nanoparticles (AgNPs) using *Ficus retusa* leaf extract for potential application as antibacterial and dye decolourising agents. *Inorg Nano-Met Chem.* 2017; 47: 1520-1529.
113. Shivani Tiwari, Jyotsna Gade, Abhishek Chourasia. Research Article Biosynthesis of silver nanoparticles using *Bacillus* sp. for Microbial Disease Control: An in-vitro and in-silico approach. *Sch Acad J Pharm.* 2015; 4: 389-397.
114. Majeed S, Ansari MT, Dash GK, bin Abdullah S. Fungal mediated synthesis of silver nanoparticles and its role in enhancing the bactericidal property of Amoxicillin. *Der Pharm Lett.* 2015; 7: 119-123.
115. Ottoni CA, Simões MF, Fernandes S, Dos Santos JG, Da Silva ES, de Souza RFB, et al. Screening of filamentous fungi for antimicrobial silver nanoparticles synthesis. *AMB Express.* 2017; 7: 31.
116. Salaheldin T, Hussein S, Al-Enizi A, Elzathary A, Cowley A. Evaluation of the cytotoxic behavior of fungal extracellular synthesized Ag nanoparticles using confocal laser scanning microscope. *Int J Mol Sci.* 2016; 17: 329.
117. Neethu S, Midhun SJ, Radhakrishnan E, Jyothis M. Green synthesized silver nanoparticles by marine endophytic fungus *Penicillium polonicum* and its antibacterial efficacy against biofilm forming, multidrug-resistant *Acinetobacter baumannii*. *Microb Pathog.* 2018; 116: 263-272.
118. Seetharaman PK, Chandrasekaran R, Gnanasekar S, Chandrakasan G, Gupta M, Manikandan DB, et al. Antimicrobial and larvicidal activity of eco-friendly silver nanoparticles synthesized from endophytic fungi *Phomopsis liquidambaris*. *Biocatal Agric Biotechnol.* 2018; 16: 22-30.
119. Elegbede JA, Lateef A, Azeez MA, Asafa TB, Yekeen TA, Oladipo IC, et al. Fungal xylanases-mediated synthesis of silver nanoparticles for catalytic and biomedical applications. *IET Nanobiotechnol.* 2018; 12: 857-863.
120. Devi LS, Joshi S. Ultrastructures of silver nanoparticles biosynthesized using endophytic fungi. *J Microsc Ultrastruct.* 2015; 3: 29-37.
121. Michalak I, Chojnacka K. Algae as production systems of bioactive compounds. *Eng Life Sci.* 2015; 15: 160-176.
122. Alassali A, Cybulska I, Brudecki GP, Farzanah R, Thomsen MH. Methods for upstream extraction and chemical characterization of secondary metabolites from algae biomass. *Adv Tech Biol Med.* 2016; p: 1-16.
123. Khanna P, Kaur A, Goyal D. Algae-based metallic nanoparticles: synthesis, characterization and applications. *J Microbiol Methods.* 2019; 163: 105656.
124. Aziz N, Faraz M, Pandey R, Shakir M, Fatma T, Varma A, et al. Facile algae-derived route to biogenic silver nanoparticles: synthesis, antibacterial, and photocatalytic properties. *Langmuir.* 2015; 31: 11605-11612.
125. Aboelfetoh EF, El-Shenody RA, Ghobara MM. Eco-friendly synthesis of silver nanoparticles using green algae (*Caulerpa serrulata*): reaction optimization, catalytic and antibacterial activities. *Environ Monit Assess.* 2017; 189: 349.
126. Rajeshkumar S, Bharath L. Mechanism of plant-mediated synthesis of silver nanoparticles—a review on biomolecules involved, characterisation and antibacterial activity. *Chem Biol Interact.* 2017; 273: 219-227.
127. Ovais M, Khalil AT, Islam NU, Ahmad I, Ayaz M, Saravanan M, et al. Role of plant phytochemicals and microbial enzymes in biosynthesis of metallic nanoparticles. *Appl Microbiol Biotechnol.* 2018; 102: 6799-6814.
128. Khorrami S, Zarrabi A, Khaleghi M, Danaei M, Mozafari M. Selective cytotoxicity of green synthesized silver nanoparticles against the MCF-7 tumor cell line and their enhanced antioxidant and antimicrobial properties. *Int J Nanomedicine.* 2018; 13: 8013.
129. Jain S, Mehata MS. Medicinal plant leaf extract and pure flavonoid mediated green synthesis of silver nanoparticles and their enhanced antibacterial property. *Sci Rep.* 2017; 7: 15867.
130. Kūūnāl S, Visnapuu M, Volubujeva O, Rosario MS, Rauwel P, Rauwel E. Optimisation of plant mediated synthesis of silver nanoparticles by common weed *Plantago major* and their antimicrobial properties. *IOP Conf Ser Mater Sci Eng.* 2019; p:8-12.
131. Abdi V, Sourinejad I, Yousefzadi M, Ghasemi Z. Mangrove-mediated synthesis of silver nanoparticles using native *Avicennia marina* plant extract from southern Iran. *Chem Eng Commun.* 2018; 205: 1069-1076.
132. Sivasankar P, Seedeivi P, Poongodi S, Sivakumar M, Murugan T, Sivakumar L, et al. Characterization, antimicrobial and antioxidant property of exopolysaccharide mediated silver nanoparticles synthesized by *Streptomyces violaceus* MM72. *Carbohydr Polym.* 2018; 181: 752-759.
133. Neethu S, Midhun SJ, Sunil MA, Soumya S, Radhakrishnan EK, Jyothis M. Efficient visible light induced synthesis of silver nanoparticles by *Penicillium polonicum* ARA 10 isolated from *Chetomorpha antennina* and its antibacterial efficacy against *Salmonella enterica* serovar *Typhimurium*. *J Photochem Photobiol B.* 2018; 180: 175-185.
134. Kohsari I, Mohammad-Zadeh M, Minaeian S, Rezaee M, Barzegari A, Shariatnia Z, et al. *In vitro* antibacterial property assessment of silver nanoparticles synthesized by *Falcaria vulgaris* aqueous extract against MDR bacteria. *J Solgel Sci Technol.* 2019; 90: 380-389.
135. Singh H, Du J, Singh P, Yi TH. Extracellular synthesis of silver nanoparticles by *Pseudomonas* sp. THG-LS1. 4 and their antimicrobial application. *J Pharm Anal.* 2018; 8: 258-264.
136. Monowar T, Rahman MS, Bhore SJ, Raju G, Sathasivam KV. Silver Nanoparticles Synthesized by Using the Endophytic Bacterium *Pantoea ananatis* are Promising Antimicrobial Agents against Multidrug Resistant Bacteria. *Molecules.* 2018; 23.
137. Akther T, Mathipi V, Kumar NS, Davoodbasha M, Srinivasan H. Fungal-mediated synthesis of pharmaceutically active silver nanoparticles and anticancer property against A549 cells through apoptosis. *Environ Sci Pollut Res.* 2019; 26: 13649-13657.
138. Koli SH, Mohite BV, Suryawanshi RK, Borase HP, Patil SV. Extracellular red *Monascus* pigment-mediated rapid one-step synthesis of silver nanoparticles and its application in biomedical and environment. *Bioprocess Biosyst Eng.* 2018; 41: 715-727.
139. El-Naggar NE, Hussein MH, El-Sawah AA. Bio-fabrication of silver nanoparticles by phycocyanin, characterization, *in vitro* anticancer activity against breast cancer cell line and *in vivo* cytotoxicity. *Sci Rep.* 2017; 7: 10844.
140. Vieira AP, Stein EM, Andreguetti DX, Colepicolo P, da Costa Ferreira AM. Preparation of silver nanoparticles using aqueous extracts of the red algae *Laurencia aldingensis* and *Laurenciaella* sp. and their cytotoxic activities. *J Appl Phycol.* 2015; 28: 2615-2622.
141. Balachandrar R, Gurumoorthy P, Karmegam N, Barabadi H, Subbaiya R, Anand K, et al. Plant-mediated synthesis, characterization and bactericidal potential of emerging silver nanoparticles using stem extract of *Phyllanthus pinnatus*: a recent advance in phytonanotechnology. *J Clust Sci.* 2019; 30: 1481-1488.
142. Ravichandran V, Vasanthi S, Shalini S, Shah SAA, Tripathy M, Paliwal N. Green synthesis, characterization, antibacterial, antioxidant and photocatalytic activity of *Parkia speciosa* leaves extract mediated silver nanoparticles. *Results Phys.* 2019; 15: 102565.
143. Shaik M, Khan M, Kuniyil M, Al-Warthan A, Alkhatlan H, Siddiqui M, et al. Plant-Extract-Assisted Green Synthesis of Silver Nanoparticles Using *Origanum vulgare* L. Extract and Their Microbicidal Activities. *Sustainability.* 2018; 10: 913.
144. Vanti GL, Nargund VB, N BK, Vanarchi R, Kurjogi M, Mulla SI, et al. Synthesis of *Gossypium hirsutum*-derived silver nanoparticles and their antibacterial efficacy against plant pathogens. *Appl Organomet Chem.* 2019; 33: e4630.
145. Nandhini T, Monajkumar S, Vadivel V, Devipriya N, Devi JM. Synthesis of spheroid shaped silver nanoparticles using Indian traditional medicinal plant *Flacourtia indica* and their *in vitro* anti-proliferative activity. *Mater Res Express.* 2019; 6: 045032.
146. G L, A S, P T K, K M. Plant-mediated synthesis of silver nanoparticles using fruit extract of *Cleome viscosa* L.: Assessment of their antibacterial and anticancer activity. *Karbala Int J Mod Sci.* 2018; 4: 61-68.
147. He Y, Wei F, Ma Z, Zhang H, Yang Q, Yao B, et al. Green synthesis of silver nanoparticles using seed extract of *Alpinia katsumadai*, and their antioxidant, cytotoxicity, and antibacterial activities. *RSC Adv.* 2017; 7: 39842-39851.
148. Greenivasulu V. Biosynthesis of Silver Nanoparticles using *Mimosa pudica* Plant root extract: Characterization, Antibacterial Activity and Electrochemical Detection of Dopamine. *Int J Electrochem Sci.* 2016; p: 9959-9971.
149. Tippayawat P, Phromviyo N, Boueroy P, Chompoosor A. Green synthesis of silver nanoparticles in aloe vera plant extract prepared by a hydrothermal method and their synergistic antibacterial activity. *PeerJ.* 2016; 4: e2589.
150. Mane Gavade SJ, Nikam GH, Dhabbe RS, Sabale SR, Tamhankar BV, Mulik GN. Green synthesis of silver nanoparticles by using carambola fruit extract and their antibacterial activity. *Adv Nat Sci-Nanosci.* 2015; 6: 045015.
151. Kora AJ, Sashidhar RB. Antibacterial activity of biogenic silver nanoparticles synthesized with gum ghatti and gum olibanum: a comparative study. *J Antibiot (Tokyo).* 2015; 68: 88-97.
152. Ahn J-M, Eom H-J, Yang X, Meyer JN, Choi J. Comparative toxicity of silver nanoparticles on oxidative stress and DNA damage in the nematode, *Caenorhabditis elegans*. *Chemosphere.* 2014; 108: 343-352.
153. Li L, Wu H, Peijnenburg WJ, van Gestel CA. Both released silver ions and particulate Ag contribute to the toxicity of AgNPs to earthworm *Eisenia fetida*. *Nanotoxicology.* 2015; 9: 792-801.
154. Burkowska-But A, Sionkowski G, Walczak M. Influence of stabilizers on the antimicrobial properties of silver nanoparticles introduced into natural water. *J Environ Sci.* 2014; 26: 542-549.
155. Oei JD, Zhao WW, Chu L, DeSilva MN, Ghimire A, Rawls HR, et al. Antimicrobial acrylic materials with *in situ* generated silver nanoparticles. *J Biomed Mater Res B Appl Biomater.* 2012; 100: 409-415.
156. Abbaszadegan A, Ghahramani Y, Gholami A, Hemmateenejad B, Dorostkar S, Nabavizadeh M, et al. The effect of charge at the surface of silver nanoparticles on antimicrobial activity against gram-positive and gram-negative bacteria: a preliminary study. *J Nanomater.* 2015; 16: 53.
157. Ishida T. Anticancer activities of silver ions in cancer and tumor cells and DNA damages by Ag<sup>+</sup>-DNA base-pairs reactions. *MOJ Tumor Res.* 2017; 1(1):8-16.
158. Gurunathan S, Park JH, Han JW, Kim JH. Comparative assessment of the apoptotic potential of silver nanoparticles synthesized by *Bacillus tequilensis* and *Calocybe indica* in MDA-MB-231 human breast cancer cells: targeting p53 for anticancer therapy. *Int J Nanomedicine.* 2015; 10: 4203-4222.

159. Haseeb M, Khan MS, Baker A, Khan I, Wahid I, Jaabir MM. Anticancer and antibacterial potential of MDR Staphylococcus aureus mediated synthesized silver nanoparticles. *Biosci Biotech Res Comm*. 2019; 12: 26-35.
160. Zhang Y, Lu H, Yu D, Zhao D. AgNPs and Ag/C225 Exert Anticancerous Effects via Cell Cycle Regulation and Cytotoxicity Enhancement. *J Nanomater*. 2017; 2017: 1-10.
161. Yang T, Yao Q, Cao F, Liu Q, Liu B, Wang X-H. Silver nanoparticles inhibit the function of hypoxia-inducible factor-1 and target genes: insight into the cytotoxicity and antiangiogenesis. *Int J Nanomedicine*. 2016; 11: 6679-6692.
162. Marsich E, Bellomo F, Turco G, Travan A, Donati I, Paoletti S. Nano-composite scaffolds for bone tissue engineering containing silver nanoparticles: preparation, characterization and biological properties. *J Mater Sci Mater Med*. 2013; 24: 1799-1807.
163. Chowdhury S, De M, Guha R, Batabyal S, Samanta I, Hazra SK, et al. Influence of silver nanoparticles on post-surgical wound healing following topical application. *Eur J Nanomed*. 2014; 237-247.
164. Salomoni R, Léo P, Rodrigues M. Antibacterial activity of silver nanoparticles (AgNPs) in Staphylococcus aureus and cytotoxicity effect in mammalian cells. *substance*. 2015; 851-857.
165. Paredes D, Ortiz C, Torres R. Synthesis, characterization, and evaluation of antibacterial effect of Ag nanoparticles against Escherichia coli O157: H7 and methicillin-resistant Staphylococcus aureus (MRSA). *Int J Nanomedicine*. 2014; 9: 1717-1729.
166. Salomoni R, Léo P, Montemor A, Rinaldi B, Rodrigues M. Antibacterial effect of silver nanoparticles in Pseudomonas aeruginosa. *Nanotechnol Sci Appl*. 2017; 10: 115-121.
167. Rónavári A, Igaz N, Gopisetty MK, Szerencsés B, Kovács D, Papp C, et al. Biosynthesized silver and gold nanoparticles are potent antimycotics against opportunistic pathogenic yeasts and dermatophytes. *Int J Nanomedicine*. 2018; 13: 695-703.
168. Kumar SD, Singaravelu G, Ajithkumar S, Murugan K, Nicoletti M, Benelli G. Mangrove-mediated green synthesis of silver nanoparticles with high HIV-1 reverse transcriptase inhibitory potential. *J Clust Sci*. 2017; 28: 359-367.
169. Sun RW-Y, Chen R, Chung NP-Y, Ho C-M, Lin C-LS, Che C-M. Silver nanoparticles fabricated in Hepes buffer exhibit cytoprotective activities toward HIV-1 infected cells. *Chem Commun*. 2005; 5059-5061.
170. Chatterjee T, Chatterjee BK, Majumdar D, Chakrabarti P. Antibacterial effect of silver nanoparticles and the modeling of bacterial growth kinetics using a modified Gompertz model. *Biochim Biophys Acta Gen Subj*. 2015; 1850: 299-306.
171. Raza M, Kanwal Z, Rauf A, Sabri A, Riaz S, Naseem S. Size-and shape-dependent antibacterial studies of silver nanoparticles synthesized by wet chemical routes. *Nanomaterials*. 2016; 10:3390.
172. Agnihotri S, Mukherji S, Mukherji S. Size-controlled silver nanoparticles synthesized over the range 5-100 nm using the same protocol and their antibacterial efficacy. *Rsc Adv*. 2014; 4: 3974-3983.
173. Jiraroj D, Tungasmita S, Tungasmita DN. Silver ions and silver nanoparticles in zeolite A composites for antibacterial activity. *Powder Technol*. 2014; 264: 418-422.
174. Hong X, Wen J, Xiong X, Hu Y. Shape effect on the antibacterial activity of silver nanoparticles synthesized via a microwave-assisted method. *Environ Sci Pollut Res Int*. 2016; 23: 4489-4497.
175. Mandal B, Dash SK, Das B, Chattopadhyay S, Ghosh T, Das D, et al. Bio-fabricated silver nanoparticles preferentially targets Gram positive depending on cell surface charge. *Biomed Pharmacother*. 2016; 83: 548-558.
176. van der Wal A, Norde W, Zehnder AJ, Lyklema J. Determination of the total charge in the cell walls of Gram-positive bacteria. *Colloids Surf B Biointerfaces*. 1997; 9: 81-100.
177. dos Santos CA, Jozala AF, Pessoa Jr A, Seckler MM. Antimicrobial effectiveness of silver nanoparticles co-stabilized by the bioactive copolymer pluronic F68. *J Nanobiotechnology*. 2012; 10: 43.
178. Lee K-J, Park S-H, Govarthanan M, Hwang P-H, Seo Y-S, Cho M, et al. Synthesis of silver nanoparticles using cow milk and their antifungal activity against phytopathogens. *Mater Lett*. 2013; 105: 128-131.
179. Mallmann EJJ, Cunha FA, Castro BN, Maciel AM, Menezes EA, Fachine PBA. Antifungal activity of silver nanoparticles obtained by green synthesis. *Rev Inst Med Trop Sao Paulo*. 2015; 57: 165-167.
180. Kim SW, Jung JH, Lamsal K, Kim YS, Min JS, Lee YS. Antifungal effects of silver nanoparticles (AgNPs) against various plant pathogenic fungi. *Mycobiology*. 2012; 40: 53-58.
181. Lu L, Sun R, Chen R, Hui C-K, Ho C-M, Luk JM, et al. Silver nanoparticles inhibit hepatitis B virus replication. *Antivir Ther*. 2008; 13: 253-262.
182. Gaikwad S, Ingle A, Gade A, Rai M, Falanga A, Incoronato N, et al. Antiviral activity of mycosynthesized silver nanoparticles against herpes simplex virus and human parainfluenza virus type 3. *Int J Nanomedicine*. 2013; 8: 4303-4314.
183. Etemadzade M, Ghamarypour A, Zabiollahi R, Shirazi M, Sahebamee H, Vaziri AZ, et al. Synthesis and evaluation of antiviral activities of novel sonochemical silver nanorods against HIV and HSV viruses. *Asian Pac J Trop Dis*. 2016; 6: 854-858.
184. Mori Y, Ono T, Miyahira Y, Nguyen VQ, Matsui T, Ishihara M. Antiviral activity of silver nanoparticle/chitosan composites against H1N1 influenza A virus. *Nanoscale Res Lett*. 2013; 8: 93.
185. Elechiguerra JL, Burt JL, Morones JR, Camacho-Bragado A, Gao X, Lara HH, et al. Interaction of silver nanoparticles with HIV-1. *J Nanobiotechnology*. 2005; 3: 6.
186. Pangestika R, Ernawati R. Antiviral Activity Effect of Silver Nanoparticles (AgNPs) Solution Against the Growth of Infectious Bursal Disease Virus on Embryonated Chicken Eggs with Elisa Test. *KnE Life Sciences*. 2017; 3: 536-548.
187. Yun'an Qing LC, Li R, Liu G, Zhang Y, Tang X, Wang J, et al. Potential antibacterial mechanism of silver nanoparticles and the optimization of orthopedic implants by advanced modification technologies. *Int J Nanomedicine*. 2018; 13: 3311-3327.
188. Wang L, Xu H, Gu L, Han T, Wang S, Meng F. Bioinspired synthesis, characterization and antibacterial activity of plant-mediated silver nanoparticles using purple sweet potato root extract. *Materials Technology*. 2016; 31: 437-442.
189. Radhakrishnan VS, Mudiam MKR, Kumar M, Dwivedi SP, Singh SP, Prasad T. Silver nanoparticles induced alterations in multiple cellular targets, which are critical for drug susceptibilities and pathogenicity in fungal pathogen (Candida albicans). *Int J Nanomedicine*. 2018; 13: 2647-2663.
190. Sharma V, Kaushik S, Pandit P, Dhull D, Yadav JP, Kaushik S. Green synthesis of silver nanoparticles from medicinal plants and evaluation of their antiviral potential against chikungunya virus. *Appl Microbiol Biotechnol*. 2019; 103: 881-891.
191. Trefry JC, Wooley DP. Silver nanoparticles inhibit vaccinia virus infection by preventing viral entry through a macropinocytosis-dependent mechanism. *J Biomed Nanotechnol*. 2013; 9: 1624-1635.
192. Yang XX, Li CM, Huang CZ. Curcumin modified silver nanoparticles for highly efficient inhibition of respiratory syncytial virus infection. *Nanoscale*. 2016; 8: 3040-3048.
193. Bharti B, Bharti S, Khurana S. Worm infestation: Diagnosis, treatment and prevention. *Indian J Pediatr*. 2018; 85: 1017-1024.
194. Taylor-Robinson DC, Maayan N, Soares-Weiser K, Donegan S, Garner P. Deworming drugs for soil-transmitted intestinal worms in children: effects on nutritional indicators, haemoglobin, and school performance. *Cochrane Database Syst Rev*. 2015; 7: CD000371.
195. Saha SK, Roy P, Saini P, Mondal MK, Chowdhury P, Babu SPS. Carbohydrate polymer inspired silver nanoparticles for filaricidal and mosquitoicidal activities: A comprehensive view. *Carbohydr Polym*. 2016; 137: 390-401.
196. Saini P, Saha SK, Roy P, Chowdhury P, Babu SPS. Evidence of reactive oxygen species (ROS) mediated apoptosis in Setaria cervi induced by green silver nanoparticles from Acacia auriculiformis at a very low dose. *Exp Parasitol*. 2016; 160: 39-48.
197. Tomar R, Preet S. Evaluation of anthelmintic activity of biologically synthesized silver nanoparticles against the gastrointestinal nematode, Haemonchus contortus. *J Helminthol*. 2017; 91: 454-461.
198. Preet S, Tomar RS. Anthelmintic effect of biofabricated silver nanoparticles using Ziziphos jujuba leaf extract on nutritional status of Haemonchus contortus. *Small Rumin Res*. 2017; 154: 45-51.
199. Rashid MMO, Ferdous J, Banik S, Islam MR, Uddin AM, Robel FN. Anthelmintic activity of silver-extract nanoparticles synthesized from the combination of silver nanoparticles and M. charantia fruit extract. *BMC Complement Altern Med*. 2016; 16: 242.
200. Subarani S, Sabhanayakam S, Kamaraj C. Studies on the impact of biosynthesized silver nanoparticles (AgNPs) in relation to malaria and filariasis vector control against Anopheles stephensi Liston and Culex quinquefasciatus Say (Diptera: Culicidae). *Parasitol Res*. 2013; 112: 487-499.
201. McDaniel JT, Nuhu K, Ruiz J, Alorbi G. Social determinants of cancer incidence and mortality around the world: an ecological study. *Glob Health Promot*. 2019; 26: 41-49.
202. Pilleron S, Sarfati D, Janssen-Heijnen M, Vignat J, Ferlay J, Bray F, et al. Global cancer incidence in older adults, 2012 and 2035: A population-based study. *Int J Cancer*. 2019; 144: 49-58.
203. Schirrmacher V. From chemotherapy to biological therapy: A review of novel concepts to reduce the side effects of systemic cancer treatment (Review). *Int J Oncol*. 2019; 54: 407-419.
204. Choudhury H, Pandey M, Yin TH, Kaur T, Jia GW, Tan SQL, et al. Rising horizon in circumventing multidrug resistance in chemotherapy with nanotechnology. *Mater Sci Eng C Mater Biol Appl*. 2019; 101: 596-613.
205. Shi J, Kantoff PW, Wooster R, Farokhzad OC. Cancer nanomedicine: progress, challenges and opportunities. *Nat Rev Cancer*. 2017; 17: 20-37.
206. da Silva PB, Machado RTA, Pironi AM, Alves RC, de Araújo PR, Dragalzew AC, et al. Recent Advances in the Use of Metallic Nanoparticles with Antitumoral Action-Review. *Curr Med Chem*. 2019; 2108-2146.
207. Machado R, Pironi A, Alves R, Dragalzew A, Dalberto I, Chorilli M. Recent Advances in the Use of Metallic Nanoparticles with Antitumoral Action-Review. *Curr Med Chem*. 2019; 26: 2108-2146.
208. Al-Sheddi ES, Farshori NN, Al-Oqail MM, Al-Massarani SM, Saquib Q, Wahab R, et al. Anticancer Potential of Green Synthesized Silver Nanoparticles Using Extract of Nepeta deflersiana against Human Cervical Cancer Cells (HeLa). *Bioinorg Chem Appl*. 2018; 9390784.
209. Gurunathan S, Qasim M, Park C, Yoo H, Kim JH, Hong K. Cytotoxic Potential and Molecular Pathway Analysis of Silver Nanoparticles in Human Colon Cancer Cells HCT116. *Int J Mol Sci*. 2018; 19: 2269.
210. Yuan YG, Peng QL, Gurunathan S. Silver nanoparticles enhance the apoptotic potential of gemcitabine in human ovarian cancer cells: combination therapy for effective cancer treatment. *Int J Nanomedicine*. 2017; 12: 6487-6502.

211. Zielinska E, Zauszkiewicz-Pawlak A, Wojcik M, Inkielewicz-Stepniak I. Silver nanoparticles of different sizes induce a mixed type of programmed cell death in human pancreatic ductal adenocarcinoma. *Oncotarget*. 2018; 9: 4675-4697.
212. Fard NN, Noorbazargan H, Mirzaie A, Hedayati Ch M, Moghimiyani Z, Rahimi A. Biogenic synthesis of AgNPs using *Artemisia oliveriana* extract and their biological activities for an effective treatment of lung cancer. *Artif Cells Nanomed Biotechnol*. 2018; 46: S1047-S1058.
213. Ahmadian E, Dizaj SM, Rahimpour E, Hasanzadeh A, Eftekhari A, Hosain Zadegan H, et al. Effect of silver nanoparticles in the induction of apoptosis on human hepatocellular carcinoma (HepG2) cell line. *Mater Sci Eng C Mater Biol Appl*. 2018; 93: 465-471.
214. Tavakoli F, Jahanban-Esfahlan R, Seidi K, Jabbari M, Behzadi R, Pilehvar-Soltanahmadi Y, et al. Effects of nano-encapsulated curcumin-chrysin on telomerase, MMPs and TIMPs gene expression in mouse B16F10 melanoma tumour model. *Artif Cells Nanomed Biotechnol*. 2018; 46: 75-86.
215. Kovacs D, Igaz N, Keskeny C, Belteky P, Toth T, Gaspar R, et al. Silver nanoparticles defeat p53-positive and p53-negative osteosarcoma cells by triggering mitochondrial stress and apoptosis. *Sci Rep*. 2016; 6: 27902.
216. Yeamin S, Datta HK, Chaudhuri S, Malik D, Bandyopadhyay A. In-vitro anti-cancer activity of shape controlled silver nanoparticles (AgNPs) in various organ specific cell lines. *J Mol Liq*. 2017; 242: 757-766.
217. Wu M, Guo H, Liu L, Liu Y, Xie L. Size-dependent cellular uptake and localization profiles of silver nanoparticles. *Int J Nanomedicine*. 2019; 14: 4247-4259.
218. Liu W, Wu Y, Wang C, Li HC, Wang T, Liao CY, et al. Impact of silver nanoparticles on human cells: effect of particle size. *Nanotoxicology*. 2010; 4: 319-330.
219. Fullstone G, Wood J, Holcombe M, Battaglia G. Modelling the Transport of Nanoparticles under Blood Flow using an Agent-based Approach. *Sci Rep*. 2015; 5: 10649.
220. Avalos A, Haza AI, Mateo D, Morales P. Cytotoxicity and ROS production of manufactured silver nanoparticles of different sizes in hepatoma and leukemia cells. *J Appl Toxicol*. 2014; 34: 413-423.
221. Roy E, Patra S, Saha S, Kumar D, Madhuri R, Sharma PK. Shape effect on the fabrication of imprinted nanoparticles: Comparison between spherical-, rod-, hexagonal-, and flower-shaped nanoparticles. *Chem Eng J*. 2017; 321: 195-206.
222. Sen Gupta A. Role of particle size, shape, and stiffness in design of intravascular drug delivery systems: insights from computations, experiments, and nature. *Wiley Interdiscip Rev Nanomed Nanobiotechnol*. 2016; 8: 255-270.
223. Li Y, Kroger M, Liu WK. Shape effect in cellular uptake of PEGylated nanoparticles: comparison between sphere, rod, cube and disk. *Nanoscale*. 2015; 7: 16631-16646.
224. He Y, Park K. Effects of the microparticle shape on cellular uptake. *Mol Pharm*. 2016; 13: 2164-2171.
225. Ahmed MJ, Murtaza G, Rashid F, Iqbal J. Eco-friendly green synthesis of silver nanoparticles and their potential applications as antioxidant and anticancer agents. *Drug Dev Ind Pharm*. 2019; 45: 1682-1694.
226. Sriram MJ, Kanth SB, Kalishwaralal K, Gurunathan S. Antitumor activity of silver nanoparticles in Dalton's lymphoma ascites tumor model. *Int J Nanomedicine*. 2010; 5: 753-762.
227. Hamouda RA, Hussein MH, Abo-elmagd RA, Bawazir SS. Synthesis and biological characterization of silver nanoparticles derived from the cyanobacterium *Oscillatoria limnetica*. *Sci Rep*. 2019; 9: 1-17.
228. Xiao H, Chen Y, Alnaggar M. Silver nanoparticles induce cell death of colon cancer cells through impairing cytoskeleton and membrane nanostructure. *Micron*. 2019; 126: 102750.
229. Vasanth K, Ilango K, MohanKumar R, Agrawal A, Dubey GP. Anticancer activity of *Moringa oleifera* mediated silver nanoparticles on human cervical carcinoma cells by apoptosis induction. *Colloids Surf B Biointerfaces*. 2014; 117: 354-359.
230. Mousavi B, Tafvizi F, Zaker Bostanabad S. Green synthesis of silver nanoparticles using *Artemisia turcomanica* leaf extract and the study of anti-cancer effect and apoptosis induction on gastric cancer cell line (AGS). *Artif Cells Nanomed Biotechnol*. 2018; 46: 499-510.
231. Suresh AK, Pelletier DA, Wang W, Morrell-Falvey JL, Gu B, Doktycz MJ. Cytotoxicity induced by engineered silver nanocrystallites is dependent on surface coatings and cell types. *Langmuir*. 2012; 28: 2727-2735.
232. Mahmood M, Casciano DA, Mocan T, Iancu C, Xu Y, Mocan L, et al. Cytotoxicity and biological effects of functional nanomaterials delivered to various cell lines. *J Appl Toxicol*. 2010; 30: 74-83.
233. Zhang XF, Shen W, Gurunathan S. Silver Nanoparticle-Mediated Cellular Responses in Various Cell Lines: An *in vitro* Model. *Int J Mol Sci*. 2016; 17:101603.
234. Schlinkert P, Casals E, Boyles M, Tischler U, Hornig E, Tran N, et al. The oxidative potential of differently charged silver and gold nanoparticles on three human lung epithelial cell types. *J Nanobiotechnology*. 2015; 13: 1.
235. Monopoli MP, Bombelli FB, Dawson KA. Nanoparticle coronas take shape. *Nat Nanotechnol*. 2010; 6: 11-12.
236. Eigenheer R, Castellanos ER, Nakamoto MY, Gerner KT, Lampe AM, Wheeler KE. Silver nanoparticle protein corona composition compared across engineered particle properties and environmentally relevant reaction conditions. *Environ Sci: Nano*. 2014; 1: 238-247.
237. Gorshkov V, Bubis JA, Solovyeva EM, Gorshkov MV, Kjeldsen F. Protein corona formed on silver nanoparticles in blood plasma is highly selective and resistant to physicochemical changes of the solution. *Environ Sci Nano*. 2019; 6: 1089-1098.
238. Barbalinardo M, Caicci F, Cavallini M, Gentili D. Protein corona mediated uptake and cytotoxicity of silver nanoparticles in mouse embryonic fibroblast. *Small*. 2018; 201801219.
239. Barabadi H, Hosseini O, Kamali KD, Shoushtari FJ, Rashedi M, Haghi-Aminjan H, et al. Emerging theranostic silver nanomaterials to combat lung cancer: a systematic review. *J Clust Sci*. 2019; p: 1-10.
240. Chen B, Zhang Y, Yang Y, Chen S, Xu A, Wu L, et al. Involvement of telomerase activity inhibition and telomere dysfunction in silver nanoparticles anticancer effects. *Nanomedicine*. 2018; 13: 2067-2082.
241. Farah MA, Ali MA, Chen SM, Li Y, Al-Hemaid FM, Abou-Tarboush FM, et al. Silver nanoparticles synthesized from *Adenium obesum* leaf extract induced DNA damage, apoptosis and autophagy via generation of reactive oxygen species. *Colloids Surf B Biointerfaces*. 2016; 141: 158-169.
242. Mytych J, Zebrowski J, Lewinska A, Wnuk M. Prolonged Effects of Silver Nanoparticles on p53/p21 Pathway-Mediated Proliferation, DNA Damage Response, and Methylation Parameters in HT22 Hippocampal Neuronal Cells. *Mol Neurobiol*. 2017; 54: 1285-1300.
243. Yang T, Yao Q, Cao F, Liu Q, Liu B, Wang XH. Silver nanoparticles inhibit the function of hypoxia-inducible factor-1 and target genes: insight into the cytotoxicity and antiangiogenesis. *Int J Nanomedicine*. 2016; 11: 6679-6692.
244. Panzarini E, Mariano S, Vergallo C, Carata E, Fimia GM, Mura F, et al. Glucose capped silver nanoparticles induce cell cycle arrest in HeLa cells. *Toxicol In vitro*. 2017; 41: 64-74.
245. Kemp MM, Kumar A, Mousa S, Dyskin E, Yalcin M, Ajayan P, et al. Gold and silver nanoparticles conjugated with heparin derivative possess anti-angiogenesis properties. *Nanotechnology*. 2009; 20: 455104.
246. Swanner J, Fahrenholtz CD, Tenvooren J, Bernish BW, Sears JJ, Hooker A, et al. Silver nanoparticles selectively treat triple-negative breast cancer cells without affecting non-malignant breast epithelial cells *in vitro* and *in vivo*. *FASEB Bioadv*. 2019; 1: 639-660.
247. Jeong J-K, Gurunathan S, Kang M-H, Han JW, Das J, Choi Y-J, et al. Hypoxia-mediated autophagic flux inhibits silver nanoparticle-triggered apoptosis in human lung cancer cells. *Sci Rep*. 2016; 6: 21688.
248. Asharani PV, Hande MP, Valiyaveetil S. Anti-proliferative activity of silver nanoparticles. *BMC Cell Biol*. 2009; 10: 65.
249. Mukherjee S, Chowdhury D, Kotcherlakota R, Patra S, B V, Bhadra MP, et al. Potential theranostics application of bio-synthesized silver nanoparticles (4-in-1 system). *Theranostics*. 2014; 4: 316-335.
250. George BPA, Kumar N, Abrahamse H, Ray SS. Apoptotic efficacy of multifaceted biosynthesized silver nanoparticles on human adenocarcinoma cells. *Sci Rep*. 2018; 8: 14368.
251. Prasad S, Gupta SC, Tyagi AK. Reactive oxygen species (ROS) and cancer: Role of antioxidative nutraceuticals. *Cancer Lett*. 2017; 387: 95-105.
252. Mao BH, Chen ZY, Wang YJ, Yan SJ. Silver nanoparticles have lethal and sublethal adverse effects on development and longevity by inducing ROS-mediated stress responses. *Sci Rep*. 2018; 8: 2445.
253. Nayak D, Kumari M, Rajachandrar S, Ashe S, Thatapudi NC, Nayak B. Biofilm impeding AgNPs target skin carcinoma by inducing mitochondrial membrane depolarization mediated through ROS production. *ACS Appl Mater Interfaces*. 2016; 8: 28538-28553.
254. Mukherjee S, Chowdhury D, Kotcherlakota R, Patra S. Potential theranostics application of bio-synthesized silver nanoparticles (4-in-1 system). *Theranostics*. 2014; 4: 316.
255. Rao PV, Nallappan D, Madhavi K, Rahman S, Jun Wei L, Gan SH. Phytochemicals and Biogenic Metallic Nanoparticles as Anticancer Agents. *Oxid Med Cell Longev*. 2016; 2016: 1-15.
256. Garrido C, Galluzzi L, Brunet M, Puig PE, Didelot C, Kroemer G. Mechanisms of cytochrome c release from mitochondria. *Cell Death Differ*. 2006; 13: 1423-1433.
257. Hsin YH, Chen CF, Huang S, Shih TS, Lai PS, Chueh PJ. The apoptotic effect of nanosilver is mediated by a ROS- and JNK-dependent mechanism involving the mitochondrial pathway in NIH3T3 cells. *Toxicol Lett*. 2008; 179: 130-139.
258. Barcinska E, Wierzbicka J, Zauszkiewicz-Pawlak A, Jaczewicz D, Dabrowska A, Inkielewicz-Stepniak I. Role of Oxidative and Nitro-Oxidative Damage in Silver Nanoparticles Cytotoxic Effect against Human Pancreatic Ductal Adenocarcinoma Cells. *Oxid Med Cell Longev*. 2018; 8251961.
259. Baharara J, Namvar F, Ramezani T, Mousavi M, Mohamad R. Silver nanoparticles biosynthesized using *Achillea biebersteinii* flower extract: apoptosis induction in MCF-7 cells via caspase activation and regulation of Bax and Bcl-2 gene expression. *Molecules*. 2015; 20: 2693-2706.
260. AshaRani P, Sethu S, Lim HK, Balaji G, Valiyaveetil S, Hande MP. Differential regulation of intracellular factors mediating cell cycle, DNA repair and inflammation following exposure to silver nanoparticles in human cells. *Genome Integr*. 2012; 3: 2.
261. Al-Sheddi ES, Farshori NN, Al-Oqail MM, Al-Massarani SM, Saquib Q, Wahab R, et al. Anticancer Potential of Green Synthesized Silver Nanoparticles Using Extract of *Nepeta deflersiana* against Human Cervical Cancer Cells (HeLa). *Bioinorg Chem Appl*. 2018; p:1-12.
262. Bandyopadhyay A, Roy B, Shaw P, Mondal MK, Chowdhury P, et al. Cytotoxic effect of green synthesized silver nanoparticles in MCF7 and MDA-MB-231 human breast cancer cells *in vitro*. *Nucleus*. 2019; p: 191-202.
263. Wang M, Zhao J, Zhang L, Wei F, Lian Y, Wu Y, et al. Role of tumor microenvironment in tumorigenesis. *J Cancer*. 2017; 8: 761-773.

264. Quail DF, Joyce JA. Microenvironmental regulation of tumor progression and metastasis. *Nat Med.* 2013; 19: 1423-1437.
265. Joyce JA, Pollard JW. Microenvironmental regulation of metastasis. *Nat Rev Cancer.* 2009; 9: 239-252.
266. Kim Y, Lin Q, Glazer PM, Yun Z. Hypoxic tumor microenvironment and cancer cell differentiation. *Curr Mol Med.* 2009; 9: 425-434.
267. Gialeli C, Theocharis AD, Karamanos NK. Roles of matrix metalloproteinases in cancer progression and their pharmacological targeting. *FEBS J.* 2011; 278: 16-27.
268. Jabłońska-Trypuć A, Matejczyk M, Rosochacki S. Matrix metalloproteinases (MMPs), the main extracellular matrix (ECM) enzymes in collagen degradation, as a target for anticancer drugs. *J Enzyme Inhib Med Chem.* 2016; 31: 177-183.
269. Buttacavoli M, Albanese NN, Di Cara G, Alduina R, Faleri C, Gallo M, et al. Anticancer activity of biogenerated silver nanoparticles: an integrated proteomic investigation. *Oncotarget.* 2018; 9: 9685.
270. Fulbright LE, Ellermann M, Arthur JC. The microbiome and the hallmarks of cancer. *PLoS Pathog.* 2017; 13: e1006480.
271. Gurunathan S, Lee KJ, Kalishwaralal K, Sheikpranbabu S, Vaidyanathan R, Eom SH. Antiangiogenic properties of silver nanoparticles. *Biomaterials.* 2009; 30: 6341-6350.
272. Kalishwaralal K, Banumathi E, Ram Kumar Pandian S, Deepak V, Muniyandi J, Eom SH, et al. Silver nanoparticles inhibit VEGF induced cell proliferation and migration in bovine retinal endothelial cells. *Colloids Surf B Biointerfaces.* 2009; 73: 51-57.
273. Hu X, Saravanakumar K, Jin T, Wang M-H. Mycosynthesis, characterization, anticancer and antibacterial activity of silver nanoparticles from endophytic fungus *Talaromyces purpureogenus*. *Int J Nanomedicine.* 2019; 14: 3427-3438.
274. Chen Z, Ye X, Qingkui G, Wenliang Q, Wen Z, Ning W, et al. Anticancer activity of green synthesised AgNPs from *Cymbopogon citratus* (LG) against lung carcinoma cell line A549. *IET Nanobiotechnol.* 2018; 13: 178-182.
275. Jeyaraj M, Sathishkumar G, Sivanandhan G, MubarakAli D, Rajesh M, Arun R, et al. Biogenic silver nanoparticles for cancer treatment: an experimental report. *Colloids Surf B Biointerfaces.* 2013; 106: 86-92.
276. Baharara J, Namvar F, Ramezani T, Mousavi M, Mohamad R. Silver nanoparticles biosynthesized using *Achillea biebersteinii* flower extract: apoptosis induction in MCF-7 cells via caspase activation and regulation of Bax and Bcl-2 gene expression. *Molecules.* 2015; 20: 2693-2706.
277. Mussa Farkhani S, Asoudeh Fard A, Zakeri-Milani P, Shahbazi Mojarrad J, Valizadeh H. Enhancing antitumor activity of silver nanoparticles by modification with cell-penetrating peptides. *Artif Cells Nanomed Biotechnol.* 2017; 45: 1029-1035.
278. El-Naggar NE-A, Hussein MH, El-Sawah AA. Phycobiliprotein-mediated synthesis of biogenic silver nanoparticles, characterization, *in vitro* and *in vivo* assessment of anticancer activities. *Sci Rep.* 2018; 8: 8925.
279. Bhanumathi R, Vimala K, Shanthi K, Thangaraj R, Kannan S. Bioformulation of silver nanoparticles as berberine carrier cum anticancer agent against breast cancer. *Nouv J Chim.* 2017; 41: 14466-14477.
280. Dadashpour M, Firouzi-Amandi A, Pourhassan-Moghaddam M, Maleki MJ, Soozangar N, Jeddi F, et al. Biomimetic synthesis of silver nanoparticles using *Matricaria chamomilla* extract and their potential anticancer activity against human lung cancer cells. *Mater Sci Eng C.* 2018; 92: 902-912.
281. Ghanbar F, Mirzaie A, Ashrafi F, Noorbazargan H, Jalali MD, Salehi S, et al. Antioxidant, antibacterial and anticancer properties of phyto-synthesised *Artemisia qutensis* Podlech extract mediated AgNPs. *IET Nanobiotechnol.* 2016; 11: 485-492.
282. Kuppusamy P, Ichwan SJ, Al-Zikri PNH, Suriyah WH, Soundharajan I, Govindan N, et al. *In vitro* anticancer activity of Au, Ag nanoparticles synthesized using *Commelina nudiflora* L. aqueous extract against HCT-116 colon cancer cells. *Biol Trace Elem Res.* 2016; 173: 297-305.
283. Fageria L, Pareek V, Dilip RV, Bhargava A, Pasha SS, Laskar IR, et al. Biosynthesized protein-capped silver nanoparticles induce ros-dependent proapoptotic signals and pro-survival autophagy in cancer cells. *ACS omega.* 2017; 2: 1489-1504.
284. Zhang Y, Lu H, Yu D, Zhao D. AgNPs and Ag/C225 exert anticancerous effects via cell cycle regulation and cytotoxicity enhancement. *J Nanomater.* 2017; 7920368.
285. He Y, Du Z, Ma S, Cheng S, Jiang S, Liu Y, et al. Biosynthesis, antibacterial activity and anticancer effects against prostate cancer (PC-3) cells of silver nanoparticles using *Dimocarpus Longan* Lour. peel extract. *Nanoscale Res Lett.* 2016; 11: 300.
286. Sriram MI, Kanth SBM, Kalishwaralal K, Gurunathan S. Antitumor activity of silver nanoparticles in Dalton's lymphoma ascites tumor model. *Int J Nanomedicine.* 2010; 5: 753-762.
287. Chakraborty B, Pal R, Ali M, Singh LM, Rahman DS, Ghosh SK, et al. Immunomodulatory properties of silver nanoparticles contribute to anticancer strategy for murine fibrosarcoma. *Nanoscale Res Lett.* 2016; 13: 191-205.
288. Tian J, Wong KK, Ho CM, Lok CN, Yu WY, Che CM, et al. Topical delivery of silver nanoparticles promotes wound healing. *ChemMedChem.* 2007; 2: 129-136.
289. Rigo C, Ferroni L, Tocco I, Roman M, Munivrana I, Gardin C, et al. Active silver nanoparticles for wound healing. *Int J Mol Sci.* 2013; 14: 4817-4840.
290. Liu X, Lee PY, Ho CM, Lui VC, Chen Y, Che CM, et al. Silver nanoparticles mediate differential responses in keratinocytes and fibroblasts during skin wound healing. *ChemMedChem.* 2010; 5: 468-475.
291. Franková J, Pivodová V, Vágnerová H, Juráňová J, Ulrichová J. Effects of silver nanoparticles on primary cell cultures of fibroblasts and keratinocytes in a wound-healing model. *J Appl Biomater Funct Mater.* 2016; 14: 137-142.
292. Soucacos PN, Johnson EO, Babis G. An update on recent advances in bone regeneration. *Injury.* 2008; 39: S1-S4.
293. Qing T, Mahmood M, Zheng Y, Biris AS, Shi L, Casciano DA. A genomic characterization of the influence of silver nanoparticles on bone differentiation in MC3T3-E1 cells. *J Appl Toxicol.* 2018; 38: 172-179.
294. Zhang R, Lee P, Lui VC, Chen Y, Liu X, Lok CN, et al. Silver nanoparticles promote osteogenesis of mesenchymal stem cells and improve bone fracture healing in osteogenesis mechanism mouse model. *Nanomed Nanotechnol Bio Med.* 2015; 11: 1949-1959.
295. Velusamy P, Su CH, Venkat Kumar G, Adhikary S, Pandian K, Gopinath SC, et al. Biopolymers Regulate Silver Nanoparticle under Microwave Irradiation for Effective Antibacterial and Antibiofilm Activities. *PLoS One.* 2016; 11: e0157612.
296. Talbird SE, Graham J, Mauskopf J, Masseria C, Krishnarajah G. Impact of tetanus, diphtheria, and acellular pertussis (Tdap) vaccine use in wound management on health care costs and pertussis cases. *J Manag Care Spec Pharm.* 2015; 21: 88-99.
297. Xu Y, Tang H, Liu J-h, Wang H, Liu Y. Evaluation of the adjuvant effect of silver nanoparticles both *in vitro* and *in vivo*. *Toxicol Lett.* 2013; 219: 42-48.
298. Asgary V, Kord Mafi O, Khosravy MS, Janani A, Namvar Asl N, Bashar R, et al. Evaluation of the Effect of Silver Nanoparticles on Induction of Neutralizing Antibodies against Inactivated Rabies Virus. *Vaccine Res.* 2014; 1: 31-34.
299. Asgary V, Shoari A, Baghbani-Arani F, Shandiz SAS, Khosravy MS, Janani A, et al. Green synthesis and evaluation of silver nanoparticles as adjuvant in rabies veterinary vaccine. *Int J Nanomedicine.* 2016; 11: 3597-3605.
300. Association AD. 9. Pharmacologic approaches to glycemic treatment: Standards of Medical Care in Diabetes—2019. *Diabetes care.* 2019; 42: 90-102.
301. Sengottaiyan A, Aravinthan A, Sudhakar C, Selvam K, Srinivasan P, Govarthanam M, et al. Synthesis and characterization of Solanum nigrum-mediated silver nanoparticles and its protective effect on alloxan-induced diabetic rats. *J Nanostructure Chem.* 2016; 6: 41-48.
302. Hussein J, El Naggar ME, Latif YA, Medhat D, El Bana M, Refaat E, et al. Solvent-free and one pot synthesis of silver and zinc nanoparticles: activity toward cell membrane component and insulin signaling pathway in experimental diabetes. *Colloids Surf B Biointerfaces.* 2018; 170: 76-84.
303. Yamamoto YS, Ishikawa M, Ozaki Y, Itoh T. Fundamental studies on enhancement and blinking mechanism of surface-enhanced Raman scattering (SERS) and basic applications of SERS biological sensing. *Front Phys.* 2014; 9: 31-46.
304. Jiang Y, Zhang X, Pei L, Yue S, Ma L, Zhou L, et al. Silver nanoparticles modified two-dimensional transition metal carbides as nanocarriers to fabricate acetylcholinesterase-based electrochemical biosensor. *Chem Eng J.* 2018; 339: 547-556.
305. Anderson K, Poulter B, Dudgeon J, Li S-E, Ma X. A highly sensitive nonenzymatic glucose biosensor based on the regulatory effect of glucose on electrochemical behaviors of colloidal silver nanoparticles on MoS<sub>2</sub>. *Sensors.* 2017; 17: 1807.
306. Zeng F, Xu D, Zhan C, Liang C, Zhao W, Zhang J, et al. Surfactant-free synthesis of graphene oxide coated silver nanoparticles for sers biosensing and intracellular drug delivery. *ACS Appl Nano Mater.* 2018; 1: 2748-2753.
307. Guo C, Irudayaraj J. Fluorescent Ag clusters via a protein-directed approach as a Hg(II) ion sensor. *Anal Chem.* 2011; 83: 2883-2889.
308. Sun Z, Li S, Jiang Y, Qiao Y, Zhang L, Xu L, et al. Silver nanoclusters with specific ion recognition modulated by ligand passivation toward fluorimetric and colorimetric copper analysis and biological imaging. *Sci Rep.* 2016; 6: 20553.
309. Guo W, Yuan J, Dong Q, Wang E. Highly sequence-dependent formation of fluorescent silver nanoclusters in hybridized DNA duplexes for single nucleotide mutation identification. *J Am Chem Soc.* 2010; 132: 932-934.
310. Singh SP, Bhargava C, Dubey V, Mishra A, Singh Y. Silver nanoparticles: Biomedical applications, toxicity, and safety issues. *Int J Res Pharm Pharm Sci.* 2017; 4: 01-10.
311. Lansdown AB. Silver in health care: antimicrobial effects and safety in use. *Curr Probl Dermatol.* 2006; p: 17-34.
312. Saha SK, Das S, Chowdhury P, Saha SK. Biocompatibility of a sonochemically synthesized poly(N-isopropyl acrylamide)/silica nanocomposite. *RSC Adv.* 2014; 4: 14457.
313. Wang L, Zhang T, Li P, Huang W, Tang J, Wang P, et al. Use of synchrotron radiation-analytical techniques to reveal chemical origin of silver-nanoparticle cytotoxicity. *ACS nano.* 2015; 9: 6532-6547.
314. William E, Donald M. Argyria. The pharmacology of silver. *Arch Dermatol.* 1940; 41: 995.
315. Hiep NT, Khon HC, Niem VVT, Toi VV, Ngoc Quyen T, Hai ND, et al. Microwave-assisted synthesis of chitosan/polyvinyl alcohol silver nanoparticles gel for wound dressing applications. *Int J Polym Sci.* 2016; 1584046.
316. Wadhwa A, Fung M. Systemic argyria associated with ingestion of colloidal silver. *Dermatol Online J.* 2005; 11: 12.
317. DiVincenzo G, Giordano C, Schriever L. Biologic monitoring of workers exposed to silver. *Int Arch Occup Environ Health.* 1985; 56: 207-215.

318. Baker JW, Leidy KL, Smith KM, Okeke S. Argyria associated with use of systemic colloidal silver. *Fed Pract.* 2011; 28: 39-42.
319. George R, Merten S, Wang TT, Kennedy P, Maitz P. *In vivo* analysis of dermal and systemic absorption of silver nanoparticles through healthy human skin. *Australas J Dermatol.* 2014; 55: 185-190.
320. Lekki J, Stachura Z, Dąbrosz W, Stachura J, Menzel F, Reinert T, et al. On the follicular pathway of percutaneous uptake of nanoparticles: Ion microscopy and autoradiography studies. *Nucl Instrum Methods Phys Res B.* 2007; 260: 174-177.
321. Lademann J, Weigmann H-J, Rickmeyer C, Barthelmes H, Schaefer H, Mueller G, et al. Penetration of titanium dioxide microparticles in a sunscreen formulation into the horny layer and the follicular orifice. *Skin Pharmacol Physiol.* 1999; 12: 247-256.
322. Jung S, Otberg N, Thiede G, Richter H, Sterry W, Panzner S, et al. Innovative liposomes as a transfollicular drug delivery system: penetration into porcine hair follicles. *J Invest Dermatol.* 2006; 126: 1728-1732.
323. Tak YK, Pal S, Naoghare PK, Rangasamy S, Song JM. Shape-dependent skin penetration of silver nanoparticles: does it really matter? *Sci Rep.* 2015; 5: 16908.
324. Laresse FF, D'Agostin F, Crosera M, Adami G, Renzi N, Bovenzi M, et al. Human skin penetration of silver nanoparticles through intact and damaged skin. *Toxicology.* 2009; 255: 33-37.
325. Szymd R, Goralczyk AG, Skalniak L, Cierniak A, Lipert B, Filon FL, et al. Effect of silver nanoparticles on human primary keratinocytes. *Biol Chem.* 2013; 394: 113-123.
326. Maneewattanapinyo P, Banlunara W, Thammacharoen C, Ekgasit S, Kaewamatawong T. An evaluation of acute toxicity of colloidal silver nanoparticles. *J Vet Med Sci.* 2011; p: 11-0038.
327. Wu Y, Zhou Q, Li H, Liu W, Wang T, Jiang G. Effects of silver nanoparticles on the development and histopathology biomarkers of Japanese medaka (*Oryzias latipes*) using the partial-life test. *Aquat Toxicol.* 2010; 100: 160-167.
328. Shimada A, Kawamura N, Okajima M, Kaewamatawong T, Inoue H, Morita T. Translocation pathway of the intratracheally instilled ultrafine particles from the lung into the blood circulation in the mouse. *Toxicol Pathol.* 2006; 34: 949-957.
329. Kaewamatawong T, Shimada A, Okajima M, Inoue H, Morita T, Inoue K, et al. Acute and subacute pulmonary toxicity of low dose of ultrafine colloidal silica particles in mice after intratracheal instillation. *Toxicol Pathol.* 2006; 34: 958-965.
330. Kaewamatawong T, Banlunara W, Maneewattanapinyo P, Thammacharoen C, Ekgasit S. Acute pulmonary toxicity caused by single intratracheal instillation of various doses of colloidal silver nanoparticles in mice: Pathological changes, particle bioaccumulation and metallothionein protein expression. *The Thai J Vet Med.* 2013; 43: 383-390.
331. Recordati C, De Maglie M, Bianchessi S, Argenti S, Cella C, Mattiello S, et al. Tissue distribution and acute toxicity of silver after single intravenous administration in mice: nano-specific and size-dependent effects. *Part Fibre Toxicol.* 2015; 13: 12.
332. Heydarnejad MS, Yarmohammadi-Samani P, Mobini Dehkordi M, Shadkhat M, Rahnama S. Histopathological effects of nanosilver (Ag-NPs) in liver after dermal exposure during wound healing. *Nanomed J.* 2014; 1: 191-197.
333. Sadauskas E, Wallin H, Stoltenberg M, Vogel U, Doering P, Larsen A, et al. Kupffer cells are central in the removal of nanoparticles from the organism. *Part Fibre Toxicol.* 2007; 4: 10.
334. Davies LC, Jenkins SJ, Allen JE, Taylor PR. Tissue-resident macrophages. *Nat Immunol.* 2013; 14: 986-995.
335. Buzea C, Pacheco II, Robbie K. Nanomaterials and nanoparticles: sources and toxicity. *Biointerphases.* 2007; 2: 17-71.
336. Peters A, Veronesi B, Calderón-Garcidueñas L, Gehr P, Chen LC, Geiser M, et al. Translocation and potential neurological effects of fine and ultrafine particles a critical update. *Part Fibre Toxicol.* 2006; 3: 13.
337. Sun C, Yin N, Wen R, Liu W, Jia Y, Hu L, et al. Silver nanoparticles induced neurotoxicity through oxidative stress in rat cerebral astrocytes is distinct from the effects of silver ions. *Neurotoxicology.* 2016; 52: 210-221.
338. Xu L, Dan M, Shao A, Cheng X, Zhang C, Yokel RA, et al. Silver nanoparticles induce tight junction disruption and astrocyte neurotoxicity in a rat blood-brain barrier primary triple coculture model. *Int J Nanomedicine.* 2015; 10: 6105-6119.
339. Huang C-L, Hsiao I-L, Lin H-C, Wang C-F, Huang Y-J, Chuang C-Y. Silver nanoparticles affect on gene expression of inflammatory and neurodegenerative responses in mouse brain neural cells. *Environ Res.* 2015; 136: 253-263.
340. Kim W-Y, Kim J, Park JD, Ryu HY, Yu IJ. Histological study of gender differences in accumulation of silver nanoparticles in kidneys of Fischer 344 rats. *J Toxicol Environ Health A.* 2009; 72: 1279-1284.
341. Kim YS, Song MY, Park JD, Song KS, Ryu HR, Chung YH, et al. Subchronic oral toxicity of silver nanoparticles. *Part Fibre Toxicol.* 2010; 7: 20.
342. Milić M, Leitinger G, Pavičić I, Zebić Avdičević M, Dobrović S, Goessler W, et al. Cellular uptake and toxicity effects of silver nanoparticles in mammalian kidney cells. *Journal of Applied Toxicology.* 2015; 35: 581-592.
343. Guo H, Zhang J, Boudreau M, Meng J, Yin J-j, Liu J, et al. Intravenous administration of silver nanoparticles causes organ toxicity through intracellular ROS-related loss of inter-endothelial junction. *Part Fibre Toxicol.* 2015; 13: 21.
344. Klippstein R, Fernandez-Montesinos R, Castillo PM, Zaderenko AP, Pozo D. Silver nanoparticles interactions with the immune system: implications for health and disease. *Silver Nanoparticles.* Seville, Spain: InTech. 2010.
345. Shin S-H, Ye M-K, Kim H-S, Kang H-S. The effects of nano-silver on the proliferation and cytokine expression by peripheral blood mononuclear cells. *Int Immunopharmacol.* 2007; 7: 1813-1818.
346. Xue Y, Zhang S, Huang Y, Zhang T, Liu X, Hu Y, et al. Acute toxic effects and gender-related biokinetics of silver nanoparticles following an intravenous injection in mice. *J Appl Toxicol.* 2012; 32: 890-899.
347. Zhang X-F, Choi Y-J, Han JW, Kim E, Park JH, Gurunathan S, et al. Differential nanorepotoxicity of silver nanoparticles in male somatic cells and spermatogonial stem cells. *Int J Nanomedicine.* 2015; 10: 1335-1357.
348. Fathi N, Hoseinipannah SM, Alizadeh Z, Assari MJ, Moghimbeigi A, Mortazavi M, et al. The effect of silver nanoparticles on the reproductive system of adult male rats: A morphological, histological and DNA integrity study. *Adv Clin Exp Med.* 2019; 28: 299-305.
349. Chen SX, Yang XZ, Deng Y, Huang J, Li Y, Sun Q, et al. Silver nanoparticles induce oocyte maturation in zebrafish (*Danio rerio*). *Chemosphere.* 2017; 170: 51-60.
350. Samberg ME, Oldenburg SJ, Monteiro-Riviere NA. Evaluation of silver nanoparticle toxicity in skin *in vivo* and keratinocytes *in vitro*. *Environ Health Perspect.* 2010; 118: 407-413.
351. Yang L, Kuang H, Zhang W, Aguilar ZP, Wei H, Xu H. Comparisons of the biodistribution and toxicological examinations after repeated intravenous administration of silver and gold nanoparticles in mice. *Sci Rep.* 2017; 7: 3303.
352. Park E-J, Bae E, Yi J, Kim Y, Choi K, Lee SH, et al. Repeated-dose toxicity and inflammatory responses in mice by oral administration of silver nanoparticles. *Environ Toxicol Pharmacol.* 2010; 30: 162-168.
353. Wang X, Ji Z, Chang CH, Zhang H, Wang M, Liao YP, et al. Use of coated silver nanoparticles to understand the relationship of particle dissolution and bioavailability to cell and lung toxicological potential. *Small.* 2014; 10: 385-398.
354. Pani JP, Singh R. Small Size Nanosilver Multi Organ Toxicity: A Higher Dose Negative Response in In-Vivo and In-Vitro Experimental Application. *Biomed J Sci & Tech Res.* 2017; 1: 000360.
355. Yousef MI, Abuzreda AA, Kamel MAE-N. Neurotoxicity and inflammation induced by individual and combined exposure to iron oxide nanoparticles and silver nanoparticles. *J Taibah Univ Sci.* 2019; 13: 570-578.
356. Sarhan OMM, Hussein RM. Effects of intraperitoneally injected silver nanoparticles on histological structures and blood parameters in the albino rat. *Int J Nanomedicine.* 2014; 9: 1505-1517.
357. Wen H, Dan M, Yang Y, Lyu J, Shao A, Cheng X, et al. Acute toxicity and genotoxicity of silver nanoparticle in rats. *PLoS One.* 2017; 12: e0185554.
358. De Jong WH, Van Der Ven LT, Sleijffers A, Park MV, Jansen EH, Van Loveren H, et al. Systemic and immunotoxicity of silver nanoparticles in an intravenous 28 days repeated dose toxicity study in rats. *Biomaterials.* 2013; 34: 8333-8343.
359. Kim K-T, Tanguay RL. The role of chorion on toxicity of silver nanoparticles in the embryonic zebrafish assay. *Environ Health Toxicol.* 2014; 29: e2014021.
360. Thiagarajan K, Bharti VK, Tyagi S, Tyagi PK, Ahuja A, Kumar K, et al. Synthesis of non-toxic, biocompatible, and colloidal stable silver nanoparticle using egg-white protein as capping and reducing agents for sustainable antibacterial application. *RSC adv.* 2018; 8: 23213-23229.
361. Kim JH, Lee SH, Cha YJ, Hong SJ, Chung SK, Park TH, et al. C. elegans-on-a-chip for *in situ* and *in vivo* Ag nanoparticles' uptake and toxicity assay. *Sci Rep.* 2017; 7: 40225.
362. Gao X, Topping VD, Keltner Z, Sprando RL, Yourick JJ. Toxicity of nano-and ionic silver to embryonic stem cells: a comparative toxicogenomic study. *J Nanobiotechnology.* 2017; 15: 31.
363. Gonzalez-Carter DA, Leo BF, Ruenraroengsak P, Chen S, Goode AE, Theodorou IG, et al. Silver nanoparticles reduce brain inflammation and related neurotoxicity through induction of H 2 S-synthesizing enzymes. *Sci Rep.* 2017; 7: 42871.
364. Salazar-García S, Silva-Ramírez AS, Ramírez-Lee MA, Rosas-Hernandez H, Rangel-López E, Castillo CG, et al. Comparative effects on rat primary astrocytes and C6 rat glioma cells cultures after 24-h exposure to silver nanoparticles (AgNPs). *J Nanopart Res.* 2015; 17: 450.
365. Flores CY, Miñan AG, Grillo CA, Salvarezza RC, Vericat C, Schilardi PL. Citrate-capped silver nanoparticles showing good bactericidal effect against both planktonic and sessile bacteria and a low cytotoxicity to osteoblastic cells. *ACS Appl Mater Interfaces.* 2013; 5: 3149-3159.
366. Zuberek M, Wojciechowska D, Krzyzanowski D, Meczynska-Wielgosz S, Kruszewski M, Grzelak A. Glucose availability determines silver nanoparticles toxicity in HepG2. *J Nanobiotechnology.* 2015; 13: 72.
367. Ikrumullah A, Salve D, Pai G, Rathore M, Joshi D. *In vitro* cytotoxicity testing of silver nano-particles in lymphocyte and sperm cells. *Ind J Fund Appl Life Sci.* 2013; 3: 44-47.